UNIVERSITÀ DEGLI STUDI DI PALERMO

Scienze Agrarie, Forestali e Ambientali

Dipartimento SAF – Scienze Agrarie e Forestali

SSD AGR/03 – AGR/15

CHARACTERIZATION AND DEVELOPMENT OF DIFFERENT METHODS TO EXTEND THE SHELF LIFE OF FRESH-CUT FRUIT

IL DOTTORE

PIVA GIULIO

IL COORDINATORE

PROF. BAGARELLO VINCENZO

IL TUTOR

PROF. INGLESE PAOLO

IL CO-TUTOR

DR. TODARO ALDO

CICLO XXIX

2017

A tutte le persone incontrate
durante questi tre anni

RINGRAZIAMENTI

Volgono ormai al termine tre anni molto intensi, ricchi di cambiamenti, di strada se n'è fatta tanta, adesso siamo all'epilogo.

Questo percorso di Dottorato mi ha riservato sorprese che mai avrei immaginato, ricco di episodi, insegnamenti e di tante care persone.

Iniziando dal primo anno, vorrei ringraziare Giorgia, Giuseppe, Alessio e Francesca per avermi aiutato con la sperimentazione e per i momenti di divertimento e crescita personale durante il convegno ISHS del 2016 a Palermo. Ringrazio anche Vincenzo per l'aiuto datomi al primo anno ma soprattutto Filippo con il quale ho condiviso bei momenti durante la sperimentazione estiva del 2014. Sono stato molto contento di aver avuto la possibilità di conoscere Giuseppe, collega fidato e compagno di stanza. Ringrazio la dott.sa Giacalone e la dott.sa Chiabrando per l'ospitalità ricevuta all'Università di Torino nel 2014 e per tutto quanto mi hanno insegnato in quel breve periodo. Ringrazio Stefano Farris perché in quel settembre 2014 mi diede l'idea di svolgere un soggiorno di ricerca PackLAB che fosse più del mese inizialmente preventivato. E così i mesi divennero 18, scelta che comportò numerosi cambiamenti nella mia vita, dal punto di vista personale e professionale, purtroppo non condiviso da alcune persone importanti.

Vorrei ringraziare Luciano, per avermi accolto al PackLAB, per avermi guidato in questi due anni e per avermi messo a disposizione le risorse e le competenze necessarie a svolgere lo studio sul food packaging. Ringrazio Erika Mascheroni, per avermi aiutato durante il secondo anno e mi rammarico di non aver potuto continuare insieme anche durante il terzo anno di dottorato. Ringrazio tutte le persone incontrate al PackLAB: Carlo Cozzolino, Gerald Marin, Alice Leone, Begum, Lea, Daniela Fracassetti, Sara Limbo, Sara Pozzo, Ghislain, Alida Musatti, Nicola, Martina Zanetta, Alessandro Adobati e Miriam Zanoletti per tutti i momenti condivisi insieme e per il sostegno professionale. Ringrazio tantissimo Manuela, che mi ha seguito in questi ultimi due anni, aiutandomi a portare avanti le sperimentazioni e gli articoli, grazie davvero di cuore; e Chiara per il suo ottimismo, il sorriso sempre presente e il supporto "calorico".

Thanks to Prof. Julien Bras and Dr. Daniele Oliveira for giving the opportunity to stay at Pagora of Grenoble INP and to experiment chemistry of materials. Un ringraziamento affettuoso alle persone conosciute durante l'esperienza francese, in particolare Lorenzo Zolin, Antonio Vulcano e i fratelli del C.C. Veymont.

Voglio ringraziare Vittorio che fin dal primo momento, nel lontano 2008, ha creduto in me e mi ha sostenuto e accompagnato in tutti questi anni come un fratello maggiore. Anche se le

circostanze professionali ci hanno allontanato non ho mai dimenticato tutti gli insegnamenti e i tanti momenti passati insieme.
Ringrazio tutti gli amici che durante l'esperienza milanese hanno attenuato il distacco dalla Sicilia: Adriana, Matteo, Francesco, Paola, Gianfranco, Lucia, Miriam e Giuseppe.

Ringrazio tutti i ragazzi della Residenza Universitaria Torrescalla con cui ho passato un periodo importante della mia vita durante quest'ultimo anno di Dottorato. Ringrazio i miei amici di sempre: Francesco e Serena, Mirko e Rossella, su cui posso sempre contare e che sempre sono al mio fianco. Ringrazio la mia famiglia, quella naturale e soprannaturale, per il costante sostegno durante questi tre anni. Un ringraziamento particolare ad Antonio e Riccardo che in questi anni sono stati colleghi fedeli e sinceri e grandi compagni di avventura. Ringrazio infine Virginia, mia moglie, che ho potuto sposare durante questo Dottorato, per tutto il supporto, l'affetto e la sopportazione.

Grazie a tutti per questa fantastica esperienza.

CHARACTERIZATION AND DEVELOPMENT OF DIFFERENT METHODS TO EXTEND THE SHELF LIFE OF FRESH-CUT FRUIT

ABSTRACT

Fresh-cut fruit is among the most highly perishable food product, characterized by short shelf-life (5-7 days), affected by microbiological spoilage and reactions caused by the presence of oxygen, such as enzymatic browning or oxidation reactions. The high added value of this product may justify the use of expensive storage solutions. Several methods exist to preserve ready-to-eat fruit, like dipping in natural or synthetic substances, or the use of active packaging and modified atmosphere packaging. These storage solutions affect differently on the final costs of the product but also on the preservation of the fruit, and on the maintenance of its quality during shelf-life.

In the present doctoral period it was decided to address some factors that influence fresh-cut fruit quality during storage, particularly, enzymatic browning, the pomological decay and microbiological spoilage. To limit these factors it is chosen to use different solutions: the dipping in natural extracts, the active packaging based on natural antioxidants and antimicrobials compounds, as well as the development of a flexible high barrier film, by cellulose nanocrystals, for possible applications on fresh-cut fruit stored under modified atmosphere. The results we obtained on fresh-cut peach or pineapple, gave us many indications. The dipping into plant extract solutions allows a good maintenance of qualitative characteristics though lower than the active packaging. Furthermore, the use of the dipping technique exposes the product to water and air for excessive time, influencing the storage, when compared to the other used storage methods. Concerning the high barrier material developed we obtained very promising results, both for a longer shelf-life, and for a higher sustainability. The active packaging was the most efficient technique both in terms of costs, employing low cost substances, and in terms of automation of the process, as well as the quality preservation. Active packaging allows, in fact, to have longer lasting effect over the time, not exhausting its efficacy in the first days of storage but carrying out its role during all the shelf-life and assuming its minimum increase.

In particular, we developed the technique of "layer-by-layer" that resulted very interesting in terms of antioxidant and antimicrobial effect, and a high device customization. In fact, this device can be applied to many types of fresh food, as well as on longer shelf-life food, giving the possibility to obtain a controlled release over the time. Indeed, it is suitable for an easy scale-up production.

SVILUPPO E CARATTERIZZAZIONE DI METODI DIFFERENTI PER L'ESTENSIONE DELLA CONSERVAZIONE DELLA FRUTTA DI IV GAMMA

RIASSUNTO

La frutta di IV gamma è un prodotto altamente deperibile, con una *shelf-life* molto corta (5-7 giorni) influenzata dalle numerose variabili che entrano in gioco accelerando la senescenza del prodotto. Il suo alto valore aggiunto può giustificare l'utilizzo di soluzioni di conservazione più o meno costose. I metodi attualmente esistenti sono numerosi, spaziano dal dipping in sostanze naturali o sintetiche, all'utilizzo di packaging attivi, all'impiego di atmosfere modificate, ecc. Queste metodiche di conservazione incidono in maniera diversa sui costi finali del prodotto ma soprattutto sulla conservazione dello stesso e sul mantenimento della sua qualità lungo tutto il periodo di *shelf-life*.

Durante il periodo di Dottorato si è scelto di intervenire su alcuni fattori che influenzano la qualità del prodotto durante il periodo di conservazione, in particolare l'imbrunimento enzimatico, il decadimento pomologico e il deterioramento microbiologico. Per limitare questi fattori si è scelto di utilizzare diverse soluzioni: il *dipping* in estratti naturali, l'*active packaging* a base di antiossidanti e antimicrobici di origine naturale, nonché la messa a punto di un film flessibile ad alta barriera, con utilizzo di nanocristalli di cellulosa, per possibili applicazioni di frutta di IV gamma in atmosfera modificata. I risultati ottenuti, applicando le diverse soluzioni proposte su pesche o su ananas, hanno fornito numerose indicazioni. Il *dipping* in soluzioni con estratti di piante permettono una buona tenuta delle caratteristiche qualitative, tuttavia inferiore all'impiego degli active packaging. Inoltre, l'utilizzo della tecnica del *dipping* espone per tempi eccessivi il prodotto all'acqua e all'aria, influenzandone la conservazione, se paragonata alle altre soluzioni impiegate. Riguardo il film flessibile ad alta barriera sviluppato, I risultati ottenuti sono molto promettenti sia per un'applicazione su prodotti caratterizzati da un'elevata *shelf-life*, sia per l'elevata sostenibilità del materiale di confezionamento. L'*active packaging* è la tecnica più efficiente, in termini di costi, impiegando sostanze *low cost*, in termini di automatizzazione del processo, e dal punto di vista dei risultati ottenuti sulla conservazione del prodotto. Permette, infatti, di avere un effetto più duraturo nel tempo, non esaurendo la sua efficacia nei primi giorni di conservazione ma espletando le sue funzioni lungo tutto il periodo di *shelf-life* e facendo ipotizzare una minima estensione di quest'ultima.

L'*active packaging* messo a punto utilizzando la tecnica del "layer-by-layer", si è rivelato molto interessante sotto l'aspetto dell'efficacia antiossidante e antimicrobica e dal punto di vista della personalizzazione del dispositivo. Esso, infatti, si dimostra applicabile a numerose tipologie di

alimento fresco, nonché ad alimenti con *shelf-life* più duratura, data la possibilità di ottenere un rilascio controllato nel tempo. La sua facilità di costruzione ne permette, inoltre, un facile *scale-up* di produzione.

I. PREFACE

Layout of the Thesis

This Doctoral Thesis is organized in five different sections. A "general introduction" where the issues addressed and the proposed solutions are explained. The "objectives" section about the goals of the topics of the Thesis. The "chapters" section is organized in 5 chapters about the experimental works developed during these 3 years. "Final remarks" section includes the final highlights of this Thesis. All the experimental works were developed in collaboration with PackLAB – DeFENS, Department of Food, Environmental and Nutritional Sciences of University of Milan.

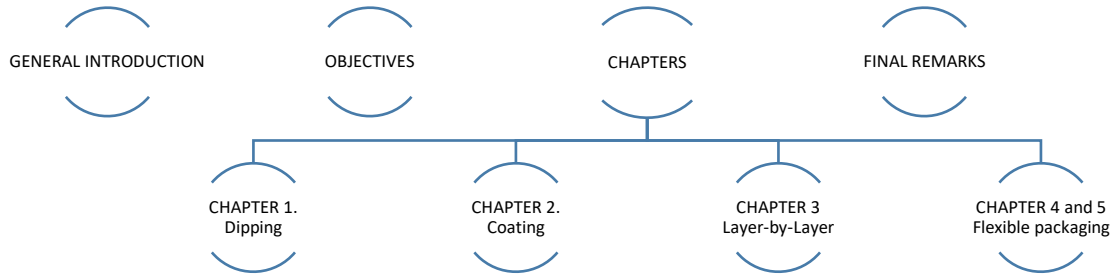

Figure I.1. The scheme of the Doctoral Thesis.

Chapter 1. In *Evaluation of the antioxidant/antimicrobial performance of Posidonia oceanica in comparison with three commercial natural extracts and as a treatment on fresh-cut peaches (Prunus persica Batsch)*, four plant extracts, *Posidonia oceanica*, Green Tea, Grape seeds and Grape skin, were analyzed to determine their total phenolic content, antioxidant activity and in vitro antimicrobial performance. The best performing extracts were applied by dipping on peach slices in storage trials. Microbiological and pomological parameters were evaluated during 7 d storage. For the first time an extract of *Posidonia oceanica* was used on food.

Chapter 2. *Characterization of paper pad coated with chitosan-tetrahydrocurcumin (THC) mix and its application on fresh-cut pineapple (Ananas comosus* L. Merr*)*, presents the in vitro and in vivo studies of a new active packaging paper-based coated with antioxidant and antimicrobial compound. The in vitro section was about the best configuration of the active packaging and its microbiological, antioxidant and mechanical properties. The *in vivo* part was on the application of

this new active packaging solution on fresh-cut fruit. For the first time tetrahydrocurcumin was applied on food and in combination with chitosan.

Chapter 3. In the topic *Novel controlled release system by layer-by-layer assembly and its application on fresh-cut peaches* (*Prunus persica* Batsch), another new active packaging device was developed using the layer-by-layer technique, employed in biomedical field. An alternate deposition of several nanolayers consisting in biopolymers with antioxidant and antimicrobial behavior. The device was characterized and, then, applied on fresh-cut peach.

Chapter 4 and 5. *Comparison of cellulose nanocrystals obtained by sulfuric acid hydrolysis and ammonium persulfate, to be used as coating on flexible food-packaging materials* and *Cellulose nanocrystals from lignocellulosic raw materials, for oxygen barrier coatings of food packaging films.* These two topics were on new flexible packaging solution with oxygen barrier properties. This new solution was developed as a possible packaging for fresh-cut fruit storage under modified atmosphere conditions. The novelty of this research was the replacement of the plastic materials by renewable material as cellulose in form of nano-crystals.

Dissemination of works

These three years of PhD have led to the publication of these four papers on international refereed journals:

1. **PIVA, G**., Fracassetti, D., Tirelli, A., Mascheroni, E., Musatti, A., Inglese, P., Piergiovanni, L. and Rollini, M. (2017). Evaluation of the antioxidant/antimicrobial performance of *Posidonia oceanica* in comparison with three commercial natural extracts and as a treatment on fresh-cut peaches (*Prunus persica* Batsch). Postharvest Biology and Technology. 124, 54-61.

2. Mascheroni, E., Rampazzo, R., Ortenzi, M.A., **PIVA, G**., Bonetti, S., and Piergiovanni, L. (2016). Comparison of cellulose nanocrystals obtained by sulfuric acid hydrolysis and ammonium persulfate, to be used as coating on flexible food-packaging materials. Cellulose. 1: 1-15.

3. Piergiovanni, L., Rampazzo, R. and PIVA, G. (2016). Protecting from oxygen (and from other gases). In Naturally Technological Packaging. ISBN: 978-88-902818-9-1 Ed. Dativo – Milano (Italy).

4. **PIVA, G.**, Rollini, M., Coma, V., Capretti, G., Mapelli, C., Piergiovanni, L., and Inglese, P. Characterization of a chitosan-tetrahydrocurcumin (THC) coated paper pad and application on fresh-cut pineapple (*Ananas comosus* L. Merr.). SUBMITTED TO Postharvest Biology and Technology.

5. Rampazzo, R., Alkan, D., Ortenzi, M.A., Gazzotti, S., **PIVA, G**. and Piergiovanni, L. Cellulose nanocrystals from lignocellulosic raw materials, for oxygen barrier coatings of food packaging film. SUBMITTED TO Packaging Technology and Science.

The obtained results were presented at national and international workshops:

1. **Poster presentation - PIVA**, G. (2014). Development and application of a new Edible Coating. Proceedings of XIX Workshop on the Developments in the Italian PhD Research on Food Science, Technology and Biotechnology, Bari 24-26/09/2014. Pag, 84-85.

2. **Oral communication** - Mascheroni, E., Rampazzo, R., **PIVA, G**. and Piergiovanni, L. (2015). Charged-cellulose nanocrystals produced from lignocellulosic sources for high performing PET coated film. 3rd International Meeting on Material/Bioproduct Interactions (MATBIM), Aragon Institute of Engineering Research, Zaragoza (Spain) 17-19/06/2015.

3. **Poster presentation - PIVA**, G., Mascheroni, E., Fracassetti, E., Inglese, P., Piergiovanni, L. and Rollini, M. (2015). *Posidonia Oceanica* and Green Tea Extract as active agents for shelf life extension of fresh cut peach. Shelf life international meeting. Monza (Italy) 22-23/10/2015.

4. **Poster presentation** - Demeure, L., **PIVA**, G., Capretti, G., Rollini, M., Coma, V., Piergiovanni, L. and Mascheroni, E. (2015). Interactive polyphenols-based biopackaging for food preservation an *in vitro* study. Shelf life international meeting. Monza (Italy) 22-23/10/2015.

5. **Poster presentation - PIVA**, G., Todaro, A., Saletta, F. Inglese, P. (2015). Interazione e applicazione di 1-MCP e film commestibile, a base di *Aloe arborescens*, su pesche a polpa bianca siciliane. XIII Convegno AISSA - Nutrire il pianeta con l'agricoltura: il punto di vista dei ricercatori. Torino, 26-27/11/2015.

6. **Poster presentation - PIVA,** G., Rollini, M., Piergiovanni, L. and Inglese, P. (2016). Controlled release system using layer-by-layer assembly for fresh-cut fruit application. I European Conference of Post Graduate Horticulture Scientists (ECPHS), University of Palermo, Palermo (Italy) 12-13/05/2016.

7. **Oral communication[1] - PIVA, G**. (2016). Characterization and development of different methods to extend shelf-life of fresh-cut fruit. Case study: novel controlled release system by layer-by-layer assembly. Proceedings of XXI Workshop on the Developments in the Italian PhD Research on Food Science, Technology and Biotechnology, Portici (NA) 14-16/09/2016. Pag, 312-316

Stay at foreign research institutions

One foreign period was carried out during the three years:

- **Erasmus Plus** at Institut Polytechnique de Grenoble - Laboratoire Génie des Procédés Papetiers (Grenoble, France), from September to December 2015 under the supervision of Prof. Julien Bras.

[1] Winner of the Award "The most effective presentation of the PhD Thesis results".

1. GENERAL INTRODUCTION

1.1. Some of the problematic of fresh-cut fruit storage

"Fresh-cut produce" is defined as any fresh fruit or vegetable or any their combination that has been physically altered from its original form, but remains in a fresh state. Regardless of commodity, it has been trimmed, peeled, washed and cut into 100% usable product that is subsequently bagged or prepackaged to offer consumers high nutrition, convenience and value while still maintaining freshness (IFPA).

The market sales of ready-to-use fresh vegetable have grown rapidly in the past decades as a result of changing in consumer habits. These types of products are satisfying consumer demands for fresh and healthy food while offering also convenience in quick preparation meal (Soliva-Fortuny et al., 2003).

The problem with this kind of product is their vulnerability. When fruits are cut, several alterations can appear: enzymatic browning, microbial spoilage, loss of weight and firmness, degradation of nutraceutical and organoleptic properties.

After cutting, immediate physical effects occur, such as mechanical shock of tissue, removal of protective epidermal layer or cell fluids on cut surface. Because of this deterioration of the cellular structure, enzymatic reactions can happen.

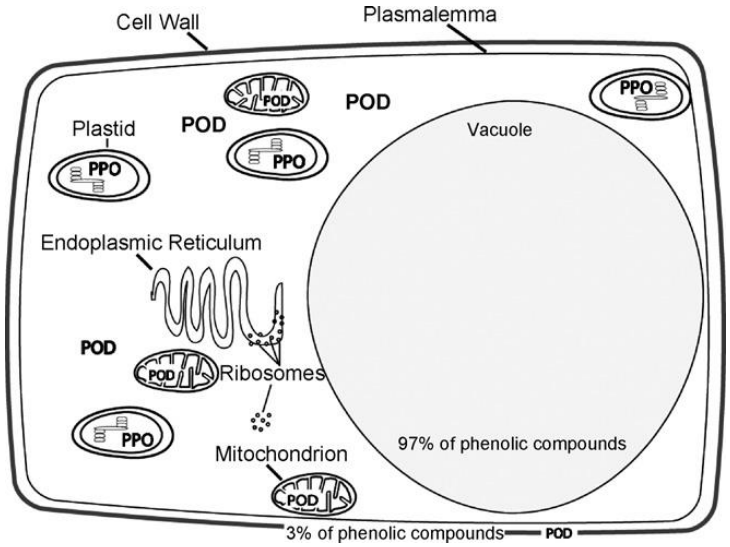

Figure 1.1. The localization of phenolic compounds and phenolic oxidizing enzymes (PPO: polyphel oxidase; POD: phenol peroxidase). (Toivonen & Brummel, 2008).

Phenolic compounds, present into the vacuole, in contact with polyphenol oxidase (PPO), inside the plastids, react and produce colored polymers (Fig. I.1); this is the onset of enzymatic browning. Enzymatic browning process consist of two parts (Fig. I.2), i.e. the hydroxylation of phenols and following oxidation that causes the formation of o-quinones, brown pigments, by PPO in the presence of oxygen (Toivonen and Brummel, 2008). Sensitivity of the fruit also makes it exposed to microbial or chemical contaminants. After that, several physiological effects take place and there is an increase of the respiration rate, in comparison with the integer fruit (Watada, 1996).

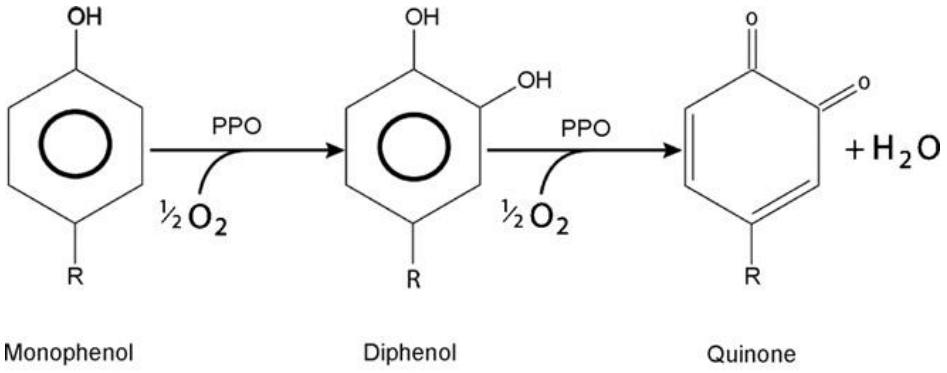

Figure 1.2. The mechanism for polyphenol oxidase action (PPO) on monophenols and Diphenols. (Toivonen & Brummel, 2008).

Also, the ethylene production rate is altered and there is an increase of other biochemical reactions (discoloration and color, texture, aroma and flavor, nutritional quality, etc) (Cantwell, 1999). Preservation of chlorophyll in vegetables, red to purple anthocyanins, yellow, orange and red carotenoids in both fruit and vegetables is of vital importance to maintain quality (Garcia & Barrett, 2002).

Consumers take product appearance into consideration as a primary criterion, and color is probably the main factor considered (Kays, 1999), for this reason in the most industrialized areas of the world (Europe, North America, part of Asia) a huge amount of fresh product waste is present.

Several solutions are put in place to avoid or limits fresh-cut decay: acidulants, chelating, complexing and reducing agents, edible coatings, antimicrobial compounds, high pressure, pulsed light, reducing temperature, heat treatments, etc.

In this study, a special focus was addressed to food packaging as one of the best better solution to protect fresh-cut products.

1.2. A possible solution to reduce quality fruit decay: the active packaging

Packaging has many functions: containment, protection, communication, convenience and logistic. For this type of product, the function of protection is very important thanks to its barrier properties between the product and the environment. Indeed, we can find different type of food alteration such as chemical reactions, enzymatic reactions or biological alteration. The evolution of food is also due to intrinsic and extrinsic factors: physical condition of food, Aw, pH, composition, temperature, humidity, light, mechanical solicitation, oxygen, migration of compound from the packaging, etc. To extend the shelf life of theses very sensitive products, a simple packaging is not enough. In the last decades, several researches have been made to develop a new kind of packaging: the active packaging.

Firstly introduce in the market of Japan in the mid 1970s, active packaging raised the attention of the industry in Europe and USA in the mid 1990s. Due to its deliberate interaction with food and its environment, this new technology posed challenges in terms of safety, compared to a traditional packaging. Migration substances between food and packaging or an incorrect use of it can be dangerous for consumer. That is why in 2004, the European Union offered for the first time a regulation for active packaging and so, the opportunity of using them in Europe. This Regulation contains also general provisions about safety of active packaging and sets framework for the European Food Safety Agency (EFSA). It is only in 2009 that a new Regulation came out for their safe use (Restuccia et al., 2010). In this Regulation, active packaging is defined as a package system that deliberately incorporates components that release or absorb substances into or from the packaged food or the environment surrounding, to extend the shelf-life or to maintain or improve the condition of food (Regulation (CE) No. 450/2009 (29/05/2009)).

Nowadays, the diversity of active packaging is large and the market is in constant evolution.

(Tab. 1.1, Ozdemir and Floros, 2004).

Table 1.1. Diversity of active packaging system currently in the market.

Type of active packaging system	Substances used and mode of action
Oxygen absorbing	Enzymatic systems, chemical systems
Carbon dioxide absorbing/emitting	Iron powder-calcium hydroxide, ferrous carbonate-metal halide
Moisture absorbing	Silica gel, propylene glycol, polyvinyl alcohol, diatomaceous earth
Ethylene absorbing	Activated charcoal, silica gel-potassium permanganate, Kieselguhr, bentonite, Fuller's earth, silicon dioxide powder, powdered Oya stone, zeolite, ozone
Ethanol emitting	Encapsulated ethanol
Antimicrobial releasing	Sorbates, benzoates, propionates, ethanol, ozone, peroxide, sulfur dioxide, antibiotics, silver-zeolite, quaternary ammonium salts
Antioxidant releasing	BHA, BHT, TBHQ, ascorbic acid, tocopherol
Flavor absorbing	Baking soda, active charcoal
Flavor releasing	Many food flavors
Color containing	Various food colors
Anti-fogging and anti-sticking	Biaxially oriented vinylon, compression rolled oriented HDPE
Light absorbing/regulating	UV blocking agents, hydroxybenzophenone

In fact, the growth of population and the changing of lifestyle increased ready-to-eat and package food. The active packaging market is expected to grow because of an increasing need of freshness, preservation of nutritional value of products and extend of shelf life at competitive prices. According to Freedonia group, active packaging demand is forecast to grow 5.4 % per year to reach $2.5 billion in 2019 (The Freedonia Group, 2015).

To answer this large demand of novelty, many researches are made on new active packaging as innovative and effective way to improve food shelf life and reduce food waste, a big and controversial problem of our society.

1.2.1. Principles of active packaging: release of useful substances

One of the last trends is to incorporated active agent such as antioxidants and antimicrobials inside the packaging material or onto its surface. The aim is release these substances into food product during their storage instead of being used in food formulations as ingredients or additives (Piergiovanni et al., 2012). This technique allows the release of active substances in the correct amount and in a controlled manner (Coma, 2008). Several studies have proved that a gradual and continues release of antimicrobial substances into food is more effective than one time addition because it is avoiding microbial adaptation phenomena (Zhang et al., 2004). The nature of active agents that can be added is very diverse (organic acid, enzymes, bacteriocins, fungicides, natural extract, ions, ethanol etc.) as well as the nature of materials into which they are included (papers, plastics, metals or combinations of these materials).

The first possible way to add active substances is the deposition of molecules on the packaging material, by coating or dipping. The term coating is generally used to refer to a procedure that leads to the deposition of a thin layer of a fluid or melted material on a support surface. The surface can be a plastic film but also paper, metallic or glass surface. Coating deposition is commonly used to improve performances of food packaging materials like barrier, mechanical and surface properties and also to add active substances. Usually, the thickness of the coating material is between 0.5 and 15 µm. Traditionally, to coat plastic materials, substances are dissolved in water or in organic solvent before his evaporation, or a thick layer of a melted polymer with a special technique, the extrusion coating. An innovative approach for coating deposition is the layer-by-layer technique; a method developed starting from Idler's studies (1996) on colloidal particles. In 1990, Decher et al. demonstrated that polyelectrolyte can be used in this technique, making it a promising technique.

Another way to integrate active substances into food packaging is to put them directly into the packaging composition. An example of active releasing materials is a plastic film commercially available in Japan, containing allylisothiocyanate (AITC), a strong antimicrobial substance extracted from mustard or wasabi. AITC is entrapped in cyclodextrins for protecting the volatile active agent from being thermally degraded during extrusion. When exposed to high moisture

conditions after the packaging of the food product, cyclodextrins have the ability to change in structure and to release the antimicrobial agent in the atmosphere surrounding the food (Lee, 2005).

1.2.2. New trends

Beside this trend related to the release of active substances, the tendency to use only natural molecules and bio-based material has to be taken into account. Indeed, over the last few decades the use of synthetic polymers as food packaging materials has increased, due to their advantages over other traditional materials such as glass or tin plate. But some serious issues such as migration phenomenon, packaging waste, environmental impact and the decrease of fossils energies have increased the desire to design alternative solutions. It is in this context that researches are carried out to develop biodegradable films for food packaging and also the use of natural active substances. Biodegradable polymers can also be manufactured from petrochemical raw materials that is why the most promising solution is the bio-based polymers. Based on U.S. Environmental Protection Agency (EPA) statistics, about 10 million pounds of plastic wastes are produced aboard government ships. These wastes can be used as an indicator for market potential for both bio-based and biodegradable materials (Wool and Sun, 2011).

The development of bio-based materials is consistent with the principles of Green Chemistry and Engineering, which pertain to the design, commercialization and use of processes and products that are technically and economically feasible while minimizing the generation of pollution at the source and the risk to human health and the environment. (Wool and Sun, 2011). Bio-based polymers are defined as polymers that are fully or partially produced from renewable raw materials. They are generally classified into three categories:

- Natural polymers extracted from animal and plant sources. Traditionally used for food and feed, plant-based materials are increasingly being used in pharmaceuticals and nutraceuticals fields. Three major plant-based polymers are protein, oil and carbohydrates. Chitin and cellulose are the main naturally occurring polymers in the large carbohydrate family (Wool and Sun, 2011);
- Polymers produced by chemical synthesis employing renewable bio-based monomers such as polylactate (PLA). It exhibits mechanical and physical properties comparable to other commercially available polymers (Krishnamurthy et al., 2004);

- Polymers produced by genetically modified bacteria or by microorganism through a fermentation process of natural substrates such as polyhydroxyalkanoates (PHA).

However, like conventional packaging, bio-based packaging must have important functions including containment and protection of food, maintaining its sensory quality and safety, and communicating information to consumers (Robertson, 1993). Unfortunately, there is some limitation of their use when high barrier properties are required, mostly because of their sensibility to water, or by legislation limits as in the case of nanotechnologies.

To obtain natural packaging, the other way to act is by replacing synthetic food additives with natural ones. Various natural substances, coming from animal, plant or microbiological sources are currently applied for this purpose. Table 1.2 shows the most commonly applied natural antioxidants and Table 1.3 natural substances manly applied for their antimicrobial properties. Most of these molecules show both antioxidant and antimicrobial activity.

Table 1.2. Most commonly applied natural antioxidant in active packaging production.

Antioxidant	**Source and efficacy**
Tocopherols	Apolar antioxidant compounds, abundant in olive, peanuts, eggs. α-tocopherols is the most effective compounds, acting as a radical scavenger.
Quercetin	Flavonol compound obtainable from diverse vegetal sources, it acts as a singlet oxygen quencher and reactivating primary antioxidants.
Ferulic Acid	Fenolic acids, obtainable from grains and fruits. It acts as a radical scavenger.
Caffeic acid	Fenolic acids, first founded into coffe extract but widely presents in others vegetables and fruits.
Catechins	Flavonol compounds, abundant in green te and cocoa, with diverse antioxidants activity depending from molecular structure.

Table 1.3. *Most commonly applied natural antioxidant in active packaging production*.

Antimicrobial	**Source and efficacy**
Citral	Aldehydic compounds coming from citrus essentials oils. Effective against *Salmonella* and *Listeria*. Water-soluble.
Carvacrol	5-isopropil-2methylphenol, extracted from oregano; volatile; effective against *E. coli*, *S. aureus*
Menthol	Cristallin substance obtained from mint essential oils. Effective against *E. coli*, *S. aureus*, *Salmonella*.
Acetic acid	Produced by *A. aceti* and *G. suboxydans*. Effective against *E. coli, L. monocytogenes, Salmonella*.
Lysozyme	Globular protein from egg albumen. Effective against Gram + and Gram -, *E. coli, P. fluorescens, S. aureus.*
Nisin A	Bacteriocins produced by *L. lactis*. Effective against Gram + and endospores
Sakacin	Bacteriocins produced by *L. sakei*. effective against *Enterobacteriaceae, L. monocytogenes, S. aureus.*

The use of natural active compounds is often limited by their sensorial impact on food. A possible strategy to overcome this problem is to search for good sensorial-matching between active compounds and foods, such as for examples rosemary extract and chicken meat products. According to these trends, several studies are made with antimicrobial and antioxidant natural agents.

For example, some essentials oils or plant extracts can be added to the coating mixture in order to prevent microbiology growth. It has been done by Rodriguez et al (2007) with clove, cinnamon and oregano essential oils, on common fungal and bacterial contaminants of foods. Another trend example is the realisation of a bio-based active film with antimicrobial and antioxidant activities thanks to chitosan. Chitosan exhibits high antimicrobial activity against pathogenic and spoilage

micro-organisms, including fungi and both Gram positive and Gram negative bacteria (Aider, 2010).

1.3. References

Ahvenainen, R. 1996. New approaches in improving the shelf life of minimally processed fruit and vegetables. Trends Food Sci. Technol. 7, 179-187.

Aider, M. 2010. Chitosan application for active bio-based films production and potential in the food industry: Review. LWT-Food Sci. Technol. 43, 837-842.

Cantwell, M. and Suslow, T. 1999. Fresh-cut fruits and vegetables: aspects of physiology, preparation and handling that affect quality. In Annual Workshop Fresh-Cut Products: Maintaining Quality and Safety. Vol. 5, pp. 1-22.

Coma, V. 2008. Bioactive packaging technologies for extended shelf life of meat-based products. Meat Sci. 78, 90-103.

Garcia, E. and Barrett, D. M. 2002. Preservative treatments for fresh-cut fruits and vegetables. Fresh-Cut Fruits and Vegetables. CRC Press, Boca Raton, FL, 267-304.

Gontard, N. 1997. Les emballages actifs: Panorama. Industries alimentaires et agricoles, 114, 117-119.

IFPA (The International Fresh-cut Produce Association).

http://www.creativew.com/sites/ifpa/fcf.html (Consulted 05/11/2016)

Kays, S.J. 1999. Preharvest factors affecting appearance. Postharv. Biol. Technol. 15, 233-247.

Krishnamurthy, K., Demirci, A., Puri, V.M. and Cutter, C.N. 2004. Effect of packaging materials on inactivation of pathogenic microorganisms on meat during irradiation. Transactions of the ASAE. 47, 1141.

Lee, D.S. 2005. Chapter 7 - Packaging containing natural antimicrobial or antioxidative agents, In Food Science and Technology, edited by Jung H. Han,, Academic Press, London, 2005, Pp. 108-122, Innovations in Food Packaging.

Ozdemir, M. and Floros, J.D. 2004. Active food packaging technologies. Critic. Rev. Food Sci. Nutr. 44, 185-193.

Piergiovanni, L. and Limbo, S. 2010. Food packaging: Materiali, tecnologie e soluzioni. Springer Science & Business Media.

Restuccia, D., Spizzirri, G., Parisi, O., Cirillo, G., Curcio, M., Iemma, F., Puoci, F., Vinci, G. and Picci, N. 2010. New EU regulation aspects and global market of active and intelligent packaging for food industry applications. Food Control. 21, 1425–1435.

Robertson, G.L. 1993. Food packaging. Principles and practice, Marcel Dekker, New York, NY.

Rodriguez, A. Batlle, R. and Nerin, C. 2007. The use of natural essential oils as antimicrobial solutions in paper packaging. Part II. Progress Organic Coat. 60, 33-38.

Soliva-Fortuny, R.C and Martın-Belloso, O. 2003. New advances in extending the shelf life of fresh-cut fruits: a review. Trends Food Sci. Technol. 14, 341–353.

The Freedonia Group. 2015. Active & Intelligent Packaging - US Industry Study with Forecasts for 2019 & 2024 - Study #3338. Pp. 4-34.

Toivonen, P.M. and Brummell, D.A. 2008. Biochemical bases of appearance and texture changes in fresh-cut fruit and vegetables. Postharv. Biol. Technol., 48, 1-14.

Watada, A.E., Ko, N.P. and Minott, D.A. 1996. Factors affecting quality of fresh-cut horticultural products. Postharv. Biol. Technol. 9, 115-125.

Wool, R. and Sun, X.S. 2005. Bio-based polymers and composites". Elsevier academic press.

Zhang, Y., Yam, K.L, Chikindas, M.L. 2004. Effective control of *Listeria monocytogenes* by combination of nisin formulated and slowly released into a broth system. Int. J. Food Microbiol. 1, 15-22.

2. OBJECTIVES

The main goal of this doctoral thesis is to preserve fresh-cut fruit from qualitative decay that occurs as a result of cutting, responsible for the senescence acceleration of the product. In particular, the topics addressed in this work have the objective to reduce enzymatic browning, preserve the polyphenolic substances and pomological traits and reduce the microbiological spoilage, in order to have a product of best quality for consumers and to reduce the food waste.

To satisfy these objectives, different strategies to preserve fresh-cut fruit, using new packaging solutions and/or new active substances as additives, have been developed. The proposed solutions are four.

Solution 1: use of a new plant extract ever used on food, applied directly on fresh-cut fruit by the dipping technique.

Solution 2: set up of a new active packaging cellulose-based, containing THC, with antioxidant properties and used for the first time on food, and chitosan, with antimicrobial properties, applied by coating technique.

Solution 3: development and characterization of a new controlled release system consists of active polymers and green tea extract, assembled by layer-by-layer technique, used for the first time in the food field.

Solution 4: development of a new flexible packaging made up cellulose nanocrystals, extracted from lignocellulosic raw materials and coated on PET, with high gas barrier activity (not applied *in vivo*).

3. CHAPTER I:

Evaluation of the antioxidant/antimicrobial performance of *Posidonia oceanica* in comparison with three commercial natural extracts and as a treatment on fresh-cut peaches (*Prunus persica* Batsch)

(Main Author of the article Published on Postharvest Biology and Technology, 2017, 124: 54-61)

3.1. ABSTRACT

This research aimed at extending the choice of natural antimicrobials/antioxidants for food applications. Four plant extracts, *Posidonia oceanica* (PO), Green Tea (GT), Grape seeds (GS) and Grape skin (GK), were analyzed to determine their total phenolic content, antioxidant activity and *in vitro* antimicrobial performance. PO extract showed the highest total phenolic content (711 mg gallic acid g^{-1} extract) and antifungal activity against *Aspergillus niger* and *Penicillium chrysogenum*. The highest antioxidant (3.81 mg L^{-1} EC_{50}) and antibacterial activities (bactericidal against Gram positives and bacteriostatic against Gram negatives) were found for GT extract.
The best performing extracts (PO and GT) were applied by dipping on peach slices in storage trials. Microbiological and pomological parameters were evaluated during 7 d storage. Total aerobic count, *Pseudomonas* as well as yeasts and moulds populations, were reduced by about 0.5 log cfu g^{-1}, mainly up to 5 d in all treated samples compared to the control. Total soluble solids, titratable acidity and colour (L*a*b*) changes were also delayed in treated fruit.

KEYWORDS: ready-to-eat fruit, green tea, *Posidonia oceanica*, dipping, antimicrobials, antioxidants.

3.2. INTRODUCTION

One of the most important research areas as rated by a large majority of food companies is the development of healthy foods, and the introduction of fresh cut produce onto the market, in order facilitate fruit consumption, is rapidly growing (Jung and Zhao, 2016).

Nevertheless, the high perishability of minimally processed fruit may lead to an increase in food waste and economic losses (Amani and Gadde, 2015). Throughout the production process, cell breakage takes place causing juice leakage and leading to microbial contamination and growth. Moreover, the contact between enzymes and cell juice under oxygen exposure increases cell respiration and activation of fruit senescence. Specifically, minimally processed fruit, and peaches in particular, are very susceptible to flesh browning (Denoya et al., 2016). Therefore one of the current challenges for the agro-food companies is to lengthen cut fruit shelf life, consequently improving attractiveness to customers as well as food safety.

The food industry has been increasingly employing polyphenols to limit enzymatic oxidation which affects the shelf life of ready-to-eat fruit (Gyawali and Ibrahim, 2014). The beneficial properties of polyphenols on human health also have to be taken into account (Pandey and Rizvi, 2009).

As sources of polyphenols, several trials have been carried out using plant extracts from common or endemic species (Perumalla and Hettiarachchy, 2011) or alternatively from by-products of the agro-food industry (Balasundram et al., 2006). Nowadays, exploitation of by-products and/or residues represents one of the environmental and economic priorities. Several substances discarded from agro-food production can find alternative applications in different contexts. As examples, grape skin (GK) and seeds (GS) are the main wastes from the wine industry, nevertheless they are appreciated for their high phenolic content which includes flavonoids, phenolic acids and non-flavonoid compounds (Poudel et al., 2008). The hydroxyl groups of gallic acid, present in grape by-products, showed antimicrobial activity against *Bacillus cereus*, *B. subtilis*, *B. coagulans*, *Staphylococcus aureus*, *Escherichia coli* and *Pseudomonas aeruginosa*; also all the substituents of the benzene rings were found effective against *S. aureus* (evaluated by Minimal Inhibitory Concentration assay) (Jayaprakasha et al., 2003).

The antioxidant capacity of polyphenols can also be used to prevent or slow down enzymatic oxidation of vitamins and pigments contained in ready-to-eat fruit and vegetables (e.g. enzymatic browning), thus preventing the loss of nutritional elements and increasing attractiveness to consumers due to the maintenance of their sensorial characteristics (Rojas-Grau et al., 2009).

Moreover, they can be added as antimicrobials thus increasing product shelf life (Guillen et al., 2013).

Flavonoids from plants have high antioxidant capacity and they are widely used substances, including catechin, epicatechin, gallocatechin, epigallocatechin, catechin gallate, epigallocatechin-3-gallate (the most abundant and biologically active compound in green tea), gallocatechin gallate and epicatechin gallate (Sutherland et al., 2006). The hydroxyl groups in the ring structure of catechin can be easily oxidized (Janeiro and Brett, 2004).

Green tea (GT) is one of the plant extracts with high antioxidant and antibacterial activities, and with anti-tumor effects due to its catechin content. GT catechin showed antimicrobial activity against Gram positive and Gram negative bacteria including certain pathogens of the gastrointestinal tract such as *S. aureus, S. epidermis* and *Plesiomonas shigelloides*, but it was not effective against *E. coli, Pseudomonas aeruginosa* and *Aeromonas hydrophila* (Kusmita et al., 2014).

Posidonia oceanica (PO) is a marine endemic plant of the Mediterranean sea protected by the EU (92/43 EEC Habitat Managerial and Community Board 97/62/EEC). It is an important species in coastal waters defence, forming extensive marine grasslands (Foden et al., 2007). Twenty-three phenolic compounds were identified in this species (Cuny et al., 1995; Agostini et al., 1997) and several studies showed that PO extract is able to inhibit the growth of both Gram positive and Gram negative bacteria, and it was particularly effective against *P. aeruginosa* and *S. aureus* (Berfad and Alnour, 2014), as well as yeasts. PO extract was also assayed in the biomedical field, proving its high anti-diabetic and anti-oxidant effects (Gokce and Haznedaroglu, 2008). However, some reports found evidence for the transfer of toxins originating from toxic dinoflagellates which live as epiphytes on PO leaves (Bellassoued et al., 2012).

The present research is aimed at extending the choice of natural antimicrobials/antioxidants for food applications, derived from PO, GT, GS and GK. These extracts were analyzed to determine their total phenolic content and antioxidant activity as well as *in vitro* antimicrobial performance. The two best performing extracts were also used to set up fresh-cut storage trials on peach slices, applying the dipping procedure. Peach (*Prunus persica* L. Batsch) is a climacteric fruit that contains carbohydrates, organic acids, pigments, phenolics, vitamins, volatiles, antioxidants and trace amounts of proteins and lipids, which make it very attractive to consumers (Kader and Mitchell, 1989). However, peaches are susceptible to physiological disorders (internal breakdown and chilling injury), pathogen (moulds) and processing manipulation (browning of tissues) (Caceres et al., 2016).

3.3. MATERIALS AND METHODS

3.3.1. Chemicals

2,2-Diphenyl-1-picrylhydrazyl (DPPH), (±)-6-Hydroxy-2,5,7,8-tetramethylchromane-2-carboxylic acid (Trolox) 97%, Ethanol (≥99.8%), Ethyl acetate (anhydrous, 99.8%), Folin-Ciocalteu's phenol reagent, hydrochloric acid, sodium hydroxide and sodium sulfate (≥99.0%, anhydrous), were purchased from Sigma–Aldrich (Gallarate, MI, Italy).
Green tea, grape skin (*Vitis vinifera* L., Chardonnay variety) and seed extracts for oenological use (antioxidants) were obtained from DAL CIN GILDO S.p.A. (Concorezzo, MB, Italy).

3.3.2. *Posidonia oceanica* extract

Posidonia oceanica (L.) Delile was collected by scuba diving from Palermo (Sicily, Italy), Tyrrhenian Sea, in October 2014. Note that as this is a protected marine plant, for use in any industrial application, it should be sourced from aquaculture systems under controlled growing conditions. The epiphytes on the leaves were removed with paper towels without damaging the organs, as reported by Gokce and Haznedaroglu (2008). Leaves were dried in the dark at 20 ± 1 °C and then stored at 4 ± 1 °C before use. The extract was obtained according to the method of Gokce and Haznedaroglu (2008). Briefly, homogenized tissues were infused in 50% (v/v) ethanol-water solution for 3 h in a water bath at 40 °C with a reflux system in the dark. The homogenate was filtered and acidified at pH 3 with hydrochloric acid 2 N. After evaporation of ethanol under vacuum at 45 °C, the aqueous residue was extracted with ethyl acetate. The organic phase was filtered and evaporated under vacuum. The extract obtained, which was a green viscous material (Figure 3.1), was freeze dried and finally stored at -20 °C until use.

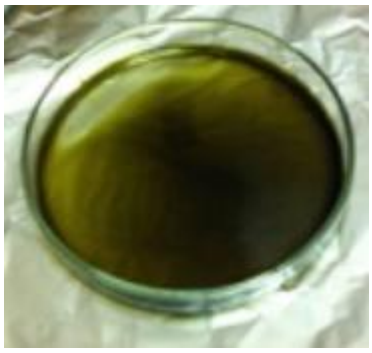

Figure 3.1. Extract of *P. oceanica*

3.3.3. Total phenolic content

Total phenols (TP) levels of the PO, GT, GS and GK extracts were estimated colorimetrically by the Folin-Ciocalteau method (Scalbert et al., 1989). Extracts (1 g L^{-1}) were dissolved in 50% (v/v) methanol/water and appropriately diluted (1:2.5, 1:5 and 1:10 v/v) in the same solvent. The Folin-Ciocalteau reagent was 10-fold diluted in water (v/v) and 2.5 mL were added to each 0.5 mL sample. Two milliliters of 75 g L^{-1} sodium carbonate solution were added and tubes kept for 1 h at 20 ± 1 °C in the dark. In the meanwhile, the calibration curve for gallic acid (5-100 mg L^{-1}) dissolved in 50% (v/v) methanol/water was achieved. The absorbance at 765 nm was measured and results were expressed as g GAE 100 g^{-1} powder. Each formulation was analyzed in triplicate.

3.3.4. Antioxidant assay

Analysis of the antioxidant capacity of PO, GT, GS and GK extracts was carried out employing the DPPH assay, following the method of Brand-Williams et al. (1995) with some modifications. The DPPH solution was diluted in methanol to obtain 1.00 ± 0.03 absorbance units at 515 nm. The extracts samples were dissolved (20 g L^{-1}) in 70 % methanol (v/v) and, after centrifugation, they were serially diluted. The DPPH solution (2.94 mL) was placed in a cuvette where a 60 µL sample was added. The absorbance readings were carried out after incubation for 50 min at 20 ± 1 °C. A calibration curve was prepared by adding increasing concentrations of Trolox ranged from 50 to 1000 µM; each concentration was assayed in triplicate. Results were expressed as mol Trolox per 100 g dry weight. Each formulation was analyzed in triplicate.

3.3.5. Microorganisms and culture conditions

Antimicrobial activity was analyzed by carrying out *in vitro* tests determining the Minimal Inhibitory Concentration (MIC) against strains belonging to official collections, i.e. *Escherichia coli* CECT 434 (Spanish Type Culture Collection), *Listeria innocua* DSM 20649 (Deutsche Sammlung von Mikroorganismen und Zellkulturen), *Pseudomonas putida* ATCC 12633 (American Type Culture Collection), *Staphylococcus aureus* ATCC 29213, *Aspergillus niger* NRRL 565 (Agricultural Research Service Culture Collection) and *Penicillium chrysogenum* CECT 2802. These microorganisms were selected among the most common spoilage and/or pathogen microorganisms that might be present in fresh food products (Mascheroni et al., 2014).

Bacterial strains were weekly maintained on TSB (Tryptic Soy Broth, Scharlau Chemie, Spain), incubated at 30 °C for 24 h and then stored at 4 °C, while moulds were maintained on MEA solid culture (MEB added with 15 g L^{-1} agar), incubated at 25 °C for 5-7 d and then stored at 4 °C until use.

3.3.6. Determination of antimicrobial activity *in vitro*

Qualitative determination of antimicrobial activity was performed as follows: 30 mL of soft TSA or MEA (TSB or MEB added with 8 g L^{-1} agar) were poured in a Petri Dish and inoculated with 300 µL of a microbial suspension prepared in sterile distilled water (OD 600nm: 0.300 ± 0.050); moulds were inoculated as spores suspension in sterile distilled water (OD 600 nm: 0.300 ± 0.050). Once solidified, holes were made by using a sterile tip and 150 µL of extracts were poured inside. Cultures were all incubated at each appropriate temperature for 24 h (up to 7 d for moulds). The presence of a growth inhibition halo around holes indicates an antimicrobial activity.
Quantitative determination of antimicrobial activity was performed only with PO and tea extracts. Ten mL of soft TSA or MEA were poured in a Petri Dish, to which aliquots of PO extract were added in order to obtain a final concentration of 0.5-1.0-1.5-2.0-2.5 and 3.0 g L^{-1}. Tea extract was tested at the following concentrations: 0.5-1.0-1.5-2.0 g L^{-1}. Once solidified, plates were all surface inoculated with aliquots (3 µL) of appropriately diluted (OD 600nm: 0.300 ± 0.050) overnight microbial cultures on TSB (bacteria). Moulds were inoculated as spore suspension in sterile distilled water (OD 600 nm: 0.300 ± 0.050). For each strain control trials were also prepared without the addition of extracts. In order to highlight any possible inhibitory effect of the solvent present in extracts, a set of solid cultures was also set up by adding ethanol (up to 3 g L^{-1}) to the culture media.
Cultures were all incubated at each appropriate temperature for 24 h or up to 7 d for moulds. MIC (Minimum Inhibitory Concentration) was determined as the lowest extract concentration (g L^{-1}) able to inhibit microbial growth. Trials were repeated twice for each extract.

3.3.7. Fresh-cut peach storage

Peaches (*Prunus persica* L. Batsch cv. 'Rich May') were purchased at the wholesale market (3 kg), 24 h after harvesting at commercial maturity and stored for 1 d at 4 °C until use. Peaches were homogenous in weight (180 ± 5 g) and ripening (10.85 ± 0.07 °Brix). Fruits were pre-washed with distilled water, sanitized for 2 min in chlorinated water (150 mg L^{-1} sodium hypochlorite), rinsed with distilled water and gently dried by hand. Peaches with skin were cut into slices (8 slices per

fruit) of about 1.5 cm thickness (15 ± 2 g each slice), using a sterile stainless-steel knife, and dipped for 3 min in the following solutions: PO extract (2% w/v), GT extract (1% w/v) and distilled water for control samples (CTRL). Slices were then left in the air for 2 min in order to drain off the excess solution. Three slices (45 ± 6 g) were placed into low-density polyethylene (LDPE) bags (22 x 15 cm, 25 µm thickness, bag volume 450 mL, ratio between fruit weight and container volume 100 g L^{-1}, surface film for each bag 660 cm^2, O_2 permeability 6200 cm^3 m^{-2} d^{-1} bar^{-1}, CO_2 permeability 24000 cm^3 m^{-2} d^{-1} bar^{-1} at 10 °C). Bags were all stored at 4 ± 1 °C up to 7 d. A total number of 48 bags were prepared, 24 used for color evaluation, and the remaining ones for the other analyses. Samples were then collected after 0, 3, 5 and 7 d. Each trial at each day was carried out in duplicate.

3.3.8. Colour evaluation

Flesh colour was evaluated using the CIE L*a*b* System by a Minolta CR-300 chromameter (Konica Minolta Sensing, Inc., Japan). Three measurements were performed on each side of slices. The instrument was calibrated using a standard white plate. The chroma (C) was calculated as follows (1):

$$C^* = \sqrt{a^{*2} + b^{*2}} \qquad (1)$$

3.3.9. Total soluble solids and titratable acidity

Total soluble solids (TSS, %) and titratable acidity (TA, g L^{-1}) were measured on the juice obtained from slices (30 g for each sample) by an electronic blender (Ariete, Italy). TSS were determined by a digital refractometer (Atago Co., Ltd, Tokyo, Japan model PR-32), while TA was determined by titrating 1:10 diluted juice using sodium hydroxide 0.1 M by an automatic titrator (Compact 44-00, Crison Instruments, SA, Barcelona, Spain).

3.3.10. Antimicrobial activity of green tea and *P. oceanica* on peach slices

After 0, 3, 5 and 7 d, peach slices (15 g) were transferred aseptically into a Stomacher bag (400 mL PE, Barloworld, France) containing 135 mL of sterile peptoned water (10 g L^{-1} bacteriological peptone, Costantino, Italy) and blended in a Stomacher (Star Blender LB 400, Biosystem, Belgium) at high speed for 3 min. Ten-fold dilution series of the obtained suspensions were made of the same solution for plating. The following culture media were used: TSA (Merck, Germany) for mesophiles, *Pseudomonas* Agar base (Himedia, India) for *Pseudomonas spp.*, VRBLA (Violet

Red Bile Agar, Merck, Germany) for *Enterobacteriaceae* and MEA for yeasts and fungi. Colonies were counted after incubation at 30 °C for 24 h for mesophiles, 30 °C for 5 d for yeasts and fungi and 25 °C for 24 h for *Pseudomonas*. Counts were performed in triplicate and reported as logarithms of the number of colony forming units (log cfu g^{-1} peach), and means and standard deviations (SD) were calculated.

3.3.11. Statistical analysis

Statistical analysis was carried out using the STATISTICA 7.1 software package (Statsoft Inc., Tulsa, OK, USA). One-way analysis of variance (ANOVA) was performed on mean values and Tukey's test was carried out for the comparison of difference among treatments for each storage time and for each treatment during storage. Differences were considered significant at $p \leq 0.05$.

3.4. RESULTS AND DISCUSSION

3.4.1. *In vitro* evaluation of total phenolic index and antioxidant activity

Total phenol index (TPI) and antioxidant capacity (AC) were evaluated for each investigated extract (Tab. 3.1). PO showed the highest TPI (711 mg g^{-1}) followed by the GS extract (526 mg g^{-1}). The highest AC was found for GT extract (3.8 ± 0.11 mg L^{-1} EC_{50}).

In case of PO, the highest polyphenols content corresponded to the lowest antioxidant capacity. Such a low value could be attributable not only to the extraction procedure but can also be related to the type of polyphenols present in the extracted matrix (Berfad and Alnour, 2014). The choice of the solvent to use (50% v/v ethanol-water solution) was based on the best results obtained by Berfad and Alnour (2014), who investigated the extraction performance of different solvent mixtures on *P. oceanica*, as well as also taking into account its food-grade nature. As reported in the literature, the principal polyphenols present in PO are acetosyringone, ferulic acid and acetovanillone, while those in GT are gallic acid, catechin gallate and epicatechin (Agostini et al., 1998). These last compounds are characterized by the presence of three proximal hydroxyl groups, able to efficiently delocalize radicals present in the aromatic ring thus acting as radical scavengers. On the contrary, the polyphenols present in PO hydroxyl groups are not in close proximity and a methyl moiety is often present, thus reducing its antioxidant capacity (Agostini et al., 1998).

Nevertheless, the polyphenols values obtained were comparable with those reported in the literature for other plants (Mensor et al., 2001). The highest antioxidant capacity of the GT extract is not surprising since GT is particularly rich in phenols, as proanthocyanidins, with low redox potential and it does not contain bi-flavanols (Lee et al., 2014).

Table 3.1. Total Phenolic Index (TPI) and Antioxidant Capacity (AC) of the extracts investigated in this study. Data are presented as mean ± SE.

Extract	**TPI**	**AC**
	mg GAE g^{-1} extract	mg L^{-1} EC_{50}
P. oceanica	710.6 ± 20.1	72.42 ± 22.9
Green tea	526.3 ± 14.9	3.80 ± 0.11
Grape skin	398.2 ± 9.5	6.14 ± 0.78
Grape seeds	596.4 ± 15.6	4.10 0.14

3.4.2. *In vitro* determination of antimicrobial activity

In qualitative trials performed employing 1 g L^{-1} extract solutions, all samples showed the highest antimicrobial activity against *L. innocua*. GT proved to be the most powerful sample, while at the tested concentration PO did not show any antibacterial activity but was the only extract possessing an antifungal action against *Aspergillus niger* (Tab. 3.2).

Table 3.2. Diameter (mm) of microbial growth inhibition halos around wells containing the analyzed extracts (1 g L^{-1}) after incubation.

Microorganism	GT	PO	GK	GS
Listeria innocua	12	n.p.*	4	6
Staphylococcus aureus	10	n.p.	2	4
Escherichia coli	6	n.p.	2	4
Pseudomonas putida	4	n.p.	n.p.	4
Aspergillus niger	n.p.	8	n.p.	n.p.
Penicillium chrysogenum	n.p.	n.p.	n.p.	n.p.

*n.p.: inhibition halo not present.

Quantitative determination of antimicrobial performance found that MIC for GT and PO extracts were 1 and 2 g L^{-1} respectively against the two Gram positive strains *L. innocua* and *S. aureus*. The two Gram negative strains showed a reduction of microbial growth attributable to a bacteriostatic, rather than a bactericidal, effect (Figure 3.2). *Aspergillus* and *Penicillium* showed a marked reduction of hyphal growth (up to 30% for *A. niger* and to 70% for *P. chrysogenum* employing 3 g L^{-1} extract) and sporulation when grown in presence of PO, while no effect was evident with GT (Figure 3.3). Only in the control plate (no extract added) after 7 d incubation the two moulds showed an antagonistic effect, while in all the other plates the hyphal growth of each strain was not influenced by the presence of the other one. Note that ethanol, the solvent used to prepare extracts, was not found to inhibit microbial growth at the tested concentrations, thus confirming literature results (Dantigny et al., 2005).

Recently, Alkan and Yemenicioglu (2016) tested the *in vitro* antimicrobial activity of various plant phenolics, finding that clove extract was the most potent antimicrobial, with MIC values of 10.24 g L^{-1} against the plant pathogens *Erwinia amylovora*, *E. carotovora*, *Pseudomonas syringae* and *Xanthomonas vesicatoria*. The reported values are much higher than those found in the present research (MIC of 1-2 g L^{-1}), at least for PO, highlighting that the tested extracts are of actual interest.

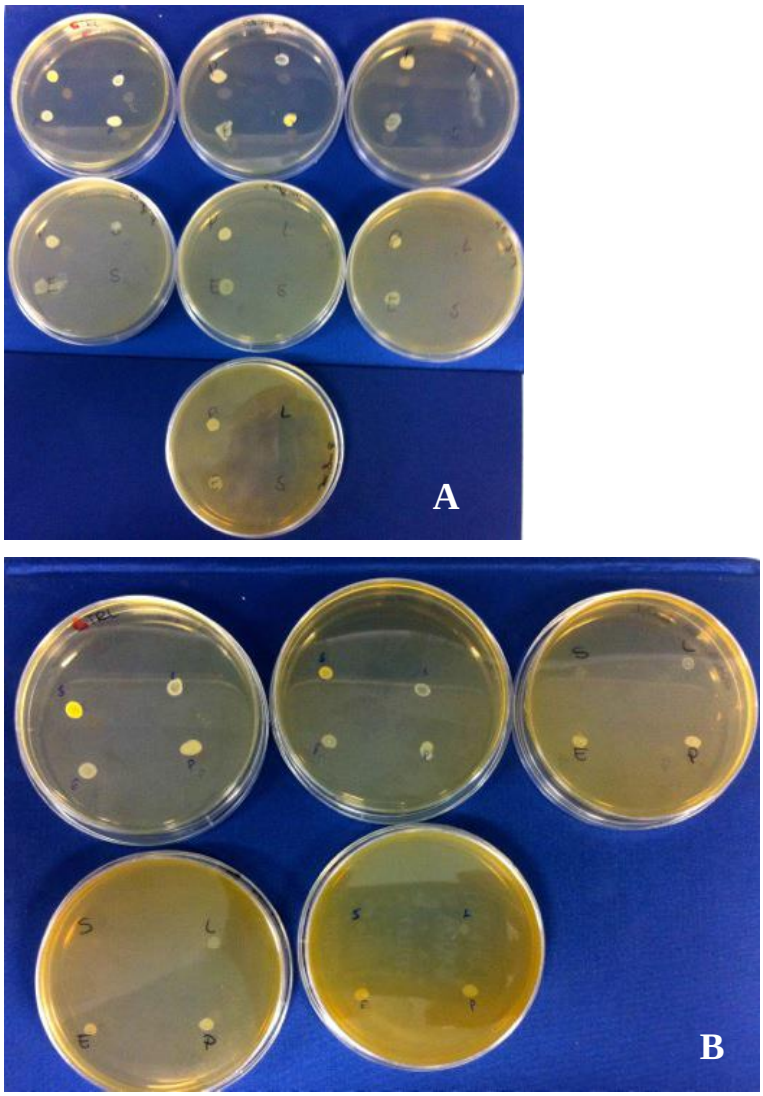

Figure 3.2. Growth of bacterial strains in presence of *P. oceanica* (A) and Green Tea (B) extracts. Concentrations used: 0-0.5-1-1.5-2-2.5-3 g L^{-1} PO; 0-0.5-1-1.5-2 g L^{-1} GT. Strains: L-*Listeria innocua*, S-*Staphylococcus aureus*, E-*Escherichia coli*, P-*Pseudomonas putida*.

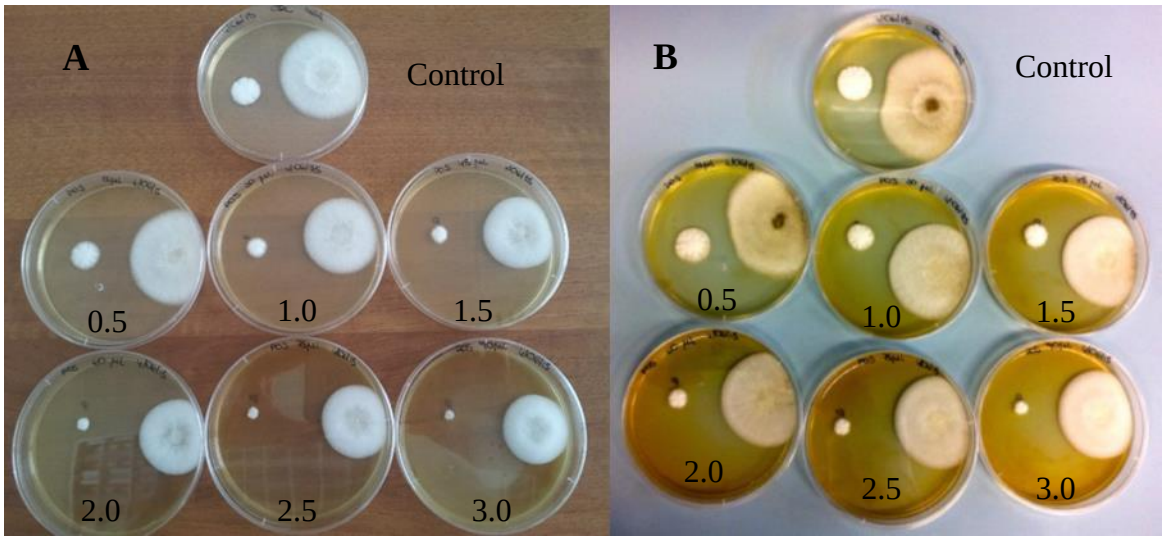

Figure 3.3. Growth after 2 days (A) or 7 days (B) incubation of *Penicillium chrysogenum* (left in each plate) and *Aspergillus niger* (right in each plate) in presence of different concentration of *P. oceanica* extract (from 0.5 to 3.0 g L^{-1}). Control: medium without extract.

3.4.3. Fresh-cut peach storage

GT and PO extracts were chosen for the dipping of fresh cut peach slices: the first of these had the most powerful antioxidant capacity, while the second was chosen for its high polyphenols content and antifungal activity. Fruits are usually quite acid and hence quite resistant to invasion by bacteria. Therefore spoilage of fruit and fruit products is often caused by fungi (Pitt and Hocking, 1999). However, recent studies have documented the exponential growth of bacteria on a variety of fresh-cut fruit (Alegre et al., 2010; John et al., 2013).

In terms of pomological traits, after 7 d storage, TSS content was found almost constant in treated samples of peach slices, while in CTRL samples this value sharply increased up to 11.8 %, mainly from 5 to 7 d (Fig. 3.4A).

Differences of TA content were significant between t 0 and 3 d, then reduced with storage. CTRL samples evidenced a significant decrease from 3 to about 1 g L^{-1}. Peach slices dipped in the two extracts showed a TA decrease of only 17 % with respect to the initial value, but with different time courses: when PO was employed, a sharp decrease of TA in the last 3 d of shelf life was evident, while in samples treated with GT the decrease was evident in the first 3 d.

Note that the sharp decrease of TA in CTRL samples occurred at the same time with the TSS increase in the last 3 d of the shelf life. For the GT treatment, no significant changes were evident in TSS between 3 and 7 d (Fig. 3.4B).

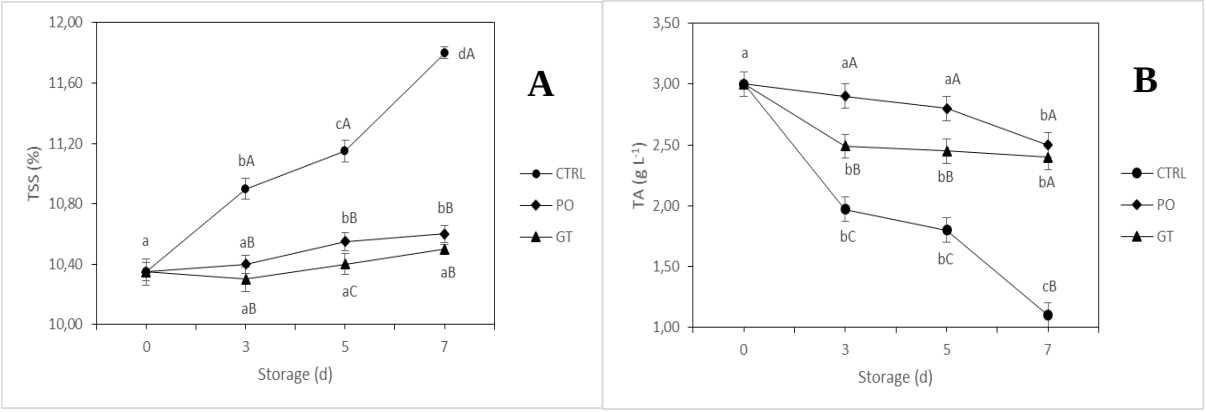

Figure 3.4. Evolution of total soluble solids (%) (A) and titratable acidity (g L^{-1}) (B) in peach (*Prunus persica*) cv. Rich May slices treated with *P. oceanica* (PO), Green Tea (GT) and untreated (CTRL). Data are means ± SE. Minor and capital letters show significant differences ($p \leq 0.05$) for each treatment and among treatments for each storage time, respectively.

After three days, lightness (L*) of peach slices decreased in all treatments (Tab. 3.3). When prolonging the incubation time up to 7 d, lightness decreased much more in CTRL sample rather than in peach slices treated by GT or PO. Caceres et al. (2016) developed a flesh browning assessment methodology for fresh whole peaches stored for a long time, and reported that ΔL* values higher than 21 can be considered symptoms of extreme flesh browning. Even if our data relate to peach slices, ΔL* values calculated at 7 d storage were found higher than 21 only in the control sample.

An indicator of chlorophyll degradation is the a* value, which decreases when color changes from green to red (Martín-Diana et al., 2008). An increase of a* values was only found for PO treatment (Tab. 3.3). This behavior can be attributed to the greenish colour imparted by the PO extract, similarly to what was found by Martín-Diana et al. (2008), after a dipping treatment with natural extracts, which they also correlated to lightness lowering.

The b* parameter indicates the color changes from yellow to blue, and its values decreased in all samples during storage (Tab. 3.3) due to phenolic degradation taking part on tissues (Fuentes-Perez, 2014). However, after 7 d storage, treated samples showed higher values than the control.

Finally, the Chroma decreased after 3 and 5 d storage more rapidly in PO samples compared to GT ones (Tab. 3.3). After 7 d, GT showed a higher value compared with samples dipped in PO.

These results, in accordance with the findings reported by Oms-Oliu et al. (2010), highlighted that dipping treatment after peeling and/or cutting can represent an effective way to control browning phenomena in fresh-cut fruit, since it can affect enzyme activity or substrates availability for

enzymatic degradation. In particular, the high polyphenols content present in both extracts can protect the cut surface of fruit products against oxidative rancidity, degradation and enzymatic browning, thus slowing their senescence process (Rojas-Grau et al., 2009).

Table 3.3. Color parameters changes during storage of fresh cut peach slices treated by *P. oceanica* (PO), Green Tea (GT) and untreated. Data are presented as mean ± SE. Minor and capital letters show significant differences ($p \leq 0.05$) for each treatment and among treatments for each storage time, respectively.

Treatment	Day	Lightness (L*)	a*	b*	C*
	0	64.07 ± 1.30^{a}	-2.22 ± 0.41^{a}	41.56 ± 0.40^{a}	41.58 ± 0.40^{a}
CTRL	3	59.63 ± 0.85^{bA}	-1.04 ± 0.18^{bB}	39.63 ± 0.55^{aA}	39.73 ± 0.54^{aA}
	5	50.01 ± 1.14^{cA}	0.40 ± 0.22^{cB}	29.60 ± 1.63^{bA}	29.61 ± 1.63^{bA}
	7	41.70 ± 0.89^{dB}	1.57 ± 0.27^{dB}	18.96 ± 0.28^{cB}	19.06 ± 0.27^{cB}
PO	3	57.11 ± 0.19^{bB}	-3.15 ± 0.19^{abA}	33.88 ± 0.72^{bB}	34.04 ± 0.71^{bB}
	5	48.69 ± 1.11^{cA}	-1.65 ± 0.40^{bA}	25.92 ± 0.84^{cA}	26.03 ± 0.84^{cA}
	7	42.99 ± 0.62^{dAB}	-0.28 ± 0.41^{cA}	20.05 ± 0.39^{dA}	20.12 ± 0.40^{dAB}
GT	3	55.19 ± 0.79^{bB}	-1.29 ± 0.24^{bB}	39.39 ± 0.45^{aA}	39.42 ± 0.45^{aA}
	5	48.56 ± 0.58^{cA}	0.43 ± 0.41^{cB}	29.02 ± 1.59^{bA}	29.07 ± 1.59^{bA}
	7	44.71 ± 0.68^{dA}	1.24 ± 0.09^{cB}	20.28 ± 0.44^{cA}	20.32 ± 0.44^{cA}

From the microbiological point of view, the applied dipping treatments were found effective in lowering the total aerobic count (TAC) and *Pseudomonas* population present in peach slices of about 0.5 log cfu g^{-1} mainly up to 5 d (Fig. 3.5). This behavior may also be favored by the fruit respiration process (Rojas-Grau et al., 2009). Yeasts and moulds were found significantly lower than the CTRL only at 3 d, with the best performance being shown by peach slices dipped in PO extract. No significant changes were found for the *Enterobacteriaceae* population. These results are in accordance with those reported by Siroli et al. (2014) for minimally processed apples dipped in different antimicrobials comparatively: shelf life of fresh cut fruit is limitedly affected by microbial growth: independently from the addition of natural antimicrobials, the end of shelf life is mainly determined by changes in colour.

Time course of CO_2 and O_2 during storage trials was not determined as it was assumed meaningless because of the high gas permeability and the geometry of the packaging system used. Assuming an oxygen respiration rate of the fruits of about 18 mg kg^{-1} h^{-1} at 10 °C and taking into account

the permeable surface of the package (0.066 m^2), the headspace volume (450 cm^3), the amount of the product (0.045 kg) and the oxygen and carbon dioxide permeabilities (respectively 6200 and 24000 cm^3 m^{-2} d^{-1} bar^{-1}, at 10 °C) using a common model for forecasting atmosphere changes in ready-to-eat vegetables (Piergiovanni et al., 1999) we estimated after 7 d a maximum CO_2 concentration equal to 0.8% and a minimum O_2 concentration of 18%.

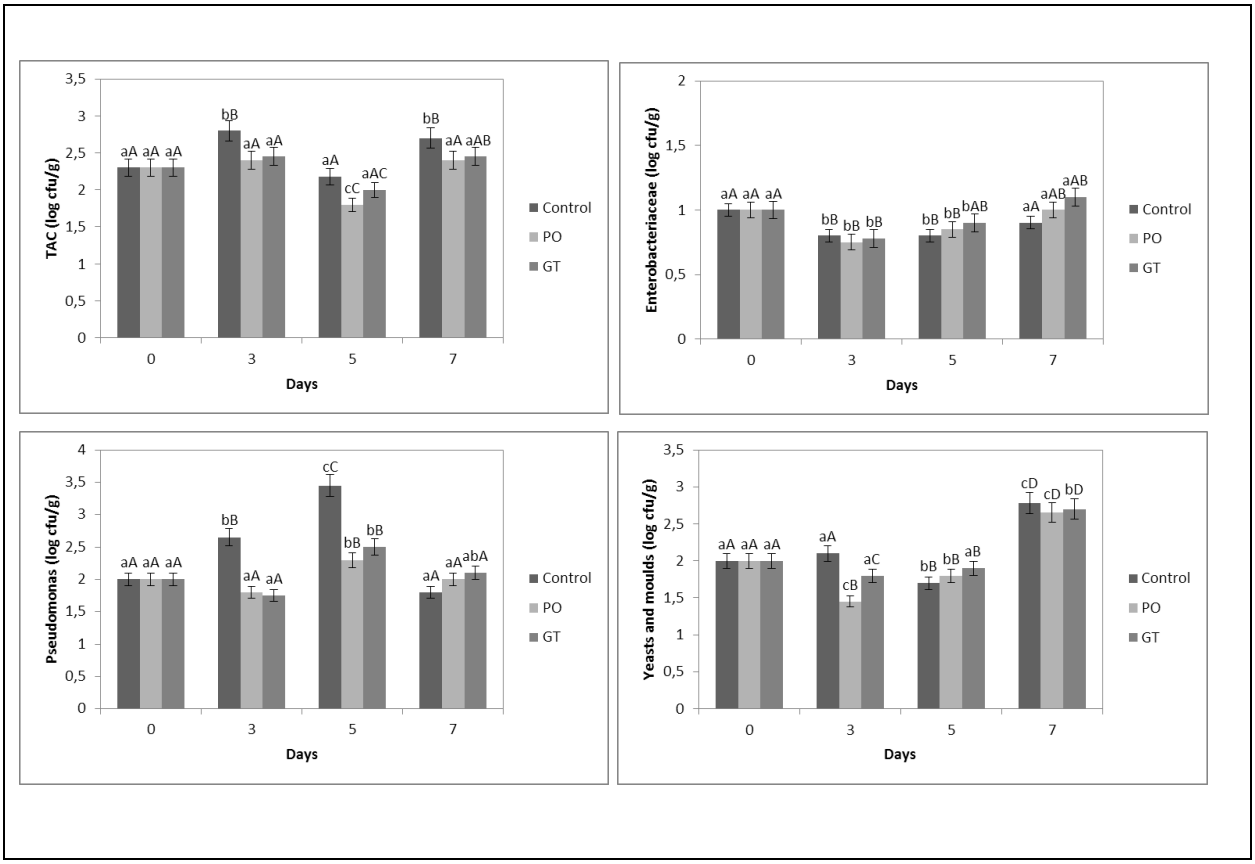

Figure 3.5. Time course of Total Aerobic Count (TAC), *Enterobacteriaceae*, *Pseudomonas* and yeasts and moulds presence (log cfu g^{-1} peach) in samples of peach slices subjected to dipping treatment with *P. oceanica* (PO) and Green Tea (GT) extracts and then stored at 4 °C. CTRL: peach slices dipped in sterile distilled water. Data are means ± SD. Minor and capital letters show significant differences ($p \leq 0.05$) for each treatment and among treatments for each storage time, respectively.

3.5. CONCLUSIONS

In this study *Posidonia oceanica* (PO) and green tea (GT) extracts were applied by dipping on peach slices, once having shown their highest total phenolic content and antifungal activity, as well as the highest antioxidant activity, respectively. Results showed that these natural extracts limited microbial spoilage of fresh-cut peach, especially the *Pseudomonas* population, and maintained the pomological parameters during storage at 4 °C while not modifying their characteristic taste.

Overall, polyphenolic extracts derived from PO and GT could provide an additional post-harvest benefit of fresh-cut produce. To the best of our knowledge, this paper represents the first report on the application of *P. oceanica* extract on fresh-cut fruit, even if this marine protected plant never should be collected from the sea for industrial application.

Although this work relates to the application of natural extracts directly on fresh-cut fruit in a traditional package, future trials will be aimed at setting up innovative active packaging solutions from which these extracts will be released. Further research will be also needed to complement antioxidant activity of plant or other extracts with digestion simulation to assess parameters such as bioaccessibility, bioavailability and *in vivo* antioxidant performance; sensorial analyses should also be performed on treated fruit.

These results can pave the way to the use of innovative natural extracts to be applied on ready-to-eat vegetables, thus improving the attractiveness for consumers of these healthy foods.

Acknowledgments

Authors wish to acknowledge Dr. Lesley Currah for her excellent language revision.

3.6. REFERENCES

Agostini, S., Desjobert. J.M., Pergent, G., 1998. Distribution of phenolic compounds in the seagrass *Posidonia oceanica*. Phytochem. 48, 611–617.

Alegre, I., Abadias, M., Anguera, M., Usall, J., Viñas, I., 2010. Fate of *E. coli* O157:H7, Salmonella and *Listeria innocua* on minimally-processed peaches under different storage conditions. Food Microbiol. 27, 862–868.

Alkan, D., Yemenicioglu, A., 2016. Potential application of natural phenolic antimicrobials and edible film technology against bacterial plant pathogens. Food Hydrocoll. 55, 1-10.

Amani, P., Gadde, L.E., 2015. Shelf life extension and food waste reduction. Proc. Food Syst. Dyn. 7-14.

Balasundram, N., Sundram, K. Samman, S., 2006. Phenolic compounds in plants and agri-industrial by-products: Antioxidant activity, occurrence and potential uses. Food Chem. 99, 191-203.

Bellassoued, K., Hamza, A., Van Pelt. J., Elfeki, A., 2012. Evaluation of cytotoxic compounds in different organs of the sea bream *Sarpa salpa* as related to phytoplankton consumption: an in vitro study in human liver cell lines HepG2 and WRL68. In Vitro Cell. Dev. Biol. Anim. 48, 528-534.

Berfad, M.A., Alnour, T.M.S., 2014. Phytochemical analysis and antibacterial activity of the 5 different extracts from the seagrasses *Posidonia oceanica*. J. Med. Plants Stud. 2, 15-18.

Bernard, P., Pesando, D., 1989. Antibacterial and antifungal activity of extracts from the rhizomes of the Mediterranean seagrass *Posidonia oceanica* (L.) Delile. Bot. Mar. 32, 85-88.

Brand-Williams, W., Cuvelier, M.E., Berset, C., 1995. Use of a free radical method to evaluate antioxidant activity. Food Sci. Technol. 28, 25–30.

Caceres, D., Diaz, M., Shinya, P., Infante, R., 2016. Assessment of peach internal flesh browning through colorimetric measures. Postharv. Biol. Technol. 111, 48-52.

Ceponis, M.J., Cappellini, R.A., Wells, J.M., Lightner, G.W., 1987. Disorders in plum, peach and nectarine shipments to the New York market, 1972–1985. Plant Dis. 71, 947–952.

Cuny, P., Serve, L., Jupin, H., Boudouresque, C.F., 1995. Water soluble phenolic compounds of the marine phanerogam *Posidonia oceanica* in a Mediterranean area colonized by the introduced chlorophyte *Caulerpa taxifolia*. Aquat. Bot. 52, 237–242.

Dantigny, P., Guilmart, A., Radoi, F., Bensoussan, M., Zwietering, M., 2005. Modelling the effect of ethanol on growth rate of food spoilage moulds. Int. J. Food Microbiol. 98, 261-269.

Denoya, G.I., Polenta, G.A., Apostolo, N.M., Budde, C.O., Sancho, A.M., Vaudagna, S.R., 2016. Optimization of high hydrostatic pressure processing for the preservation of minimally processed peach pieces. Innov. Food Sci. Emerg. Technol. 33, 84–93.

Dumay, O., Costa, J., Desjobert, J.M., Pergent, G., 2004. Variations in the concentration of phenolic compounds in the seagrass *Posidonia oceanica* under conditions of competition. Phytochem. 65, 3211–3220.

Foden, J., Brazier, D.P., 2007. Angiosperms (seagrass) within the EU water framework directive: a UK perspective. Mar. Pollut. Bull. 55, 181-195.

Fuentes-Perez, M., Nogales-Delgado, S., Ayuso, M. C., Bohoyo-Gil, D., 2014. Different peach cultivars and their suitability for minimal processing. Czech J. Food Sci. 32, 413,421.

Gokce, G., Haznedaroglu, M.Z., 2008. Evaluation of antidiabetic, antioxidant and vasoprotective effects of *Posidonia oceanica* extract. J. Ethnopharm. 115, 122–130.

Guillén, F., Díaz-Mula, H.M., Zapata, P.J., Valero, D., Serrano, M., Castillo, S., Martínez-Romero, D., 2013. *Aloe arborescens* and *Aloe vera* gels as coatings in delaying postharvest ripening in peach and plum fruit. Postharvest Biol. Technol. 83, 54-57.

Gyawali, R., Ibrahim, S.A., 2014. Natural products as antimicrobial agents. Food Control. 46, 412-429.

Janeiro, P., Brett, A.M.O., 2004. Catechin electrochemical oxidation mechanisms. Anal. Chim. Acta 518, 109-115.

Jayaprakasha, G.K., Selvi, T., Sakariah, K.K., 2003. Antibacterial and antioxidant activities of grape (*Vitis vinifera*) seed extracts. Food Res. Int. 36, 117-122.

John, A.P., Robert, M.H., Tracy, A., Robert, V.T., Christopher, R.B., Frederick, J.A., Patricia, M.G., 2013. Attribution of foodborne illnesses, hospitalizations, and deaths to food

commodities by using outbreak data, United States, 1998-2008. Emerg. Infect. Dis. J. 19, 407-415.

Kader, A.A., Mitchell, F.G., 1989. Postharvest physiology. In: LaRue, J.H., Johnson, R.S., (Eds), Peaches, Plums and Nectarines: Growing and Handling for Fresh Market. Publication No. 3331. University of California, Division of Agriculture and Natural Resources. Oakland (USA), pp. 158–164.

Kusmita, L., Puspitaningrum, I., Limantara, L., 2015. Identification, isolation and antioxidant activity of pheophytin from Green Tea (*Camellia sinensis* (L.) Kuntze). Proc. Chem. 14, 232-238.

Lan-Sook, L., Sang-Hee, K., Young-Boong, K., Young-Chan, K., 2014. Quantitative analysis of major constituents in green tea with different plucking periods and their antioxidant activity. Mol. 19, 9173-9186. [Is that abbreviated journal name adequate?]

Lung, J., Zhao, Y., 2016. Antimicrobial packaging for fresh and minimally processed fruits and vegetables, in: Barros-Velasquez, J., (Eds.), Antimicrobial Food Packaging. Elsevier, UK, pp. 243-256.

Martín-Diana, A.B., Rico, D., Barry-Ryan, C., 2008. Green tea extract as a natural antioxidant to extend the shelf life of fresh-cut lettuce. Innov. Food Sci. and Emerg. Technol. 9, 593–603.

Mascheroni, E., Figoli, A., Musatti, A., Limbo, S., Drioli, E., Suevo, R., Talarico, S., Rollini, M. (2014) An alternative encapsulation approach for production of active chitosan - propolis beads. Int. J. Food Sci. Technol. 49, 1401-1407.

Mensor, L., Menezes, F., Leitao, G., Reis, A., Dos Santos, T., Coube, C., Leitao, S., 2001. Screening of Brazilian plant extracts for antioxidant activity by the use of DPPH free radical method. Phytother. Res. 15, 127-130.

Mitchell, F.G., Kader, A.A., 1989. Factors affecting deterioration rate, in: LaRue, J.H., Johnson, R.S., (Eds) Peaches, Plums Nectarines: Growing and Handling for Fresh Market. Publication No. 3331. University of California, Division of Agriculture and Natural Resources. Oakland, (USA), pp. 165–178.

Oms-Oliu, G., Odriozola-Serrano, I., Soliva-Fortuny, R., Elez-Martínez P., Martín-Belloso, O., 2012. Stability of health-related compounds in plant foods through the application of non thermal processes. Trends Food Sci. Technol. 23, 111–123.

Oms-Oliu, G., Rojas-Graü, M.A., Alandes González, L., Varela, P., Soliva-Fortuny, R., Hernando Hernando, M.I., Pérez Munuera, I., Fiszman, S., Martín-Belloso, O., 2010. Recent approaches using chemical treatments to preserve quality of fresh-cut fruit: A review. Postharvest Biol. Technol. 57, 139-148.

Pandey, K.B., Rizvi, S.I., 2009. Plant polyphenols as dietary antioxidants in human health and disease. Oxid. Med. Cell. Longev. 2, 270-278.

Perumalla, A.V.S., Hettiarachchy, N.S., 2011. Green tea and grape seed extracts—Potential applications in food safety and quality. Food Res. Int. 44, 827-839.

Piergiovanni, L., Fava, P., Ceriani, S., 1999. A simplified procedure to determine the respiration rate of minimally processed vegetables in flexible permeable packaging. Ital. J. Food Sci. 11, 99–110.

Pitt, J., Hocking, A.D., 1999. Fungi and Food Spoilage, ed. Aspen Publishers Inc., Gaithersburg, pp. 529.

Poudel, P.R., Tamura, H., Kataoka, I., Mochioka, R., 2008. Phenolic compounds and antioxidant activities of skins and seeds of five wild grapes and two hybrids native to Japan. J. Food Compos. Anal. 21, 622-625.

Rojas-Grau, M.A., Oms-Oliu, G., Soliva-Fortuny, R., Martin-Belloso, O., 2009. The use of packaging techniques to maintain freshness in fresh-cut fruits and vegetables: a review. Int. J. Food Sci. Technol. 44, 875-889.

Scalbert, A., Monties, B., Janin, G., 1989. Tannins in wood: comparison of different estimation methods. J. Agric. Food Chem. 37, 1324-1329.

Siroli, L., Patrignani, F., Serrazanetti, D.I., Tabanelli, G., Montanari, C., Tappi, S., Rocculi, P., Gardini, F, Lanciotti, R., 2014. Efficacy of natural antimicrobials to prolong the shelf life of minimally processed apples packaged in modified atmosphere. Food Cont. 46, 403-411.

Sutherland, B.A., Rahaman, R.M.A., Appleton, I., 2006. Mechanism of action of green tea catechins with a focus on ischemia-induced [something missing here?] . J. Nutr. Biochem. 17, 291-306.

4. CHAPTER II:

Development and characterization of paper pad coated by chitosan-tetrahydrocurcumin (THC) mix and its application on fresh-cut pineapple (*Ananas comosus* L. Merr.)

(Main Author of the article Submitted to Postharvest Biology and Technology)

4.1. ABSTRACT

The aim of this work was to develop a new cellulose-based active packaging added with chitosan and tetrahydrocurcumin (THC), an antioxidant compound. The two substances were incorporated in paper either by mass or as a coating. Produced paper pads were analyzed to determine their polyphenols content, as well as their antioxidant and *in vitro* antimicrobial activities. A good EC_{50} of 4.49 mg/L and a polyphenols concentration of 0.8 % were found for THC, which was also found to be able to slowdown the growth of molds. Afterwards, the best performant combination of active paper, consisting of commercial paper coated by 10 % of THC and 3 % of chitosan was applied to fresh-cut pineapple in storage trials at 4°C (*Ananas comosus* L. Merr.). Color changes, browning potential, weight loss, pomological traits and microbiological activity were analyzed and compared with untreated, naked samples. After 7 d of storage, L* was preserved by paper pad action as confirmed by the ΔE, higher on treated sample (3.58) respect to the control (4.24). Browning was lower in treated samples (0.185 A), than in the control (0.250 A), confirming THC antioxidant action. Also for yeast and molds and total microbial counts, better results were obtained on pineapple stored in presence of the active pad.

KEYWORDS: active packaging, ready-to-eat pineapple, THC, natural antimicrobial, natural antioxidant.

4.2. INTRODUCTION

Fresh-cut fruit is among the most widely perishable food product. The major causes of degradation are microbiological spoilage and reactions caused by the presence of oxygen, such as enzymatic browning or oxidation reactions. Fresh-cut fruit faster decay than whole fruit is mainly due to the cutting action that breaks cells causing juice leakage, perfect substrate for microorganism growth and enzymatic activity. These processes lead to an acceleration of fruit metabolic response, thus increasing its respiration rate and decay (Raybaudi-Massilia, et al., 2009).

Preservation of fresh food is one of the biggest challenges faced by food industry. Researches are driven to maintain high food quality during storage as long as possible (Guerreiro et al., 2015; Rana et al., 2015; Roopa et al., 2015). One way to achieve this goal is the use of active packaging solutions. An active package involves the use of materials able to absorb or release substances in order to improve food quality or to extend food shelf life (EFSA, 2016).

One of the actual trend in food industry is the use of natural materials, also because consumers ask for natural and renewable compounds. Contrarily to all kinds of plastic materials, cellulose is the most abundant biodegradable polymer found in nature and therefore perfectly safe for the environment (Khwaldia et al., 2010).

Several studies focused on production and characterization of paper containing antioxidant and/or antimicrobial substances to obtain active packaging solutions (Barbiroli et al., 2012; Khwaldia et al., 2010; Bordenave et al., 2007). In order to obtain an entirely natural packaging, active compounds found in nature can be used for their specific properties. These molecules should present peculiar activity that can be used to avoid food degradation (Piva et al., 2017; Mascheroni et al., 2014).

Tetrahydrocurcumin (THC) is a colorless and odorless derivative of curcumin, traditionally used either as spice and food coloring in Asian cooking. Curcumin, or diferuloylmethane, is a yellow

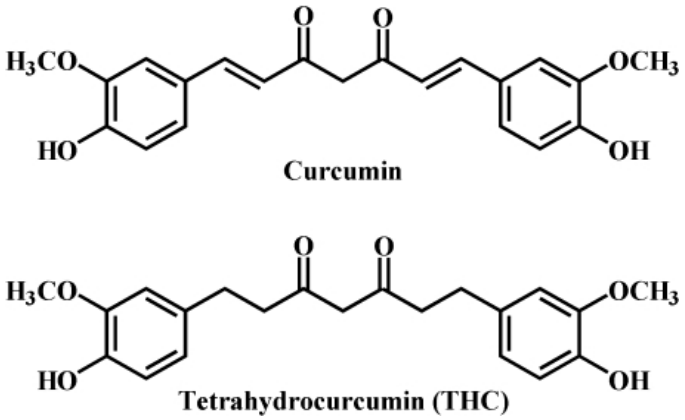

Figure 4.1. Chemical structures of Curcumin (above) and (Tetrahydrocurcumin (below).

crystalline substance that is isolated from turmeric (*Curcuma longa*). It is known to exhibit antioxidant, anti-inflammatory, antibacterial and neuroprotective properties (Aggarwal et al., 2015).

In a study of the metabolism of curcumin in human intestine, curcumin underwent extensive reduction in the gastrointestinal tract, with THC being the major metabolite of curcumin (Ireson et al., 2002). THC polyphenolic structure includes two aromatic rings (Fig. 4.1) and can be synthetized by hydrogenation of curcumin (Majeed et al., 1995). In *vivo*, THC is the major metabolite of curcumin, and takes part in the antioxidant metabolism (Portes et al., 2007). THC also possesses positive physiological effects, such as antioxidant, antidiabetic and neuroprotective properties (Murugan & Pari, 2006; Aggarval et al., 2015; Rajeswari & Sabesan, 2008).

Chitosan is a high molecular mass linear copolymer of N-acetyl-D-glucosamine and D-glucosamine units linked by β (1-4), obtained by the partial hydrolysis of the N-acetyl groups of chitin (Rinaudo, 2006). Chitosan is known to possess antimicrobial activity against a wide range of microorganisms (yeasts, moulds and bacteria) but its efficacy can vary considerably: in particular, a degree of polymerization of at least seven monomeric units is required to get significant antibacterial effect (Dutta et al., 2009; Goy et al., 2009; Coma, 2013). Chitosan charged reactive groups can also be exploited to form electrostatic interactions with biologically active molecules, i.e. polyphenols. Studies report that in association with chitosan, THC can form a film that exhibits antioxidant and antibacterial activities (Portes et al., 2009). Chitosan is also able to impart good mechanical properties to paper (Elsabee & Abdou, 2013).

In this study, we combined THC and chitosan in a paper-based material to develop an innovative active package. THC was added to the cellulose matrix in two different ways comparatively: incorporation or coating. Papers containing these natural active compounds were first tested

employing chemical, *in vitro* microbiological and mechanical assays; the best performing paper was then applied as a pad on fresh-cut pineapple with the goal of delaying fruit quality decay. Several studies exist on storage preservation of fresh-cut produce, nevertheless few report on ready-to-eat pineapple, characterized by a shelf life of 5-7 days (Montero-Calderon et al., 2008). The aims of this study were (1) to better underline THC *in vitro* antioxidant and antimicrobial activities; (2) to formulate and select an active papermaking process to obtain the best chemical, antimicrobial and mechanical paper properties. To authors' best knowledge this is the first report on the use of THC in the food area.

4.3. MATERIALS AND METHODS

4.3.1. Chemicals

Ethanol (≥99.8%), Folin-Ciocalteu's phenol reagent, 2,2-Diphenyl-1-picrylhydrazyl (DPPH), Gallic acid monohydrate (≥98.0%), (±)-6-Hydroxy-2,5,7,8-tetramethylchromane-2-carboxylic acid (Trolox) 97%, hydrochloric acid and sodium hydroxide were purchased from Sigma–Aldrich (Gallarate, MI, Italy).

Chitosan (Chitoclear - 3.38x105 Mw and 80% of Deacetylation degree) was obtained from Giusto Faravelli Spa (Milano, Italia). Tetrahydrocurcumin syntheses were obtained as reported (Portes et al., 2007).

4.3.2. THC antioxidant assay

Antioxidant power of TCH was determined through the DPPH assay, apply the method of Brand-Williams et al. (1995) with some modifications. The DPPH solution was diluted in absolute ethanol to obtain 1.00 ± 0.03 absorbance units at 515 nm. Samples to analyze were dissolved (20 g L^{-1}) in 70 % ethanol (v/v) and, after centrifugation, serially diluted. The DPPH solution (2.94 mL) was placed in a cuvette where a 60 µL sample was added. Absorbance readings were carried out after incubation for 50 min at 20 ± 1°C. A calibration curve was prepared employing increasing concentrations of Trolox ranged from 50 to 1000 µM; each concentration was assayed in triplicate. Results were expressed as mol Trolox per 100 g dry weight. Each formulation was analyzed in triplicate. The antioxidant capacity was expressed as EC_{50}, defined as the concentration of the sample leading to 50% reduction of the initial DPPH concentration, was obtained from the linear regression of plots of mean percentage of the antioxidant activity against the concentration of the test extracts (µg/ml) obtained from three replicate assays.

A cellulosic pulp was used as a basic material, composed by 64% bleached ECF Eucalyptus chemical pulp (BAHIA SUL) and 36% bleached softwood chemical pulp (BOWATER). Carboxymethylcellulose (CMC), water-soluble derivative of cellulose, was added (5% on fiber) to paper to improve its mechanical properties and facilitate molecules retention: thanks to its negative charges, CMC creates interactions with chitosan.

Polyamidoamine-epichlorohydrin resin (PAAE) is a common additive in paper production. It is used to improve the permanent wet strength of paper (2.5% on fiber).

Paper production

The paper was produced thanks to a lab-scaled sheet former sheet former Rapid Köthen (ESTANIT GmbH) according to ISO 5269-2:2004. First, the cellulosic pulp was soaked in water. Depending on the formulation, different components were added to the pulp and mixed well during 15 min (Tab. 4.1). Then the slurry was introduced in the sheet former. The machine is able to create a whirling of the suspension, and then to vacuum water through a sieve. The thin and uniform layer is placed between two special paper sheets, and then dried at 92°C for 7 min under vacuum. The final grammage of 60 g/m^2 was obtained by measuring precisely the quantity of slurry used for each sheet.

Table 4.1. Composition of papers in which THC is incorporated in mass. (pH values are ± SD)

Sample	**CMC (5% on fiber)**	**Chitosan/PAAE (2.5% on fiber)**	**Concentration of THC (% on fiber)**	**pH**
CHIT 01	CMC	Chitosan	-	5.61 ± 0.09
CHIT 1.5-8	CMC	Chitosan	1.5	8.46 ± 0.11
CHIT 1.5-4	CMC	Chitosan	1.5	4.00 ± 0.09
CHIT 3-4	CMC	Chitosan	3.0	4.04 ± 0.08
CHEM	CMC	PAAE	1.5	8.32 ± 0.10

In the case of THC-chitosan coated paper production, coating solutions were applied on either commercial food grade wet-resistant commercial paper (Burgo Group Spa, Vicenza, Italia) and paper samples produced as previously reported. Chitosan solution was prepared dissolving chitosan (6% w/v) in a diluted acetic acid solution (2 % w/v). THC solution was prepared (20 % w/v) in absolute ethanol. The two solutions were singularly stirred for 1 h at 25 °C and then mixed at 1:1 (v/v) ratio in order to obtain the desired concentrations, as reported in table 4.2.

Table 4.2. Paper samples produced with the coating technique: chitosan and THC concentration in the coating solution.

Sample	Basis	Chitosan concentration (% on coating solution)	THC concentration (% on coating solution)
Coating 3-10 comm	Commercial paper	3	10
Coating 3-10 chit	CHIT 11	3	10
Coating 3-5 comm	Commercial paper	3	5
Coating 3-5 chit	CHIT 11	3	5

A coating applicator was used (model 1137, Sheen Instruments, Kingston, UK); deposition occurred at speed of 2.5 mm/s. Coated papers were then dried for 30 min by a continuous air flux at 25 ± 0.3 °C. Paper were cut in strips (11 x 7 cm) (Fig. 4.2) and stored into desiccator until the application on fresh-cut fruit (Fig. 4.2).

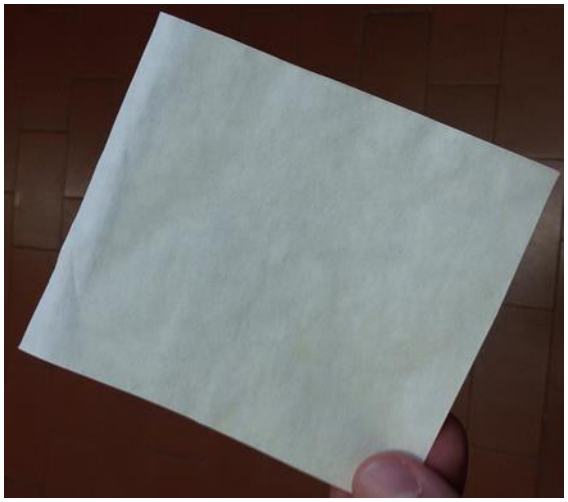

Figure 4.2. Strips of Active paper pad.

4.3.3. Physico-chemical analysis of the active paper samples

Physical analysis

Paper grammage and dry tensile strength were measured according to ISO 536: 2012 and ISO 1924-2:2008 respectively. Wet tensile strength was measured after dipping the paper into distilled H_2O for 2 h according to ISO 3781:2011. All measurements were performed in a controlled atmosphere at 23 °C and 50% R.H.

Chemical analysis

THC contained in paper samples was extracted as follows: three paper disks for each kind of paper were cut and placed in 1 mL of absolute ethanol under overnight stirring at room temperature. Then vials were placed under ultra sounds for 10 min. The liquid fraction was subjected to the determination of total phenols (TP), estimated by the Folin-Ciocalteau method (Scalbert et al., 1989). Aliquots of the liquid fraction were dissolved in 50% (v/v) methanol/water and appropriately diluted (1:2.5, 1:5 and 1:10 v/v) in the same solvent. The Folin-Ciocalteau reagent was 10-fold diluted in water (v/v) and 2.5 mL were added to each 0.5 mL sample. Two milliliters of 75 g L^{-1} sodium carbonate solution were added and tubes kept for 1 h at 20 ± 1°C in the dark. In the meanwhile, the calibration curve for gallic acid (5-100 mg L^{-1}) dissolved in 50% (v/v) methanol/water was achieved. The absorbance at 765 nm was measured and results were expressed as g gallic acid/100 g paper. Each formulation was analyzed in triplicate.
DPPH was used to determine the antioxidant power of paper samples. For each paper production, strips (1 x 3 cm) were weighed and plunged in 3 mL of 90 µM DPPH solution in absolute ethanol. After 2 h, strips were removed and absorbance of the solution were measured at 515 nm. Results are expressed as the percentage of DPPH scavenged.

4.3.4. *In vitro* microbiological analysis

Four strains of bacteria were chosen from official collections, i.e. *Escherichia coli* CECT 434 (Spanish Type Culture Collection), *Listeria innocua* DSM 20649 (Deutsche Sammlung von Mikroorganismen und Zellkulturen), *Pseudomonas putida* ATCC 12633 (American Type Culture Collection), *Staphylococcus aureus* ATCC 29213. Those strains play an important role in food contamination and are among the most common spoilage and/or pathogen microorganisms that might be present in fresh food products (Mascheroni et al., 2014).
As regards the determination of THC antibacterial activity, different THC concentration solutions, prepared by dissolving the compound in a mixture absolute ethanol:water 70:30, were added to liquid Tryptic Soy Agar (Merck, Darmstadt, Germany) before solidification, in order to obtain culture media with THC concentration ranging from 0.3 to 1.2 g L^{-1}. After pouring into plate, drops (3 µL) of fresh bacterial cultures (OD 600 nm: 0.400 ± 0.100) were deposited on the surface of each solidified medium. Four strains were employed, i.e. two Gram positive (*Staphylococcus aureus* and *Listeria innocua*) and two Gram negative (*Escherichia coli* and *Pseudomonas putida*) bacteria. Bacterial growth was observed after 24 h incubation at 30°C. For each THC

concentration, negative controls were also set-up by adding only the solvent solution without THC in culture media.

To determine the antimicrobial activity of paper samples, bacteria were inoculated in liquid TSA medium before solidification (150 µL of an overnight culture in 15 mL medium). After solidification, paper discs were placed on the surface of the medium. After 24 h incubation at 30°C, paper discs were peeled off and the absorbance of the solid culture was measured at 600 nm employing a spectrophotometer (Lambda 25 Perkin Elmer, MA). An increase in absorbance is related to microbial growth, thus indicating the absence of an antimicrobial activity. For each strain solid cultures were incubated in absence of paper discs (negative control), to determine the maximum turbidity reached by each strains in absence of any antimicrobial compound; the difference between this value and the absorbance reached in presence of an active paper sample allows to estimate the inhibition caused by the antimicrobial compound contained in paper.

4.3.5. Application of the active paper on fresh-cut pineapple

In accordance to the *in vitro* analysis, trials were carried out employing paper produced from commercial paper coated by chitosan and THC (3 and 10 %, respectively).

Fresh pineapples (*Ananas comosus* L. Merr. cv. "Super Sweet") were purchased at the wholesale market (3 kg) and immediately processed. Fruit were homogeneous in ripening (13.05 ± 0.17 °Brix); they were hand-peeled, pre-washed with distilled water and sanitized for 2 min in chlorinated water (150 mg L^{-1} sodium hypochlorite), rinsed with distilled water and gently dried by hand. Pineapples without skin were cut into slices of about 1.5 cm thickness, and the obtained slices cut to obtain half-slices (70 ± 3 g each) using a sterile stainless-steel knife. Three slices (210 ± 9 g) were placed onto PET trays (19 x 12 x 4 cm). In trials with the active paper (PAD), 4 active papers (11 x 7 cm), were put under, among and on top of the slices (Fig. 4.3). Samples were packed into low-density polyethylene (LDPE) bags (22 x 15 x 6 cm, 25 µm thickness, bag volume 600 mL, ratio between fruit weight and container volume 100 g L^{-1}, surface film for each bag 660 cm^2,

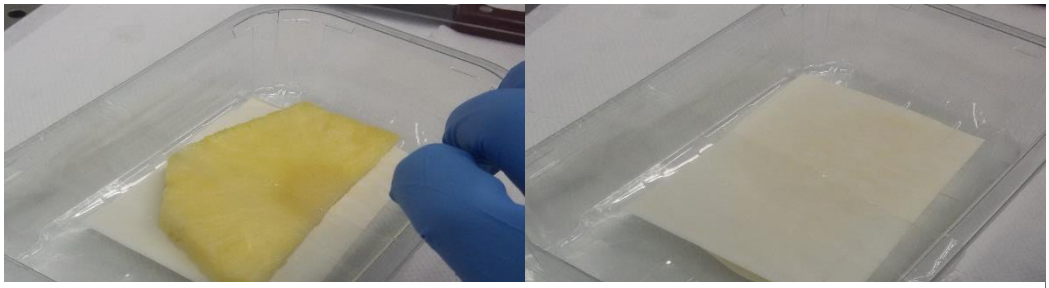

Figure 4.3. Preparation of the treated samples. The active papers were put among the slices of pineapple.

O_2 permeability 6200 cm^3 m^{-2} d^{-1} bar^{-1}, CO_2 permeability 24000 cm^3 m^{-2} d^{-1} bar^{-1} at 10 °C). Packs were all stored at 4 ± 1 °C up to 7 d. A total number of 48 packs were prepared, 24 used for color evaluation, and the remaining ones for the other analyses. Samples were then collected after 0, 2, 4 and 7 d. Each trial at each day was carried out in duplicate.

4.3.6. Color evaluation of pineapple samples

Flesh colour was evaluated using the CIE L*a*b* System by a Minolta CR-300 chromameter (Konica Minolta Sensing, Inc., Japan). Three measure

ments were performed on each side of slices. The instrument was calibrated using a standard white plate. The ΔE was calculated as follows (1):

$$\Delta E = [(\Delta L^{*2}) + (\Delta a^{*2}) + (\Delta b^{*2})]^{1/2} \quad (1)$$

where ΔL*, Δa* and Δb* were obtained from the differences among daily measures of L*, a* and b* during the 7 d of storage.

4.3.7. Physico-chemical analysis of pineapple samples

Weight loss (WL %) of pineapple samples were calculated by the difference between the initial and the actual weight. The measures were carried out after 2, 4 and 7 d of storage. Results were calculated as follows (2):

$$WL\ (\%) = \frac{(\mathrm{Wi}-\mathrm{Wf})}{\mathrm{Wi}} \mathrm{x}\ 100 \quad (2)$$

where Wi is the weight at the beginning of the experiment and Wf is the weight measured during storage.

Total soluble solids (TSS, %) and titratable acidity (TA, g L^{-1}) were measured on the juice obtained from slices (100 g for each sample) by an electronic blender (Ariete, Italy). TSS were determined by a digital refractometer (Atago Co., Ltd, Tokyo, Japan model PR-32), while TA was determined by titrating 1:10 diluted juice using sodium hydroxide 0.1 M by an automatic titrator (Compact 44-00, Crison Instruments, SA, Barcelona, Spain).

Total phenolic content (TPC) were determined by the method of Slinkard and Singleton (1977) with Folin-Ciocalteu reagent using gallic acid as a standard. Absorbance was measured at 765 nm by spectrophotometer (Lambda 25 Perkin Elmer, MA). Results were expressed as mg gallic acid equivalents (GAE) per 100 g of fresh pineapple.

4.3.8. Browning potential of pineapple samples

Browning potential (BP) was measured using the method reported by Souza et al. (2014), at t0 and after 2, 4 and 7 days of storage. 2 g pineapple slices were homogenized with 5 mL ethanol for 2 min at 13.500 rpm by Ultra-Turrax (DI25 IKA Works, Germany); obtained homogenate was centrifuged for 20 min at 4.000 rpm (Centrifuge Rotofix 32A, Hettich, Germany) and the supernatant was filtered through Whatman 4 filter paper (Whatman Intl., UK). On the filtered supernatant the absorbance was measured at 420 nm by spectrophotometer (Lambda 25 Perkin Elmer, MA). Results were expressed as browning potential (BP). For each sample, results were obtained from 5 replicates.

4.3.9. Evaluation of the microbial population of pineapple samples

Microbiological analyses were carried out at days 0, 2, 4 and 7 of storage period. 10 g of flesh pineapple were transferred aseptically into a Stomacher bag (400 mL PE, Barloworld, France) containing 135 mL of sterile peptoned water (10 g L^{-1} bacteriological peptone, Costantino, Italy) and blended in a Stomacher (Star Blender LB 400, Biosystem, Belgium) at high speed for 3 min. Ten-fold dilution series of the obtained suspensions were made of the same solution for plating. The following culture media were used: Nutrient Agar (Merck, Germany) for mesophiles, and MEA (Malt Extract Agar) for yeasts and fungi. Colonies were counted after incubation at 30 °C for 24 h for mesophiles, 30 °C for 5 d for yeasts and fungi. Counts were performed in triplicate and reported as logarithm of the number of colony forming units (log cfu g^{-1} pineapple), and means and standard deviations (SD) were calculated.

4.3.10. Statistical analysis

Statistical analysis was carried out using the STATISTICA 7.1 software package (Statsoft Inc., Tulsa, OK, USA). One-way analysis of variance (ANOVA) was performed on mean values and Tukey's test was carried out for the comparison of difference among treatments for each storage time and for each treatment during storage. Differences were considered significant at $p \leq 0.05$.

4.4. RESULTS AND DISCUSSION

4.4.1. *In vitro* THC and paper pad performances

EC_{50} value of THC was 4.49 ± 0.13 mg L^{-1}, lower than the antioxidant power of Trolox (2.86 mg L^{-1}), but still considered as good (Tab. 4.3).

Table 4.3. Antioxidant activity (EC_{50}) of some common plant extracts and flavonoids.

Plant extracts and flavonoids	**EC_{50} (mg L^{-1})**	**Source**
Ocimum basilicum L.	4.78	Souri et al., 2008
Catechin	4.80	Choi et al., 2002
Quercetin	8.10	Choi et al., 2002

The minimal inhibitory concentration (MIC) of THC was 0.4 g L^{-1} for Gram positive bacteria and higher than 0.6 g L^{-1} for Gram negative; for these last microorganisms the water/ethanol mix in which THC was dissolved showed an antimicrobial activity when added to culture; above THC concentration higher than 0.6 g L^{-1}, it was not possible to distinguish an antimicrobial activity a result of the presence of THC or of the solvent. The determination of MIC showed that THC has an interesting antimicrobial activity. In addition to its antioxidant power and antimicrobial property, THC has a natural origin, thus can be considered a suitable molecule for active packaging applications, especially for biobased material to be in contact with food.

When incorporated, THC did not affect either paper odor or color. Grammage as well as paper dry and wet strength values were significantly higher in samples produced with the synthetic PAAE resin, compared to samples produced with chitosan (Tab. 4.4). The addition of THC did not significantly modify mechanical properties.

Table 4.4. Mechanical properties of paper samples produced by chitosan and THC incorporation. Data are means ± SD. Minor letters show significant differences ($p \leq 0.05$) among treatments.

	Paper with **synthetic resin PAAE**	Paper **with chitosan without THC**	Paper **with chitosan with THC**
Grammage (g/m^2)	59.1 ± 1.7^b	64.5 ± 1.2^a	66.9 ± 2.8^a
Dry tensile strength ($Nm\ g^{-1}$)	82.8 ± 3.9^a	69.9 ± 5.0^b	71.4 ± 4.0^b
Wet tensile strength ($Nm\ g^{-1}$)	20.8 ± 0.8^a	5.5 ± 0.6^b	6.1 ± 0.8^b

About polyphenols determination, results showed that in any case extraction solutions did not contain polyphenols. This behavior showed that polyphenols contained in paper were not released, maybe due to the fact that they are strongly linked to other matrix components, such as chitosan. Nevertheless, all papers evidenced antioxidant power (Table 4.5). Antioxidant property of papers prepared by incorporating THC was found related to papermaking conditions, in particular pH could be around 5 to obtain the maximal antioxidant power. Indeed, chitosan exhibits more ionic charges at an acidic pH, probably resulting in a higher capacity of creating ionic linkage thus improving THC retention. When chitosan was substituted with the PAAE resin, the antioxidant activity was also good, at almost neutral pH. Note also that when THC concentration was doubled (from 1.5 to 3%), the scavenging activity was found 4 times higher (from 17 to 80%).

Data related to the coated paper samples evidenced that when THC was coated at 5% onto THC incorporated paper, the global THC activity increased compared to the coating on commercial paper (57 *vs.* 41%). However, this difference disappeared when THC level in the coating solution reached 10%, leading to the conclusion that when polyphenols concentration inside the coating is high, THC incorporation in paper mass can be avoided.

By combining all the results obtained by the chemical analyzes, it can be concluded that even if polyphenols are linked to the paper matrix and cannot be extracted, they still exhibit antioxidant properties.

Table 4.5. Antioxidant activity of papers where THC was incorporated in mass (CHIT series) or coated (COAT) onto paper.

Sample	Scavenging (%)
CHIT 01	2
CHIT 1.5-8	15
CHIT 1.5-4	17
CHIT 3-4	80
CHEM *	24
COAT 3-10 comm	72
COAT 3-10 chit	72
COAT 3-5 comm	41
COAT 3-5 chit	57

* Paper sample produced with the PAAE resin without chitosan.

Antimicrobial analysis of the active papers (Tab. 4.6) evidenced that CHIT01, paper produced by incorporating only chitosan, exhibited an antimicrobial activity, with a maximal effect on *L. innocua* and *S. aureus* (Δ CHIT 01: 0,47). Paper sample produced by incorporating THC (sample CHIT1.5-8) did not show any increase of antimicrobial effect compared to chitosan only paper. On the contrary, samples produced by the coating technique evidenced higher Δ Absorbance, in particular for the sample COAT 3-10 comm, produced with the highest THC concentration against the two Gram positive bacteria *S. aureus* and *L. innocua* (Δ OD: 0.52-0.53).

Table 4.6. Absorbance values (OD 600 nm) of culture media inoculated with different strains after 24 h incubation at 30 °C in presence of the active paper samples. Coefficientof variation in the range of 2-10%).

Absorbance at 600 nm	*P. putida*	*E. coli*	*S. aureus*	*L. innocua*
Maximal growth	0,607	1,021	1,133	0,784
CHIT 01	0,493	0,719	0,757	0,310
CHIT 1.5-8	-	0,783	0,832	0,393
COAT 3-10 comm	0,362	0,756	0,611	0,254
COAT 3-10 chit	0,530	0,548	0,821	0,373
Δ* CHIT 01	0,11	0,30	0,38	0,47
Δ CHIT 1.5-8	-	0,24	0,30	0,39
Δ COAT 3-10 comm	0,25	0,26	0,52	0,53
Δ COAT 3-10 chit	0,08	0,47	0,31	0,41

*Δ: calculated as difference in absorbance between the OD related to the maximal growth and the OD related to the growth in presence of the active paper. Higher Δ value, greater the inhibition.

On the overall, results highlighted that active papers produced by coating chitosan and THC exhibit the highest antimicrobial activity. This finding can be explained by the fact the THC and chitosan being concentrated on the surface of paper samples are in contact with microorganisms, and can better exert their antimicrobial activity. Although direct incorporation of antimicrobials inside the polymer matrix has been demonstrated an effective strategy, losses and/or inactivation during the papermaking process still represents the main drawback (Barbiroli et al., 2012). The efficacy of the coating technique *vs.* direct mass incorporation in influencing antimicrobial activity of active packages has already been reported in the literature (Barbiroli et al., 2016).

The obtained results can be related to previous studies dealing with the antimicrobial effect of chitosan. Portes et al. (2009), tested the association between chitosan and THC in a film and evidenced an antilisterial effect. Liu et al. (2016) underlined the inhibition of *Staphylococcus aureus* by a film composed by curcumin and chitosan.

Results also evidenced that direct incorporation of THC and chitosan during paper production was not advantageous: coating on commercial paper gave more interesting antimicrobial effect than coating onto paper samples already containing THC and chitosan. This finding has interesting applicative advantages, since only a coating facility is needed to setup the studied antimicrobial package.

4.4.2. Paper pad application on fresh-cut pineapple

Storage trials were set-up employing paper samples with the best antimicrobial effect, i.e. COAT 3-10 comm, prepared at the highest THC concentration in coating onto commercial paper. Slices of pineapple were stored at 4 °C for up to 7 d in presence (treated-PAD) or not (untreated, control - CTR) of the active paper, comparatively.

At the end of the storage period treated and untreated fruit did not show differences in terms of weight loss, both showing a 0.4% decrease. However, in the first period of storage CTR weight decreased more rapidly than the PAD sample (data not shown).

As regards pomological traits, total soluble solids (TSS, %) (Fig. 4.4A) decreased during the first 4 d of storage, in accordance with Latifah et al. (1999), which explained this behavior with the absence of respiratory stress.

Titratable acidity (TA, g L^{-1}) showed the same time course in all samples (Fig. 4.4B). After 2 d storage a decrease was present, followed by a stationary status up to day 4. A subsequent reduction

was again evidenced at the end of the storage. After 7 d treated sample showed higher TA content than the control.

Time course of pH showed a similar behavior to TA (Fig. 4.4C), with an initial decrease in PAD samples followed by stationary phase and a subsequent decrease step. At the end of the storage, PAD sample showed higher pH reduction than the CTR.

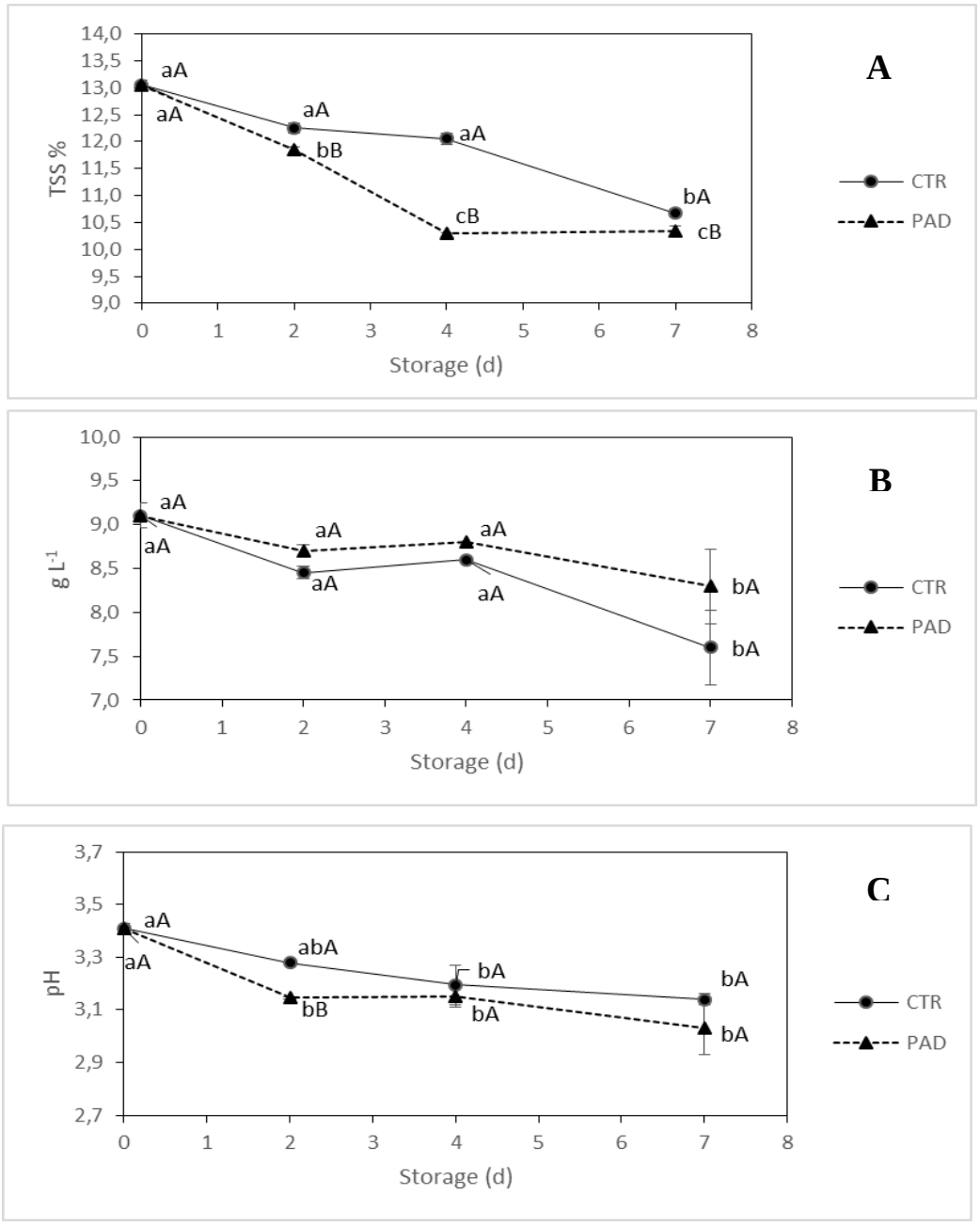

Figure 4.4. Evolution of total soluble solids (TSS %) (A), titratable acidity (TA g L^{-1}) (B) and pH (C) of pineapple slices treated by paper pad (PAD) and untreated (CTR). Data are means ± SD. Minor and capital letters show significant differences ($p \leq 0.05$) for each treatment and among treatments for each storage time, respectively.

The color monitoring of the samples indicates the ripeness evolution and the eventual arise of the browning phenomenon. Lightness (L*) of pineapple slices (Tab. 4.7) showed a constant trend for the treated sample, without significant lightness changes after 7 d, contrarily to the control sample. Several studies demonstrated that L* can be used as indicator of flesh browning (Rocha & Morais, 2003). In the study of Gonzalez-Buesa et al. (2011) the correlation between L* and visual consumer perception was showed on peach fruit. The study showed that L* values around 80 did not affect consumer perception of browning; in our study, PAD sample showed a final L* value around 80.

The a* parameter, index of color change from green to red, is an indicator of chlorophyll degradation (Martin-Diana et al., 2008) and browning presence in some fruit (McHugh & Senesi, 2000). In our study, at the end of storage trials, PAD and CTR samples showed the same a* value (Tab. 4.7), that remained negative thus not showing an excessive slices degradation. For the b* index, color change from blue to yellow, CTR sample showed the highest percentage decrease (11.71 %) respect to the treated sample (9.95 %).

For a correct determination of the color changes, it was possible to calculate the ΔE index, a better indicator than a* and b* parameters or hue angle, as it takes account the lightness (L*) and not only a* and b*. In the present work, ΔE of PAD samples (Tab. 4.7) showed lower value than the control ones, demonstrating lower color modification. This behavior can be also explained by the interaction between chitosan and fruit: Freire et al. (2005) reported that chitosan showed a positive effect on the color of mango slices.

Table 4.7. Color parameters changes during storage of pineapple slices treated by paper pad (PAD) and untreated (CTR). Data are presented as mean ± SD. Minor and capital letters show significant differences ($p \leq 0.05$) for each treatment and among treatments for each storage time, respectively.

		Storage (d)			
	Sample	0	2	4	7
L*	CTR	79.73 ± 0.88^{aB}	78.31 ± 0.88^{bA}	77.81 ± 0.63^{bB}	77.57 ± 0.70^{bB}
	PAD	81.30 ± 0.76^{aA}	79.99 ± 0.66^{aA}	80.42 ± 0.68^{aA}	80.15 ± 0.64^{aA}
a*	CTR	-5.54 ± 0.12^{aA}	-5.05 ± 0.17^{bA}	-4.89 ± 0.17^{cA}	-4.13 ± 0.34^{cA}
	PAD	-5.61 ± 0.18^{aA}	-4.94 ± 0.18^{bA}	-4.37 ± 0.15^{cB}	-4.05 ± 0.09^{cA}
b*	CTR	34.00 ± 1.03^{aA}	32.94 ± 1.18^{aA}	31.40 ± 0.85^{abA}	30.02 ± 0.94^{bA}
	PAD	30.24 ± 0.95^{aB}	29.70 ± 0.98^{abB}	29.24 ± 1.24^{bB}	27.23 ± 0.89^{bB}
ΔE	CTR	-	1.97	2.68	4.24
	PAD	-	1.57	1.82	3.58

Interesting results were obtained by browning potential analysis (Figure 4.5A). The values remained constant the first 2 d of cold storage and showed an acceleration in the following days. PAD samples showed lower values from day 4 onward.. This result, in accordance with color analysis, may evidence the effective role of THC as antioxidant on pineapple fruit, reducing the browning phenomenon. As further confirmation, PAD sample showed less decay in terms of total polyphenol content (TPC). After 2 d, TPC of PAD sample decreased sharply (Figure 4.5B) but remained stable up to 7 d. A different behavior was shown by the CTR sample: in this case the decay trend of TPC was lower but constant and, at the end of storage time, lower polyphenols were present than in PAD sample. This behavior could be explained by the fact that THC may need at least 2 d to be released from the active paper pad to the slices and play its antioxidant role. However this interesting result needs to be the focus of further research trials.

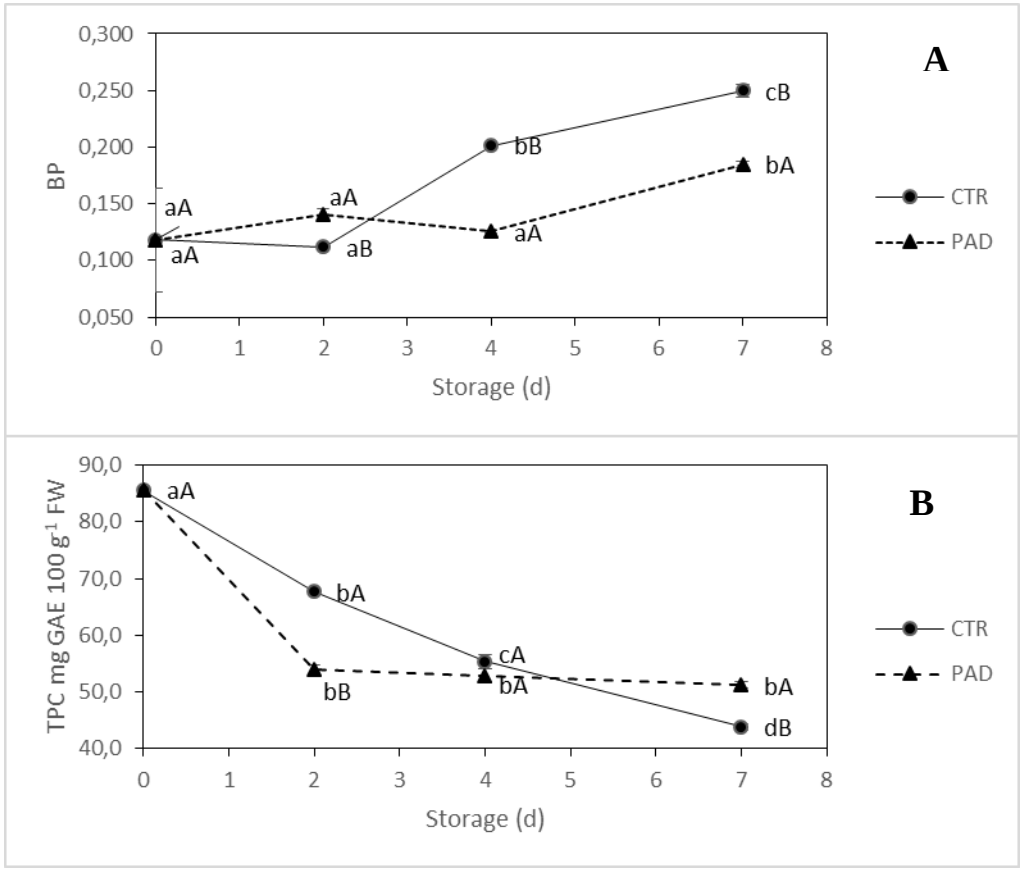

Figure 4.5. Evolution of Browning Potential (BP) (A) and Total Polyphenol Contents (TPC) (mg GAE/100 g of fresh fruit) (B) of pineapple slices treated by paper pad (PAD) and untreated (CTR). Data are means ± SD. Minor and capital letters show significant differences ($p \leq 0.05$) for each treatment and among treatments for each storage time, respectively.

Microbiological analysis performed during storage trials evidenced that molds and yeasts (Figure 4.6A) showed an increase of population in PAD sample after the first 2 d, that however remained stable until the end of storage, with lower values that what observed for the CTR sample. This behavior reflects what previously evidenced for TPC evolution. In the case of total microbial count (TAC) (Figure 4.6B), lower values were immediately visible for treated sample respect to control and visible during all 7 d of storage. At the end of storage time, CTR sample showed a value of near 1,5 log/CFU higher than the PAD sample. In accord to Martinon et al. (2014) on cantaloupe

and Brasil et al., (2012) the active package containing chitosan showed its antimicrobial role on fresh-cut pineapple.

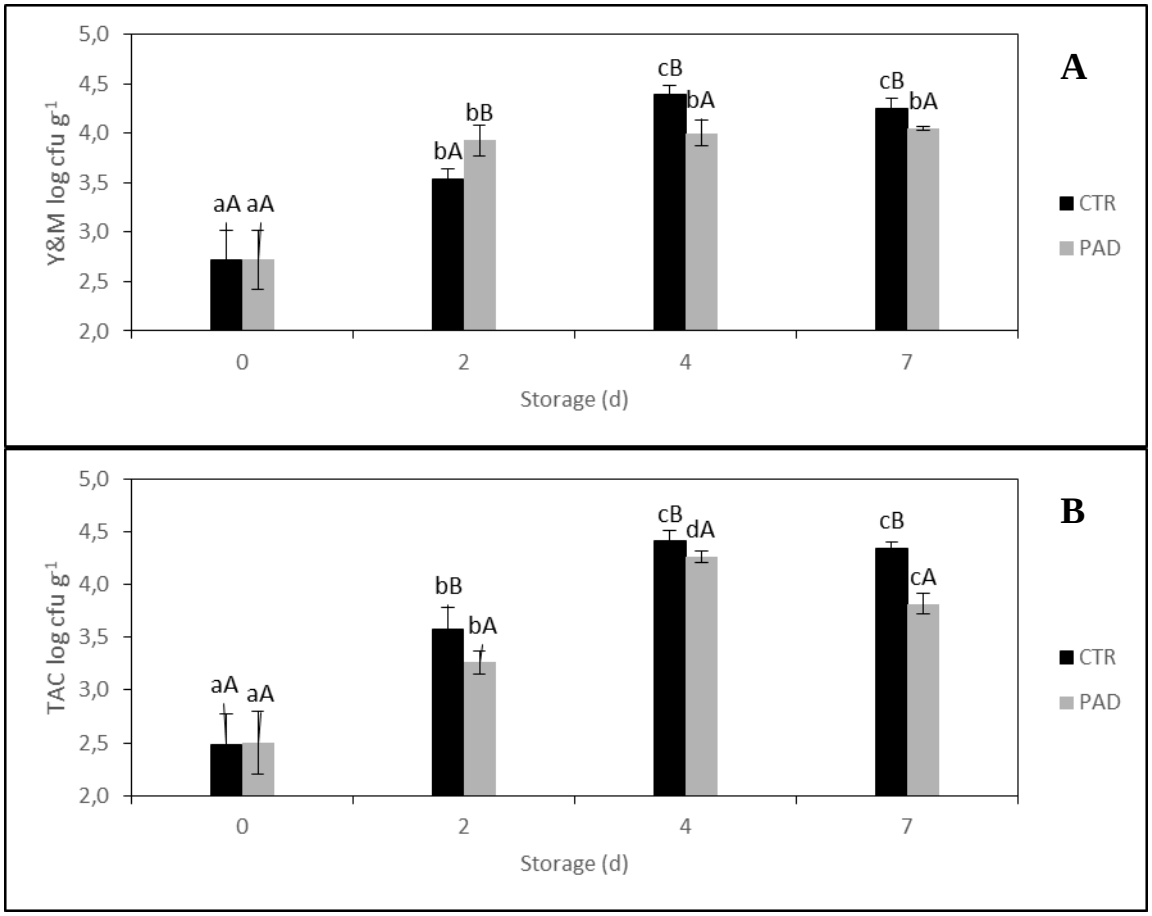

Figure 4.6. Time course of yeasts and moulds (A) and Total Aerobic Count (TAC) (B), (log cfu g^{-1} pineapple) in samples of pineapple slices treated by paper pad (PAD) and untreated (CTR). Data are means ± SD. Minor and capital letters show significant differences ($p \leq 0.05$) for each treatment and among treatments for each storage time, respectively.

4.5. CONCLUSIONS

The present paper reports on the use of chitosan and THC for the production of an active antimicrobial/antioxidant paper suitable in the food packaging area. To the best of authors' knowledge this is the first report on the exploitation of such a combination in the sector of fresh-cut fruit.

In vitro results showed THC antioxidant and antimicrobial properties. This molecule was then applied in combination with chitosan to paper samples either by mass incorporation and by coating, for the production of an active device. Paper samples produced by coating showed the best antimicrobial and antioxidant performances, in particular employing a chitosan-THC coating solution at 3 and 10 % (w/v) concentration, respectively.

This paper pad configuration was applied on fresh cut pineapple slices in storage trials in order to verify the possibility of preserving product quality. In terms of pomological traits, fruit did not show substantial changes after 7 d of cold storage. Results showed the effective preservation of flesh color in presence of the active paper pad, showing positive ΔE values. After 4^{th} d, slices stored in presence of the active pad showed lower browning potential and higher polyphenol contents than the untreated fruit. Moreover, also from a microbiological point of view, yeasts and molds and total microbial count were lower on treated pineapple slices rather than in control samples.

In conclusion, the active paper pad was found effective in maintaining fresh cut pineapple slices due to its antioxidant as well as antimicrobial properties.

Although this work relates to the application of an active pad in a traditional package, future trials will be aimed at setting up innovative active packaging solutions from which these molecules will be released. Further research will be also needed to complement antioxidant with digestion simulation to assess parameters such as bioaccessibility, bioavailability and in vivo antioxidant performance.

These results can pave the way to the use of innovative combination between THC and other natural compounds to be applied on ready-to-eat vegetables, thus improving the attractiveness for consumers of these healthy foods.

.

4.6. REFERENCES

Aggarwal B.B., Deb L., Prasad S. 2015. Curcumin Differs from Tetrahydrocurcumin for Molecular Targets, Signaling Pathways and Cellular Responses. Molecules 20, 185-205.

Barbiroli A., Bonomi F., Capretti G., Iametti S., Manzoni M., Piergiovanni L., Rollini M. 2012. Antimicrobial activity of lysozyme and lactoferrin incorporated in cellulose-based food packaging. Food Control 26, 387-392.

Barbiroli A., Farris S., Rollini M. 2016 Combinational approaches for antimicrobial packaging: lysozyme and lactoferrin. In: (J. Barros-Velazquez Ed.) Antimicrobial Food Packaging. Elsevier, Academic Press, Boston USA, pp. 589-595.

Bordenave N, Grelier S, Pichavant F, and Coma V. 2007. Water and moisture susceptibility of chitosan and paper-based materials: structure–property relationships. J. Agric. Food Chem. 55, 9479–88.

Brand-Williams, W., Cuvelier, M.E., Berset, C., 1995. Use of a free radical method to evaluate antioxidant activity. Food Sci. Technol. 28, 25–30.

Brasil, I. M., Gomes, C., Puerta-Gomez, A., Castell-Perez, M. E., and Moreira, R. G. 2012. Polysaccharide-based multilayered antimicrobial edible coating enhances quality of fresh-cut papaya. LWT- Food Sci. Technol. 47, 39-45.

Choi, C.W., Kim, S.C., Hwang, S.S., Choi, B.K., Ahn, H.J., Lee, M.Y., Park, S.H. and Kim, S.K. 2002. Antioxidant activity and free radical scavenging capacity between Korean medicinal plants and flavonoids by assay-guided comparison. Plant Sci. 163, 1161-1168.

Elsabee, M.Z., and Abdou, E.S. 2013. Chitosan based edible films and coatings: a review. Mater. Sci. Engineer. C. 33(4), 1819-1841.

European Food Safety Authority. Active and intelligent packaging substances. [Online] http://www.efsa.europa.eu/fr/topics/topic/active_intelligent_packaging (Accessed 20 Oct. 2016).

Freire, M., Lebrun, M., Ducamp, M.N. and Reynes, M. 2005. Evaluation of edible coating in fresh-cuts mango fruits. Alimentaria. 369, 85–9

Gonzalez-Buesa, J., Arias, E., Salvador, M.L., Oria, R. and Ferrer-Mairal, A. 2011. Suitability for minimal processing of non-melting clingstone peaches. Int. J. Food Sci. Technol. 46, 819-826

Guerreiro, A.C., Gago, C.M., Faleiro, M.L., Miguel, M.G., and Antunes, M.D. 2015. The use of polysaccharide-based edible coatings enriched with essential oils to improve shelf-life of strawberries. Postharv. Biol. Technol. 110, 51-60.

Ireson, C.R.; Jones, D.J.L.; Orr, S.; Coughtrie, M.W.H.; Boocock, D.J.; Williams, M.L.; Farmer, P.B.; Steward, W.P.; Gescher, A.J. 2002. Metabolism of the cancer chemopreventive agent curcumin in human and rat intestine. Cancer Epidemiol. Biomarkers Prev. 11, 105–111.

Khwaldia, K., Arab-Tehrany, E., and Desobry, S. 2010. Biopolymer coatings on paper packaging materials. Comprehensive Rev. Food Sci. Food Safety. 9(1), 82-91.

Kjellgren H, Gällstedt M, Engström G, and Järnström L. 2006. Barrier and surface properties of chitosan-coated greaseproof paper. Carbohydr. Polym. 65, 453–60.

Latifah, M.N., Abdullah, H, Selamat, M.M., Talib, Y. and Rahman, K.M. 1999. Quality evaluation of minimally processed pineapple using two packing systems. J. Trop. Agric. Food Sci. 27, 101–107

Liu, Y., Cai, Y., Jiang, X., Wu, J., and Le, X. 2016. Molecular interactions, characterization and antimicrobial activity of curcumin–chitosan blend films. Food Hydrocoll.. 52, 564-572.

Majeed, M., Badmaev, V., Shivakumar, U. and Rajendran, R. 1995. Curcuminoids: antioxidant phytonutrients. Sabinsa Corporation, NJ, USA.

Martín-Diana, A.B., Rico, D., Barry-Ryan, C., 2008. Green tea extract as a natural antioxidant to extend the shelf life of fresh-cut lettuce. Innov. Food Sci. and Emerg. Technol. 9, 593–603

Martiñon, M. E., Moreira, R. G., Castell-Perez, M. E., and Gomes, C. 2014. Development of a multilayered antimicrobial edible coating for shelf-life extension of fresh-cut cantaloupe (*Cucumis melo* L.) stored at 4 C. LWT-Food Sci. Technol. 56(2), 341-350.

Mascheroni, E., Figoli, A., Musatti, A., Limbo, S., Drioli, E., Suevo, R., Talarico, S., Rollini, M. 2014 An alternative encapsulation approach for production of active chitosan - propolis beads. Int. J. Food Sci. Technol. 49, 1401-1407.

McHugh, T.H. and Senesi, E. 2000. Apple wraps: a novel method to improve the quality and extend the shelf life of fresh-cut apples. J. Food Sci. 65,480–5

Montero-Calderón, M., Rojas-Graü, M. A. and Martín-Belloso, O. 2008. Effect of packaging conditions on quality and shelf-life of fresh-cut pineapple (*Ananas comosus*). Postharvest biology and technology, 50, 182-189

Murugan, P., and Pari, L. 2006. Antioxidant effect of tetrahydrocurcumin in streptozotocin–nicotinamide induced diabetic rats. Life Sci. 79(18), 1720-1728.

Piva, G., Fracassetti, D., Tirelli, A., Mascheroni, E., Musatti, A., Inglese, P., Piergiovanni, L and Rollini, M. 2017. Evaluation of the antioxidant/antimicrobial performance of *Posidonia oceanica* in comparison with three commercial natural extracts and as a treatment on fresh-cut peaches (*Prunus persica* Batsch). Postharv. Biol. Technol. 124, 54-61.

Portes, E., Gardrat, C., Castellan, A., and Coma, V. 2009. Environmentally friendly films based on chitosan and tetrahydrocurcuminoid derivatives exhibiting antibacterial and antioxidative properties. Carbohydr. Polym. 76(4), 578-584.

Portes, E., Gardrat, C., and Castellan, A. 2007. A comparative study on the antioxidant properties of tetrahydrocurcuminoids and curcuminoids. Tetrahedron Lett. 63(37), 9092-9099.

Rajeswari, A., and Sabesan, M. 2008. Inhibition of monoamine oxidase-B by the polyphenolic compound, curcumin and its metabolite tetrahydrocurcumin, in a model of Parkinson's disease induced by MPTP neurodegeneration in mice. Inflammopharmacol. 16(2), 96-99.

Rana, S., Siddiqui, S., and Goyal, A. 2015. Extension of the shelf life of guava by individual packaging with cling and shrink films. Journal of food science and technology, 52(12), 8148-8155.

Raybaudi-Massilia, R. M., Mosqueda-Melgar, J., Soliva-Fortuny, R. and Martín-Belloso, O. 2009, Control of Pathogenic and Spoilage Microorganisms in Fresh-cut Fruits and Fruit Juices by traditional and alternative natural antimicrobials. Compr. Rev. Food Sci. Food Saf. 8, 157-180

Rinaudo M. 2006. Chitin and chitosan: properties and applications. Progress in Polymer Science 31, 603-632.

Rocha, A.M.C.N. and Morais, A.M.M.B. 2003. Shelf life of minimally processed apple (cv.Jonagored) determined by color changes. Food Control. 14,13–20

Roopa, N., Chauhan, O.P., Madhukar, N., Ravi, N., Kumar, S., Raju, PS., and Dasgupta, D.K. 2015. Minimal processing and passive modified atmosphere packaging of bread fruit (Artocarpus altilis) sticks for shelf life extension at refrigerated temperature. J.Food Sci. Technol. 52(11), 7479-7485.

Scalbert, A., Monties, B., Janin, G., 1989. Tannins in wood: comparison of different estimation methods. J. Agric. Food Chem. 37, 1324-1329.

Slinkard, K. and Singleton, V. 1977. Total phenol analysis: automation and comparison with manual methods. Am Soc Enol Vit. 28, 49–55.

Souri, E., Amin, G. and Farsam, H. 2008. Screening of antioxidant activity and phenolic content of 24 medicinal plant extracts. DARU J. Pharm. Sci. 16, 83-87.

Souza, M.P., Vaz, A.F.M., Cerqueira, M.A., Texeira, J.A. Vicente, A.A. and Carneiro-da-Cunha, M.G. 2014. Effect of an Edible Nanomultilayer Coating by Electrostatic Self-Assembly on the Shelf Life of Fresh-Cut Mangoes. Food Bioproc. Technol. 8, 647-654.

5. CHAPTER III:

Novel controlled release system by layer-by-layer assembly and its application on fresh-cut peach (*Prunus persica* Batsch).

5.1. ABSTRACT

Fresh-cut fruit is a highly perishable product, a large amount of its surface is exposed to oxygen and moisture, due to the lack of skin layer tissue that causes arise of oxidation. Layer-by-layer assembly is a basic technique for the fabrication of multicomponent nano-films on solid supports that permits the transfer of compounds from the support to the contact food. Polyelectrolytes as chitosan (with antifungal properties) and alginate, as carrier for antioxidant compounds, were applied on a PET sheet with releasing capacity. In vitro analyses showed the effectively modulated release of polyphenols and chitosan during 48 h. The growth of *P. chrysogenum* was inhibited by the presence of the extract obtained from coated PET. The characterization study showed the controlled release of layer-by-layer system in terms of antioxidant and antimicrobial capacity, after this the new controlled release system was applied on fresh-cut peach, pomological traits, carotenoids content, polyphenoloxidase and microbiological activities were analyzed. Carotenoids content decay were mitigated by the new active packaging, enzyme activity was lower in treated sample by the new controlled release system as well as microbial activity.

KEYWORDS: ready-to-eat, chitosan, active packaging, antioxidant, storage.

5.2. INTRODUCTION

The growing demand of ready-to-eat food, associated to the need for food waste reduction, have promoted many active packaging solutions to extend the shelf-life of foods. The storage time of fresh-cut fruit can still be improved delaying quality decay and reducing microbiological spoilage. Fresh-cut white-fleshed peaches, which are very appreciated fruit, is characterized by a short shelf life due to fast quality decay and browning phenomenon. Enzymes activity causes browning of tissue by formation of quinones in the presence of O_2 and polyphenol oxidase (PPO), this is one of the most limiting factors and has been the subject of much research on fresh-cut fruit (Beaulieu and Gorny, 2004)

Active packaging materials are "materials and articles that are intended to extend the shelf-life or to maintain or improve the condition of packaged food. They are designed to deliberately incorporate components that would release or absorb substances into or from the packaged food or the environment surrounding the food" (European Commission, 2004). Several types of active packaging have been developed, containing: O_2 and ethylene scavenging (Cao et al., 2015; Di Maio et al., 2014), CO_2-scavengers and –emitters (Wang et al., 2015), moisture regulators, antimicrobial and antioxidant release (de Dicastillo et al., 2016; Mascheroni et al., 2010).

Chitosan is one of the most used natural substance in active packaging; a linear polysaccharide consisting of (1,4)-linked 2-amino-deoxy-β-d-glucan, is a deacetylated derivative of chitin, which is the second most abundant polysaccharide found in nature after cellulose (Aider, 2010). Chitosan has been extensively studied due to its biocompatibility, low toxicity, biodegradability, and antimicrobial activity (Alvarez et al., 2013). In food packaging field, chitosan is widely applied for its antimicrobial activity against various microorganisms (bacteria and fungi), which makes it useful to improve food shelf-life. The exact mechanism of chitosan antimicrobial action is still not completely known, but different mechanisms have been proposed. One explanation is its positively charged amino group which interact with negatively charged of microbial cell membranes, leading to the leakage of proteins and other intracellular constituents of the microorganisms. Chitosan also acts as a chelating agent that selectively binds trace metals and thereby inhibits the production of toxins and microbial growth (Cuero et al. 1991). It also activates several defense processes in the host tissue (El Ghaouth et al. 1992), acts as a water binding agent and inhibits various enzymes.

Alginate is a natural anionic polymer typically obtained from brown algae (*Phaeophyceae*), for its biocompatibility and interesting physical properties, alginate is widely applied in the field of food

formulations as a thickener, stabilizer agent and carrier of active compounds (Robles-Sánchez et al., 2013; Rojas-Graü et al., 2007)

Among antioxidant substances there are flavonoids from green tea extract, including gallic acid, ferulic acid, catechin, epicatechin, gallocatechine, epigallocatechin, catechin gallate, epigallocatechin-3-gallate (the most abundant and biologically active compound in green tea), gallocatechin gallate, and epicatechin gallate (Sutherland et al., 2006). The hydroxyl groups in the ring structure of catechin can be easily oxidized (Janeiro and Brett, 2004). Green tea is one of the plant extracts with high antioxidant and antibacterial activities, and with anti-tumor effects due to its catechin content (Kusmita et al., 2015). Green tea catechins are also able to act as secondary antioxidants through the chelation of metal ions (Michalak, 2006). Because of these properties, there is an increasing interest for green tea extracts incorporations into oxidations-sensitive foods (Senanayake, 2013).

Layer-by-layer (LbL) assembly is a basic technique for the fabrication of multicomponent films on solid supports by controlled adsorption from solutions or dispersions (Decher, 1997). With the LbL technique, polyelectrolyte multi-nanolayer films can be fabricated on various templates through repeat deposition, mainly due to the electrostatic attraction between oppositely charged polyelectrolytes (Donath et al, 1998). One of the use of LbL assembly is the drug delivery in biomedical field to release antibiotics or others substances (Wohl & Engbersen, 2012; Tang et al., 2006). One of the mechanism of drugs release is the immobilization of the active compound between two layers of LbL system. Drugs are released via diffusion (Chen et al., 2011) or by degradation of the layers (Flessner et al., 2011).

The aims of this work were the development and characterization of a new Controlled Release System (CRS) by the conjugation of Chitosan-Alginate using LbL assembly, including polyphenols, and the application of this novel active packaging device on fresh-cut peaches to reduce its quality decay.

5.3. MATERIALS AND METHODS

5.3.1. Chemicals

Chitosan from shellfish (CS, GiustoFaravelli S.p.A., Milan, Italy) had a degree of deacetylation of 85% and a molecular weight ranging from 50,000 to 60,000 (data provided by the supplier). 1,2-Dihydroxybenzene (≥99%), 2,2-Diphenyl-1-picrylhydrazyl (DPPH), (±)-6-Hydroxy-2,5,7,8-tetramethylchromane-2-carboxylic acid (Trolox) 97%, Acetone (≥99.5%), Citric acid monohydrate (≥99.0%), Ethanol (≥99.8%), Fluorescein 5(6)-isothiocyanate (FITC) (> 90%), Hexane (anhydrous, 95%), Hydrochloric acid, Hydrogen peroxide solution (≥30%), Poly(vinylpolypyrrolidone), Sodium alginate powder, Sodium chloride (anhydrous, ≥99%), Sodium hydroxide (≥99.0%, anhydrous), Sulfuric acid (95.0-98.0%) were purchased from Sigma–Aldrich (Gallarate, MI, Italy). HPLC grade methanol was from Panreac (Barcelona, Spain), and HPLC grade water was obtained by a Milli-Q system (Millipore Filter Corp., Bedford, MA, USA). Green tea extract were obtained from DAL CIN GILDO S.p.A. (Concorezzo, MB, Italy). Amorphous polyethylene terephthalate (PET) (∼250 μm thick) was used as the plastic substrate for LbL coating, provided from ILPA S.R.L. (Bazzano, Italy).

5.3.2. Preparation of Controlled Release System (CRS) through layer-by-layer assembly

Chitosan and alginate water dispersion, 0.2 % (w/v), was separately prepared by dissolving the chitosan in 2 % (v/v) of acetic acid, only water for alginate, at 25 °C for 3 h under stirring. The employed concentration of alginate and chitosan were chosen according to several previous reported work (Del Hoyo-Gallego et al., 2016; Medeiros et al. 2011; Caneiro da Cunha et al. 2009). Into the alginate solution was added 0.35% of green tea extract, after that, the pH was adjusted to 3.8 and 6.5 for chitosan and alginate-green tea solution, respectively. The solutions were used for LbL assembly. This (Fig. 5.1) was carried out using the method of Li *et al*. (2013). PET sheets were cleaned with distilled water and methanol for removing lipids and contaminants, after drying, they were submitted to corona treatment (BD-20 high frequency generator, Electro-Technic Products, Inc., Chicago, IL, USA) to increase surface energy and generate a negative-charge surface. The PET sheet was cut in 7 x 3 cm strips, each strip was dipped into the chitosan solution for 10 min; after, the strips were rinsed in distilled water for 5 min to remove the excess of chitosan; strips coated by chitosan were dried by filtered compressed air. Following, strips were dipped into the alginate-green tea solution for 10 min; the rinsing and drying steps were the same as the one

for chitosan. Finally, 20 bilayers were achieved by repeating the previous steps. All the samples were stored into desiccators at 0% RH, in dark and put into a cold chamber at 4 °C for the following measurements. The same treatments were used to prepare the coated glass samples intended to AFM analysis, glass slides were instead charged treating them with Piranha Solution (96 % H_2SO_4 : 30 % H_2O_2 = 3 : 1 v\v).

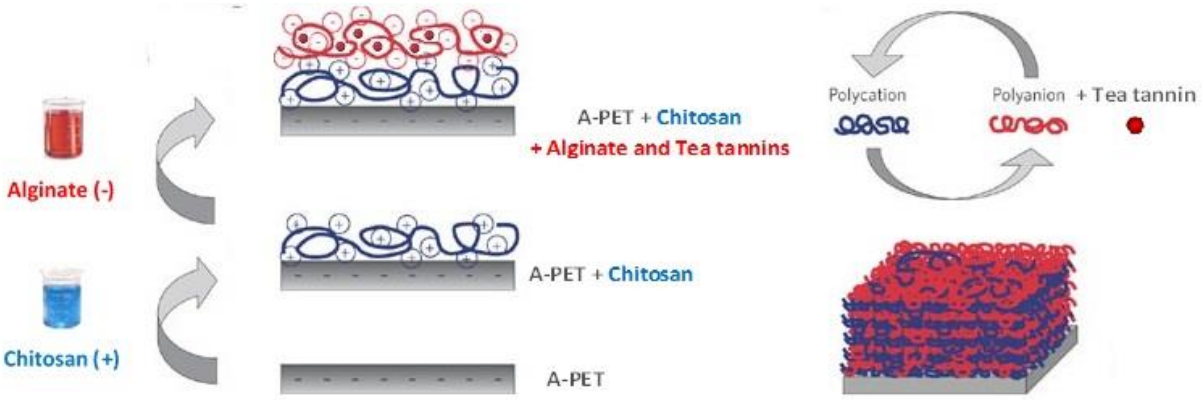

Figure 5.1. Layer-by-Layer assembly procedure.

5.3.3. Optical contact angle (OCA)

On PET surface contact angle (θ) measurement was performed using the sessile drop method (Newman and Kwok, 1999) with optical contact angle apparatus (OCA 15 Plus – Data Physics Instruments GmbH, Filderstadt, Germany) equipped with a video measuring system with a high-resolution CCD camera and a high performance digitizing adapter. SCA20 software (Data Physics Instruments GmbH, Filderstadt, Germany) was used for data acquisition.

Onto the PET surface 4 ± 0.5 μL droplet of Milli-Qwater was placed by syringe (Hamilton, Switzerland), the measures were made at 0,20 and 20 s and 20,5 ± 0,3 °C , 15 replicates of contact angle measurements were carried out.

5.3.4. FTIC-chitosan assembly

FITC-CHI was synthesized using the following procedure reported by Hoyo-Gallego et al (2016). 0,4 mg/mL of fluorescein-isothiocyanate in methanol was added into 0,2 % w/v chitosan in 0,1 M acetic acid solution; after 3 h of reaction in the dark at room temperature. The fluorescein-labeled chitosan was precipitated in 0,2 M NaOH and severally washed with distilled water until a clear supernatant was obtained. The FITC-CHIT was then dissolved into distilled water to obtain a 0,2

% solution which was employed for the layer by layer assembly as previous reported (except for the green tea mix that was not added inside alginate to avoid possible interference on absorbance analysis) and coated on PET dedicated sheets. An UV-Vis spectrophotometer (mod. L650 with a 150 mm integrating sphere, Perkin-Elmer, Milano, Italy) was employed to monitor the absorbance at 490 nm of the coated PET samples after the deposition of 5, 10, 15 and 20 layers of FIT-CHIT (9, 19, 29, 39 total layers). The obtained absorbance measures were then employed to produce a curve, absorbance vs number of layers, which was used to understand the assembly of layers.

5.3.5. Atomic Force Microscopy (AFM)

For surface measurements, the LbL coating on glass slides was gently scratched in order to expose part of the glass substrate and thus measure the surface of the coating. An atomic force microscope (AFM, AlphaSNOM, WITec GmbH, Germany) was employed to study the morphology. Topography images were acquired with soft tapping mode at low oscillation amplitudes, stabilized by an amplitude-modulation feedback system based on the optical lever deflection method. Standard AFM Si probes have been used.

5.3.6. Dissolution of the coated layers from PET support

To characterize the PET sheets coated by LbL assembly and to understand the kinetics of release, the strips were stirred for 48 h. A portion of sheet, 3 x 3 cm, was cut and put into the glass flask and immersed in 5 mL of acid aqueous solution (acidified by citric acid at pH 3.8) as food simulant. The flasks with samples were shaken for 6, 24 and 48 h using Flask Dancer (270292 Boekel Scientific, Feasterville, PA, USA). The obtained solution were used for the next analysis and the remaining strips were analyzed by Fourier Transform Infrared Spectroscopy.

5.3.7. Fourier Transform Infrared Spectroscopy (FTIR)

FTIR spectra of remaining sheets coated by LbL were obtained using a Perkin Elmer instrument (Sprectrum 100) equipped with an ATR. Spectra were recorded using a spectral width ranging from 700 to 4000 cm^{-1}, with 4 cm^{-1} resolution and an accumulation of 32 scans.

5.3.8. UV-Vis spectrophotometry, antioxidant and microbiological assays on extracted solution

The UV–Vis analyses were carried out using a UV–Vis spectrophotometer (Lambda 25 Perkin Elmer, MA), following the method of Hoyo-Gallego et al (2016) with some modifications. The

absorbance at 280 nm was measured on the extracted solution of PET-LBL at different time, after 6, 24 and 48 h.

Analysis of the antioxidant capacity of the was carried out employing the DPPH assay, following the method of Brand-Williams et al. (1995) with some modifications. The DPPH solution was diluted in ethanol to obtain 1.00 ± 0.03 absorbance units at 515 nm. The DPPH solution (2.94 mL) was placed in a cuvette where 60 µL sample were added. The absorbance readings were carried out after incubation for 50 min at 20 ± 1 °C. A calibration curve was prepared by adding increasing concentration of Trolox ranged from 50 to 1000 µM; each concentration was assayed in triplicate, as well as each sample. Results were expressed as mg Trolox per 100 g of powder.

Antimicrobial activity carried out against strains belonging to official collection, i.e. *Escherichia coli* CECT 434 (Spanish Type Culture Collection), *Staphylococcus aureus* ATCC 29213, *Aspergillus niger* NRRL 565 (Agricultural Research Service Culture Collection) and *Penicillium chrysogenum* CECT 2802.

Bacterial strains were weekly maintained on TSB (Tryptic Soy Broth, Scharlau Chemie, Spain), incubated at 30 °C for 24 h and then stored at 4 °C, while yeasts on MEB (Malt Extract Broth, g L^{-1}: malt extract 20, glucose 20, soy peptone 1, pH 5.8), incubated at 28 °C for 24-48 h and then stored at 4 °C until use. Moulds were maintained on MEA solid culture (MEB added with 15 g L^{-1} agar), incubated at 25 °C for 5-7 d and then stored at 4 °C until use. Qualitative determination of antimicrobial activity was performed as follows: thirty mL of soft TSA or MEA (TSB or MEB added with 8 g L^{-1} agar) were poured in a Petri Dish and inoculated with 300 µL of a microbial suspension prepared in sterile distilled water (OD 600nm: 0.300 ± 0.050); moulds were inoculated as spores suspension in sterile distilled water (OD 600 nm: 0.300 ± 0.050). Once solidified, holes were made by using a sterile tip and 150 µL of extracts were poured inside. Cultures were all incubated at each appropriate temperature for 24 h (up to 7 d for moulds). The presence of a growth inhibition halo around holes indicates an antimicrobial activity.

5.3.9. High Performance Liquid Chromatography (HPLC)

A sample of extracted solution after 48 hours was submitted to Acquity HClass UPLC (Waters, Milford, MA, USA) system equipped photo diode array detector 2996 (Waters), in order to identify and quantify the released polyphenols compounds. The solution was primarily filtered to remove chitosan and alginate (that can obstruct the column). Column used was Kinetex C18 150 x 3 mm, 2.6 µm particle size, 100 Å pore size (Phenomenex, Torrence, CA, USA). Flow rate: 0.8 mL/min; column temperature: 30 °C; solvents: A, 0.1% trifluoroacetic acid; B, acetonitrile acidified with

0.1% trifluoroacetic acid; gradient: 0-5 min, 0% B; 5-10 min, 5% B, 10-15 min, 5% B, 15-35 min, 15% B, 35-52 min, 32% B followed by column washing and re-equilibration. Integration: 280 nm.

5.3.10. Application on fresh-cut peach of the new CRS

Peaches (*Prunus persica* L. Batch cv. 'Alexandra") were purchased at the wholesale market (10 kg) at commercial maturity and stored for 1 d at 4 °C until use. Peaches were homogenous in size and ripening (6 ± 0.7 kg/cm^2, 9.70 ± 0.1 °Brix, 12 ± 0.6 g L^{-1} titratable acidity). Fruits were pre-washed with distilled water, sanitized for 2 min in chlorinated water (1.5 g L^{-1} sodium hypochlorite), rinsed with distilled water and gently dried by hand. Peaches with skin were cut into slices of about 1.5 cm thickness (15 g each slice), using a sterile stainless-steel knife. Four slices (60 g) were placed onto PET trays (19 x 12x 4 cm). Among each slice and on the bottom of the tray were insert PET-LbL strips, 7 x 3 cm and 7 x 7 cm respectively, (LBL) (Fig. 5.2); in uncoated samples (UNC) slices were placed with untreated strips and in control samples (CTR) without strips. The trays with slices were put into low-density polyethylene (LDPE) bags (22 x 15 x 6 cm, 25 µm thickness, bag volume 600 mL, ratio between fruit weight and container volume 100 g L^{-1}, surface film for each bag 660 cm^2, O_2 permeability 6200 cm^3 m^{-2} d^{-1} bar^{-1}, CO_2 permeability 24000 cm^3 m-2 d^{-1} bar^{-1} at 10 °C) and stored at 4 ± 1 °C up to 7 d. Each treatment was carried out in triplicate. Samples were then collected at time zero and after 3, 5 and 7 d.

Figure 5.2. Disposition of the Controlled Release System (CRS) among and below the slices of peach in treated sample (LBL).

5.3.11. Physico-chemical evaluations

Flesh colour was evaluated using the CIE L*a*b* System by a Minolta CR-300 chromameter (Konica Minolta Sensing, Inc., Japan). Three measurements were performed on each side of slices. The instrument was calibrated using a standard white plate. The Chroma (C) was calculated as following reported:

$$C^* = \sqrt{a^{*2} + b^{*2}} \qquad (1)$$

Fruit firmness was measured with digital penetrometer (53205, TR Turoni, Forlì, Italia) and expressed as kg/cm^2.

Weight loss (WL) was calculated by the difference between the initial and final weight (after 7 d) of samples. The value was expressed as a relative percentage and calculated as follows:

$$WL = \frac{(\mathrm{Wi} - \mathrm{Wf})}{\mathrm{Wi}} * 100 \qquad (2)$$

Where Wi is the initial weight and Wf is the weight measured during storage.

Total soluble solids (TSS, %) and titratable acidity (TA, g L^{-1}) were measured on the juice obtained from slices (50 g for each sample) by an electronic juicer (Moulinex, France). TSS was determined by a digital refractometer (Atago Co., Ltd, Tokyo, Japan model PR-32). Titratable acidity was measured on by titrating 1:10 diluted juice (obtained from 50 g of samples) using sodium hydroxide 0.1 M by automatic titrator (Compact 44-00, Crison Instruments, SA, Barcelona, Spain).

To determine the carotenoids content the De Ritter and Purcell (2010) method was used. Briefly, 5 g of sample were mixed for 20 min with 50 mL of extracting solvent (hexane/acetone/ethanol, 50:25:25, v/v). The organic phase was recovered and then used for analyses after suitable dilution with hexane. Total carotenoid determination was carried out on an aliquot of the hexane extract by measuring absorbance at 450 nm in a spectrophotometer Lambda 25 (Perkin Elmer, MA). Total carotenoids were calculated as follows:

$$\beta carotene\ content\ (\mu g\ 100\ g) = \frac{Abs*V*D*100*100}{W*Y} \qquad (3)$$

Where V is total volume extract, D the dilution factor, W the sample weight and Y the percentage of dry matter content of the sample. The analyses were performed in triplicate for each sample.

For the determination of polyphenol oxidase (PPO) activity, the buffer solution (1:1) at pH 6.5 was prepared using 1 M NaCl and 5% polyvinylpolypyrrolidone, peach sample (5 g) was mixed with a buffer solution and homogenized using an Ultra-Turrax DI25 (IKA Works, Germany). The homogenate mix was centrifuged at 12,000 rpm for 30 min at 4 ◦C (Centrifuge Rotofix 32A, Hettich, Germany.). The supernatant was collected and filtered, to obtain the enzymatic extract, required for enzyme activity determination. According to the method of Soliva-Fortuny *et al*. (2001) and Kołodziejczyk *et al*. (2010) PPO activity was determined spectrophotometrically, adding 3 mL of 0.05 M catechol and 75 µL of obtained extract into a quartz cuvette. The changes in absorbance at 400 nm were recorded every 1 min up to 3 min. One unit of PPO activity was defined as a change in absorbance of 0.001 min^{-1} mL^{-1} of enzymatic extract immediately after extract addition. All determinations were performed in triplicate.

5.3.12. Antimicrobial activity of CRS on peach slices

After 0, 3, 5 and 7 d, a portion of sample (10 g) were transferred aseptically into a Stomacher bag (400 mL PE, Barloworld, France) containing 135 mL of sterile peptoned water (10 g L^{-1} bacteriological peptone, Costantino, Italy) and blended in a Stomacher (Star Blender LB 400, Biosystem, Belgium) at high speed for 3 min. Ten-fold dilution series of the obtained suspension were made in the same solution for plating. The following culture media were used: Nutrient Agar (Merck, Germany) for mesophiles and psycrophiles, and MEA (Malt Extract Agar) for yeasts and fungi. Colonies were counted after incubation at 30 °C for 24 h for mesophiles, 10 °C for 10 d for psychrophiles and 30 °C for 5 d for yeasts and fungi. Counts were performed in triplicate and reported as logarithms of the number of colony forming units (log cfu g^{-1} peach).

5.3.13. Statistical analysis

Statistical analysis was carried out using the STATISTICA 7.1 software package (Statsoft Inc., Tulsa, OK, USA). One-way analysis of variance (ANOVA) was performed on mean values and Tukey's test was carried out for the comparison of difference among treatments for each storage time and for each treatment during storage. Differences were considered significant at $p \leq 0.05$.

5.4. RESULTS AND DISCUSSION

5.4.1. *In vitro* analysis

Contact angle measurement (Fig. 5.3) showed the different values for each assembled layer. Uncoated PET showed an angle of 43.32° ± 0.95, after first chitosan layer deposition the angle value increase and after alginate layer application the value decrease again. After 20 layers (10 of chitosan and 10 of alginate), was possible to see a stabilization of the angle values, in fact, after the first 10 layers, the contact angle average of chitosan layers was 81,8° ± 1,3 while the contact angle average of alginate was 68,6° ± 3,4. Therefore, the hydrophilic properties was changed by the nature of the layers. This result is the proof of individual layering and need a minimum number of layers in order to obtain a uniform covering of surface.

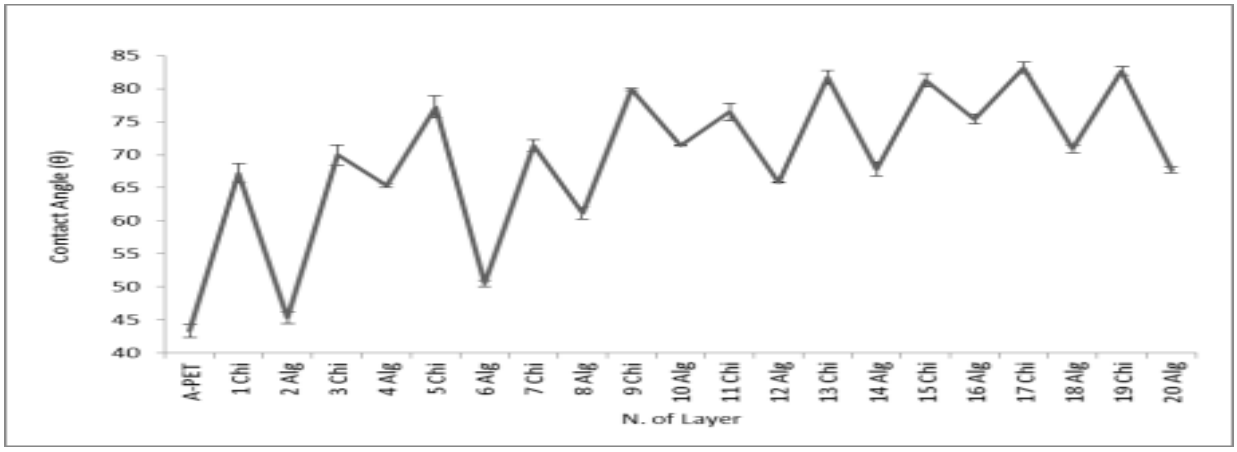

Figure 5.3. Contact angle values of uncoated PET and PET coated by 20 layers o chitosan-alginate (measured 0 s after water drop deposition). Data average ± SD.

The LbL coating assembly was also confirmed by the increasing values of absorbance observed on PET samples during the deposition of following layers employing the FITC-CHIT. As shown in (Fig. 5.4) linear growth of PET absorbance obtained, suggesting that thick constant layers were following deposited.

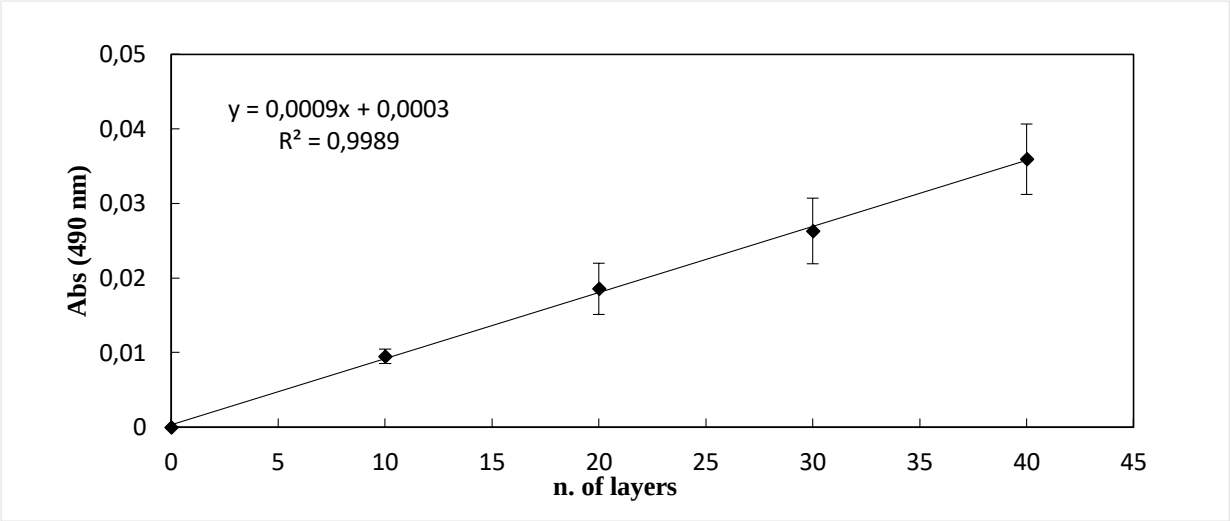

Figure 5.4. Increasing absorbance of PET sample during FIT-CHIT\ALG coating assembly. Each data is the average ± SD.

AFM topography images on the coated glass slides showed minimal differences in surface roughness of the final layer between the alginate and the chitosan, in chitosan appears punctiform discontinuities not present in the alginate surface (Fig. 5.5).

AFM thickness analysis was carried out on coated glass after 20 and 40 layers. After 20 layers the thickness value was 30 ± 5 nm while after 40 layers was 65 ± 5 nm, 1.6 ± 0.1 nm was the average thickness of each layer. Despite this minimal deposition quantity the antioxidant and antimicrobial efficacy were carried out. As reported in biomedical studies, nanometric thickness could allows a greater efficiency of active molecules, compared to the same material with the larger particles owing to the fact that the surface/volume ratio of the nanoparticles increases considerably with decrease in the particle size (Dizaj et al., 2014). Future studies will characterize the each layer provision in thickness. The AFM image ensure a spatial lateral resolution (in the plan of sample) of any nm and spatial vertical resolution (perpendicular to the sample) of about 1 nm. Black color show the shorter quote and yellow the higher quote in the sample during the AFM scan. The vertical color bar show the vertical total range of the sample while white bar in the image show the horizontal range. In accord to the OCA analysis is possible to see the uniform surface after 40 layers, respect to 20 layers that showed discontinuous part as long streaks. The AFM analysis, as the OCA, showed the effective nanoscale assembly of LbL structure.

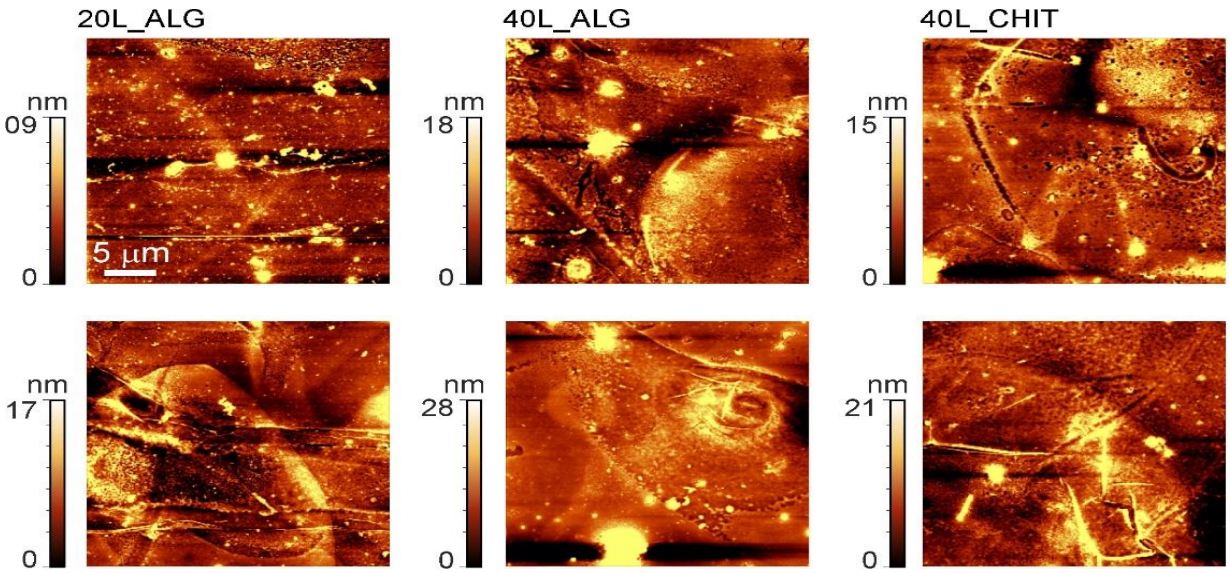

Figure 5.5. AFM topography images of alginate (left) and chitosan (right) layer surfaces after 40 layers deposition.

On extracted solution DPPH assay was carried out. DPPH activity decay from 100 % to 97,80 ± 0,49 % after 6 hours, to 94,76 ± 0,04 % after 24 hours and to 93,00 ± 0,13 % after 48 hours (Fig. 5.6). No significant differences were observed between samples in which alginate or chitosan was the last deposited layer. Based on these results was possible to conclude that green tea antioxidant species has been incorporated through the alginate layers and subsequently gradually released into the simulant solution.

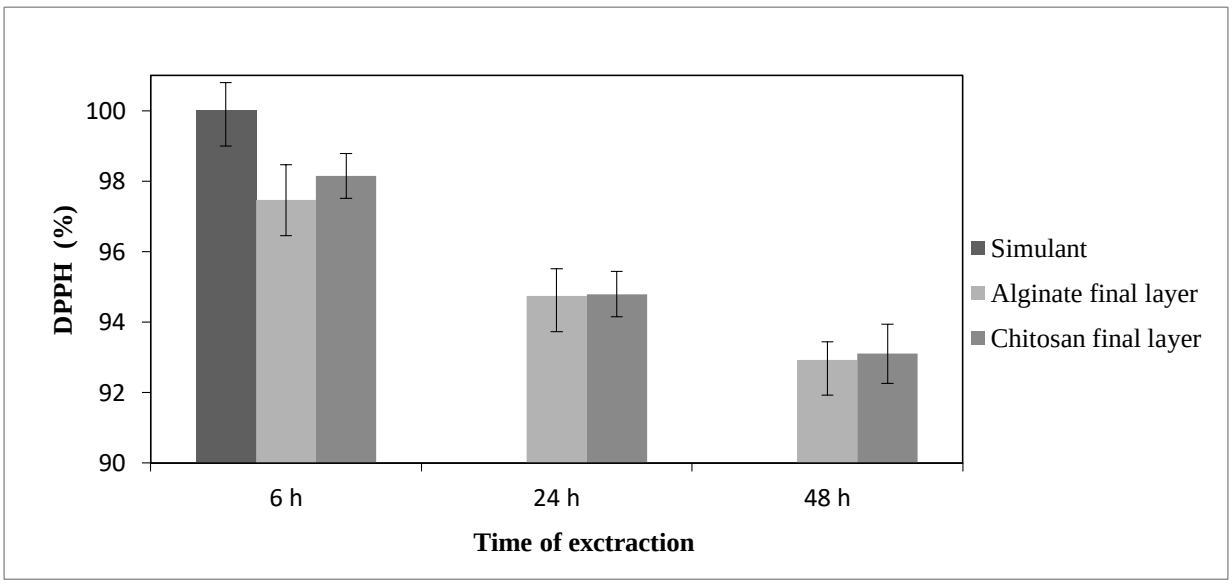

Figure 5.6. DPPH (%) decay of the extracted solution, after 6, 24 and 48 h of CRS extraction by simulant.

The absorbance increase of extracted solution of CRS was measured by spectrophotometer at 280 nm, the wavelength of maximum in absorbance of polyphenols. In this measurement, the increase

in absorbance value depends on the time of extraction. After 48 h of extraction from the CRS, the solution has higher absorbance than the other two samples (Fig. 4.7).

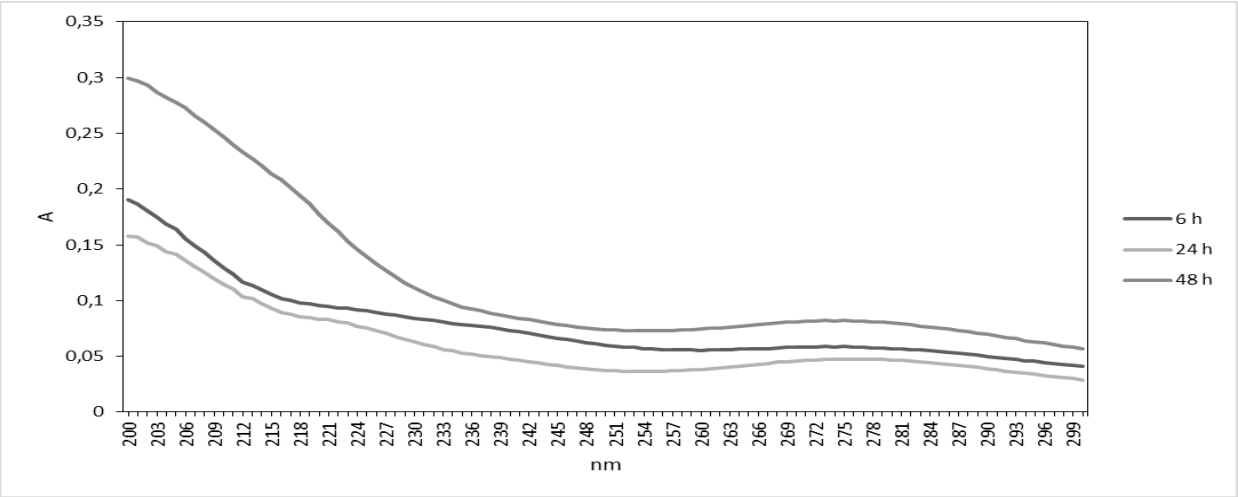

Figura 5.7. UV-spectra (range of 200-300 nm) of the three extracted solution, after 6, 24 and 48 h.

After the extraction procedure, the remaining PET samples were analyzed by FTIR. Similarly as UV-vis spectra, but in opposite way, the FTIR spectra showed the absorbance decrease, in

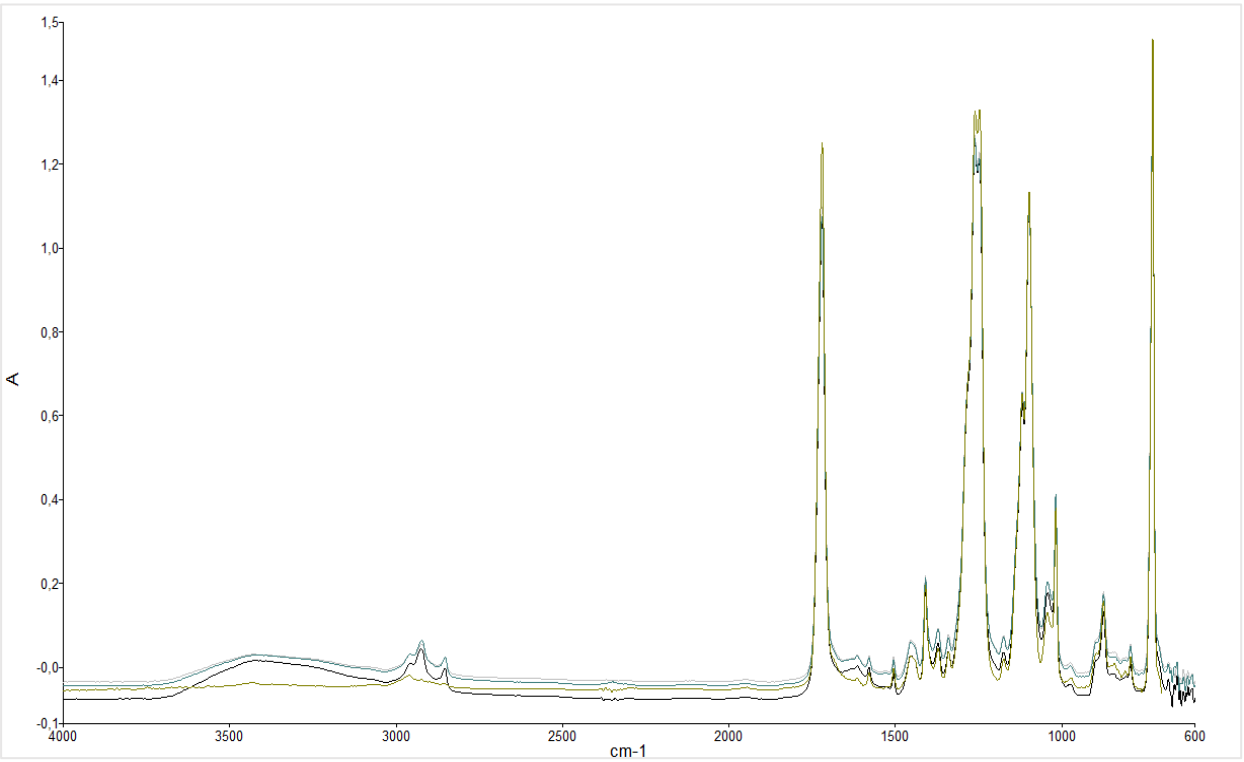

Figure 5.8. FTIR spectra of uncoated PET and coated PET samples after 6, 24 and 48 h of extraction. From above: after 6, 24, 48 and uncoated PET.

correspondence of 2900 nm the wavelength of $–CH_2$ (Fig. 5.8), present in chitosan and alginate polymers, and increase at 3425 nm, the typical wavelength of polyphenols compounds (Fig. 5.9).

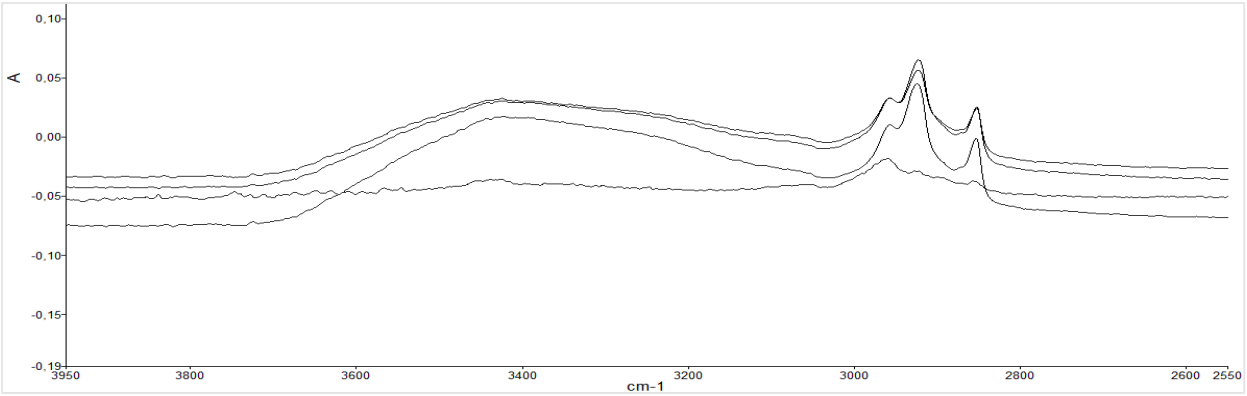

Figure 5.9. Particular of FTIR spectra of uncoated PET and coated PET samples after 6, 24 and 48 h of extraction. From above lines mean: after 6, 24, 48 h and uncoated PET.

This behavior confirms the solubilization of the layers after the extraction procedure with food simulant.

Layer-by-layer coating kinetics of releasing was further investigated by putting the FITC-CHI\ALG coated PET samples (40 layers) to a longer extraction process and monitoring the absorbance of the simulant solution over time. A gradual release of the coating was observed during 244 hours (10 d) (Fig. 5.10), the first 144 h showed a constant speed of coating release, after this moment the release reached a plateau, in accord to Hoyo-Gallego et al. (2016).

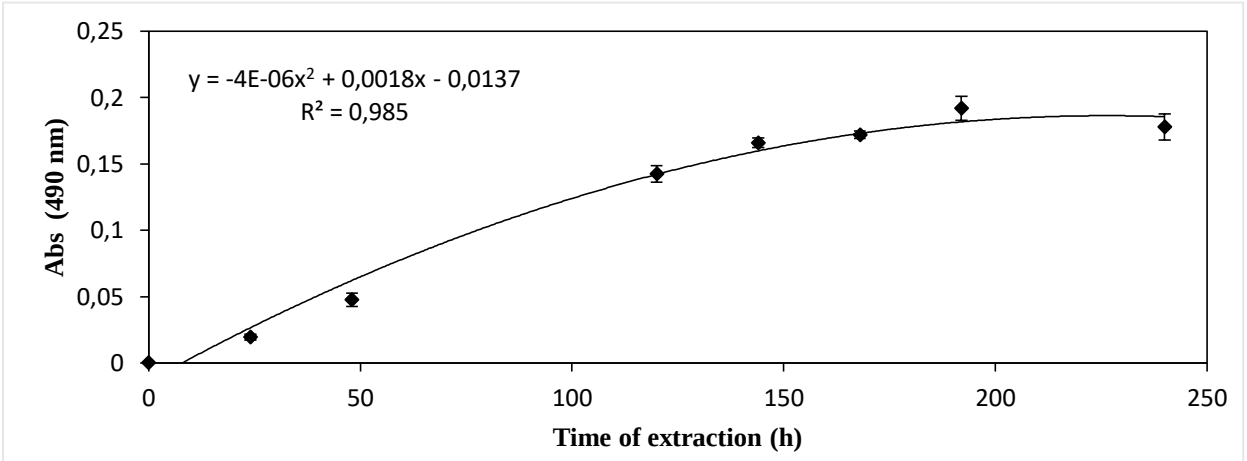

Figure 5.10. Kinetics of FITC-CHIT release over 244 hours of extraction (10 days). Each data point is an average of 3 determinations ± SD.

In microbiological qualitative trials no activity against bacteria was shown. Missed antibacterial capacity depends on the low concentration of chitosan into the LbL assembly. At the same time, any antifungal activity was present against *A. niger* (data not shown) but it was observed against

P. chrysogenum (Fig. 5.11). The antifungal activity of chitosan was evident in the sample after 48 h of extraction, in this case, *P. chrysogenum* did not grow into the hole.

Figure 5.11. Culture of *P. chrysogenum*, front of Petri-dish (left) and back of Petri-dish (right), after 6 d of incubation with different CRS extracts. The hole in the lower left showed the inhibition halo for the extract obtained after 48 h.

The presence of the green tea antioxidants species inside the citric acid simulant solutions was also confirmed by HPLC analysis (Fig. 5.12), performed on the simulant solution after 48 hours of contact by coated PET. Gallic acid was identified (retention time: 3,5 minutes) as well as different water-soluble phenols (retention times: 3,9 6,8 and 9,8 minutes) and flavons (retention times: 32,9 and 36,4 minutes). Gallic acid concentration was 75 μg\L and it represented the 11,5 % of the total detected substances.

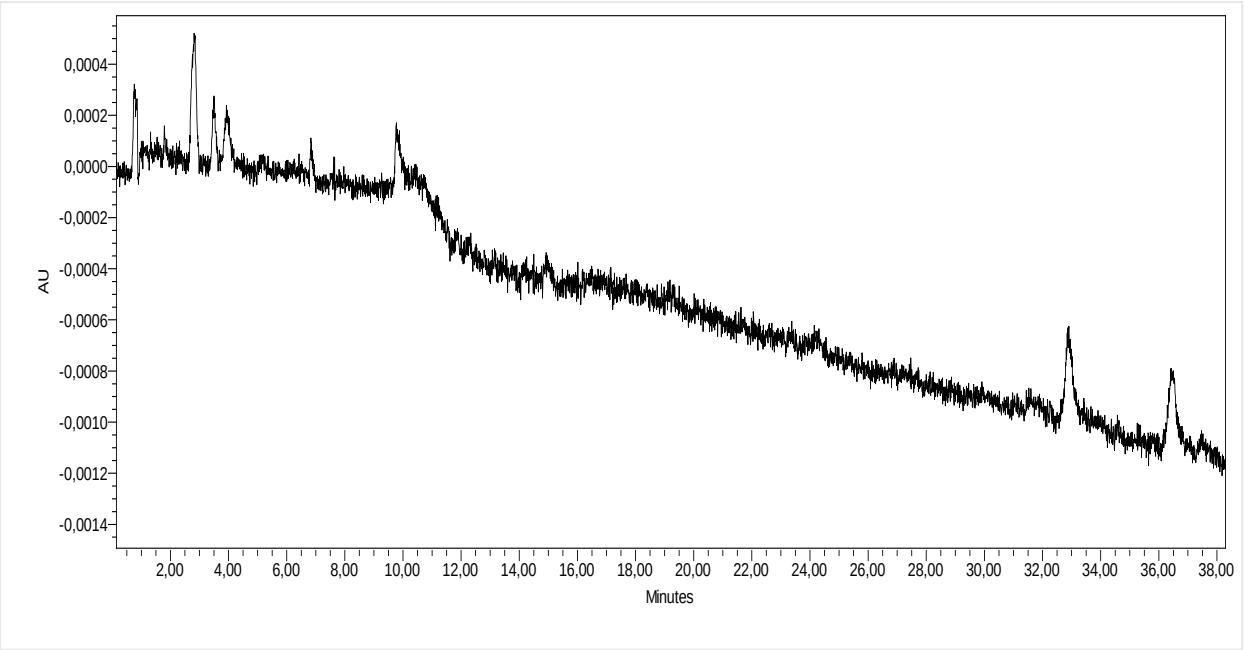

Figure 5.12. HPLC spectrum of the extracted solution after 48 h in contact by coated PET.

5.4.2. *In vivo* performance

After 7 d of storage, Lightness (L*) was higher in LBL sample (Fig. 5.13a), the same result occurred for the Chroma (C*) (Tab. 5.1). Different studies affirm that L* can be used as indicator of flesh browning (Rocha & Morais, 2003). Gonzalez-Buesa et al. (2011) have demonstrated the correlation between L* and visual consumer perception on peach fruit. The study reported that L* values higher than 75 did not affect consumer perception of browning; in our study, LBL sample showed the final L* value around 76 while 74 for the control sample. Similarly, a* index, color changes from green to red, is an indicator of chlorophyll degradation (Martin-Diana et al., 2008) and browning presence in apple fruit (McHugh & Senesi, 2000). In our study, at the end of the trial, LBL negative value of a* (Fig. 5.13b), that means the absence of an excessive degradation of the slices, CTR sample showed a* value around 0. Also from visual appearance, was possible to detect differences among the slices for the different treatment (Fig. 5.14), the slices of LBL sample showed better attractive appearance. A decrease of b* index, color changes from blue to yellow, normally indicates the phenolic degradation taking part on tissues (Fuentes-Perez, 2014).

In this study, b* increase, after 2 d for all the samples, after 7 d the LBL sample showed the higher value than the others samples (data not shown).

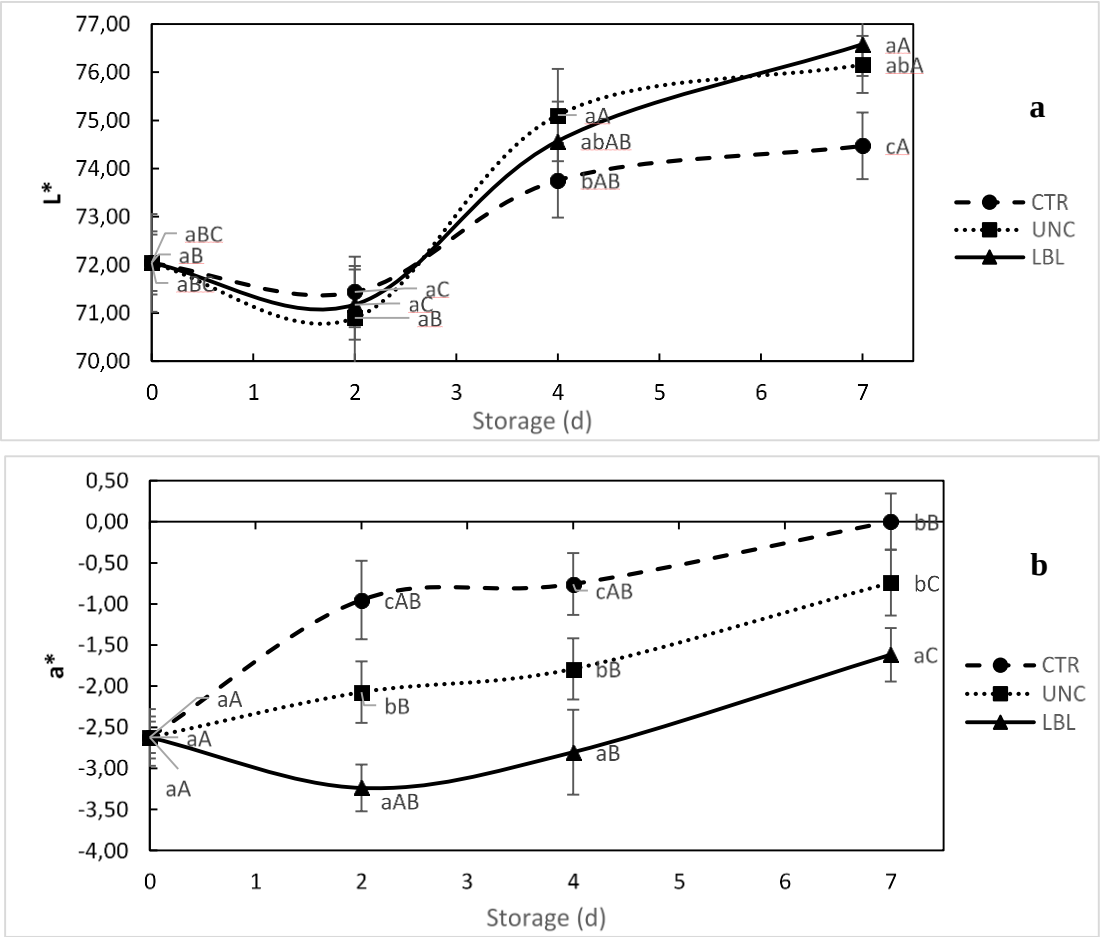

Figure 5.13. Lightness (L*) (a) and a* (b) parameter changes during storage of fresh-cut peach slices treated of CRS (LBL), uncoated strips (UNC) and untreated (CTR). Data indicate ± SE. Capital and minor letters show significant differences ($p \leq 0.05$) for each treatment and among treatments for each storage time, respectively.

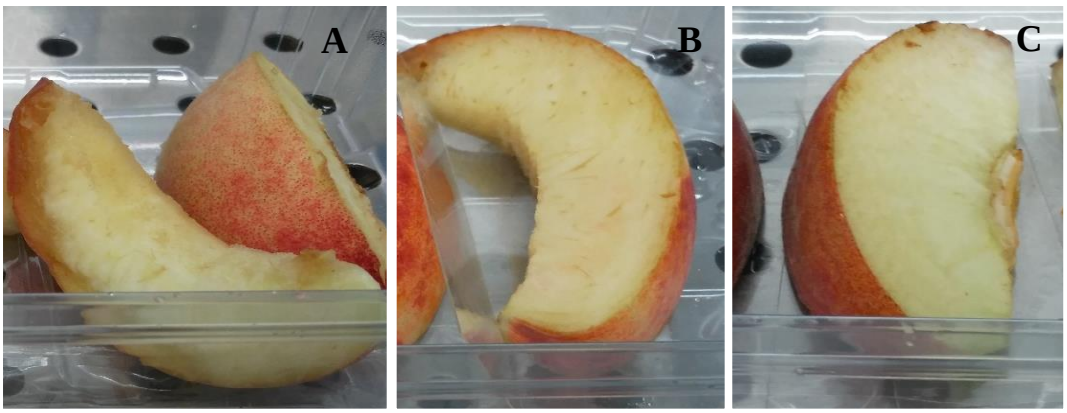

Figure 5.14. Visual appearance of peach slices for the different treatments: untreated (A), uncoated strips (B) and CRS strips (C).

In terms of flesh firmness, it was possible to see an increment of values and it is possible to explain this phenomenon trough two ways. First, arise of leatheriness phenomenon caused by storage temperature as documented by Lurie and Crisosto (2005); second, based on the cross-linking action of chitosan, investigated by several researchers (Bigucci et al., 2008; Berger et al., 2004), on flesh pectin molecules. Similarly happens with calcium complexing to cell wall and middle lamella polygalacturonic acid residues imparting improvement of structural integrity (Luna-Guzmán & Barrett, 2000). Comparing samples, LBL showed the higher value in flesh firmness. Permeability to water vapour is one of the most relevant functional properties of films during postharvest preservation of fruits and vegetables susceptible to water loss (Ayala-Zavala et al., 2013), during storage weight loss (WL) values showed higher loss for control in comparison with other treatments. The presence of PET strips influenced the weight loss of peach slices, avoiding loss around 2.50 ± 0.70 % of initial weight respect to 5.22 ± 0.09 the CTR. About TSS and TA, the values follow the normal postharvest behavior, no significant differences were observed.

Table 5.1. Evolution of chemical and physical indexes of peach slices after 7 d of storage (T7), PET coated by LbL sample (LBL), PET uncooated sample (UNC) and control (CTR). Data are means ± SD. Minor letters show significant differences ($p \leq 0.05$) among treatments.

	C*		Firmness kg cm^{-1}		WL %	TSS %		TA % of malic acid	
Time	T0	T7	T0	T7	T7	T0	T7	T0	T7
CTR	17.77 ±1.15	20.87^{b} ±3.03	3.97 ±0.46	4.08^{b} ±0.73	5.22 ±0.09	8.25 ±0.55	9.55ns ±0.02	0.808 ±0.09	0.710ns ±0.02
UNC	17.77 ±1.15	21.39^{ab} ±2.29	3.97 ±0.46	4.86^{b} ±1.33	2.48 ±0.68	8.25 ±0.55	8.99ns ±0.59	0.808 ±0.09	0.720ns ±0.06
LBL	17.77 ±1.15	22.89^{a} ±1.59	3.97 ±0.46	5.89^{a} ±1.54	2.50 ±0.70	8.25 ±0.55	9.53ns ±0.01	0.808 ±0.09	0.670ns ±0.08

Interesting results were obtained from chemical analysis. Total carotenoids content showed a decrease for all the samples. LBL treatment showed the lowest reduction of total carotenoids content (Fig. 5.15a), in accord to Srinivasa et al. (2002). Also the presence of PET strips could reduce the carotenoids decay.

About PPO activity, after 7 d of storage the results showed little increase in enzyme activity for LBL sample, while higher increase were seen in the controls (Fig. 5.15b). Although the polyphenols (added by the active packaging) represent the substrate for the PPO (for which would

expect an increase in PPO activity), chitosan, alginate and catechin exhibit metal chelation properties as reported in several studies (Li et al., 2011; Li et al., 2010; Yoneda & Nakatsubo, 1998; Facinò et al., 1996; Muzzarelli, 1973).

The oxidation slowdown, due to the presence of polyphenols substances presents in the coated LbL can protect the cut surface of ready-to-eat fruit products against oxidative processes, degradation and enzymatic browning, thus delay the senescence of the fruit (Rojas-Grau et al., 2009).

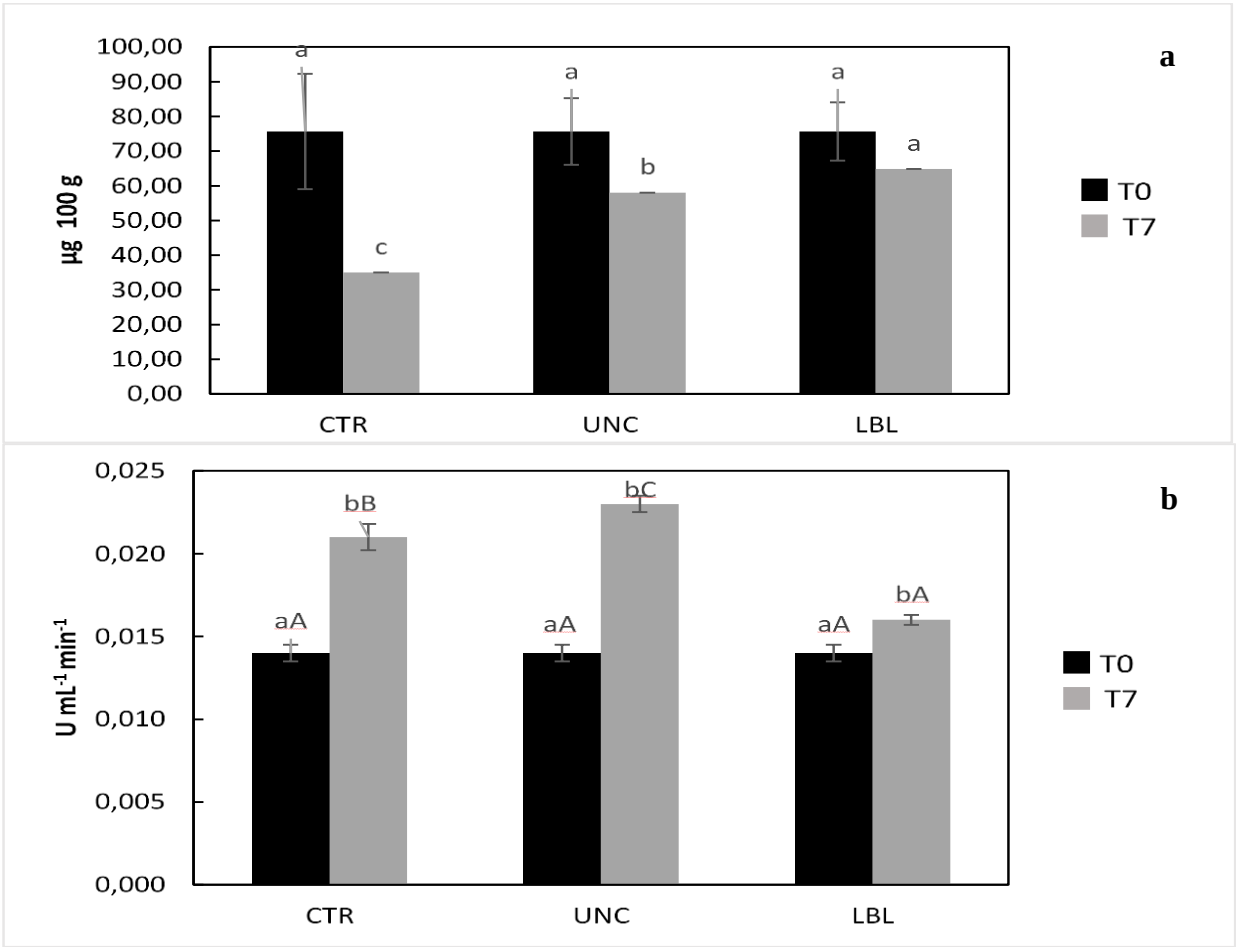

Figure 5.15. Evolution of total carotenoids content (a) and Polyphenol oxidase (PPO) (b) of peach slices, at time 0 (T0) and after 7 d of storage (T7). For CRS (LBL), uncoated strips (UNC) and untreated (CTR) samples. Data indicate ± SD. Minor and capital letters show significant differences ($p \leq 0.05$) for each treatment and among treatments for each storage time, respectively.

As regards microbiological trials, the results evidenced that psychrophiles and the total aerobic count (TAC) were the prevailing microbiota affected by the package: the first decreased to about 1 log in LBL samples respect either to CTR and UNC samples (from 2 to 1 log cfu g^{-1}) (Fig. 5.16).

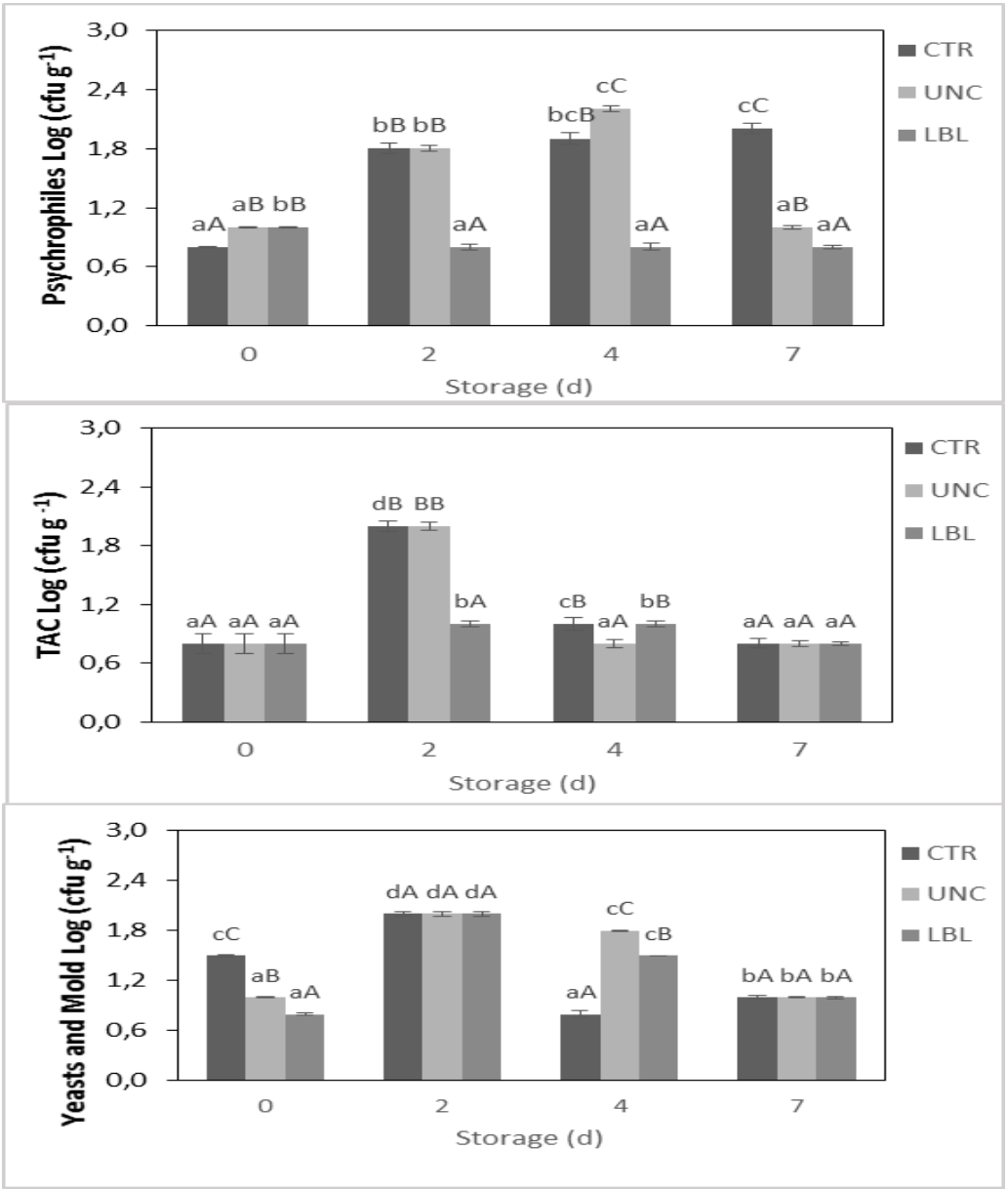

Figure 5.16. Time course of psychrophiles (above) Total Aerobic Count (TAC) (middle), yeasts and moulds (below) presence (log cfu g^{-1} peach) for CRS (LBL), uncoated strips (UNC) and untreated (CTR) samples. Data indicate ± SD. Minor and capital letters show significant differences ($p \leq 0.05$) for each treatment and among treatments for each storage time, respectively.

TAC after 2 days storage increased up to 2 log cfu g^{-1} in CTR and UNC sample, while remained around 1 log cfu g^{-1} in peach slices stored with controlled release system. After 2 d, psychrophiles were found significantly lower in LBL sample than the others two, this low value remains constant during all the storage period, while remains higher in CTR and UNC samples. Similarly occurred for the TAC population, but in this case the two controls sample showed a decrease after 4 d, keeping as the LBL sample. These results are in accordance with those reported by Siroli et al.

(2014) for minimally processed apples dipped in different antimicrobials comparatively: shelf life of fresh cut fruit is limitedly affected by microbial growth: independently from the addition of natural antimicrobials, the end of shelf life is mainly determined by changes in colour.

5.5. CONCLUSIONS

The effectives chitosan-alginate multilayers coating deposition, realised employing the Layer by Layer technique, was demonstrated by optical contact angle surface measurements and by atomic force microscopy. The coating growth followed a linear trend, as demonstrated by the increase of PET absorbance during the LbL assembly using fluorescein-isothiocianate labeled chitosan (FITC-CHIT).

The *in vitro* assays, allowed to confirm the incorporation of green tea antioxidant compounds inside the alginate layers and their gradual release from the coated PET during the extraction procedure. Indeed DPPH assay have shown an increasing antioxidant activity of the simulant solution as a function of the extraction time. HPLC analysis have confirmed the presence of gallic acid, water soluble phenols and flavonoids compounds. Also chitosan gradual release was confirmed by a qualitative microbiological assay.

The application on fresh-cut peach showed interesting results. As confirmed by colorimetric indexes, the visual appearance of peach stored with active packaging was better than the other samples. Promising results were obtained from carotenoids content evaluation and PPO activity measurements. Indeed, after 7 days of storage the LBL treated samples showed the best preservation of carotenoids and the lowest PPO activity. The observed carotenoids preservation should be related to the release of green tea antioxidants from the coating, while the lowest PPO activity could be related to chelating properties of chitosan and alginate. Microbiological trials demonstrated that psychrophiles were the prevalent microbiota affected by the active package. Indeed, while psychrophiles count increased during storage time for uncoated and control samples, it remained constant for the LbL treatment suggesting an inhibitory activity of the coating. Overall, these *in vivo* results allowed to suppose that the release of active substances from the LBL coating occurred also during the contact with food and that release could be effectiveness to produce positive effects on its shelf-life.

Further investigations will have the objective to compare the efficacy of LbL technique vs a normal coating procedure or conventional active molecules addition. Moreover: the type of active substances, various active substances should be applied to achieve the best effectiveness; the numbers of layers, the number of subsequent active layers should be modulated relating to the need.

5.6. REFERENCES

Ayala-Zavala, J.F., Silva-Espinoza, B.A., Cruz-Valenzuela, M.R., Leyva, J.M., Ortega-Ramírez, L.A., Carrazco-Lugo, D.K., Pérez-Carlón, J.J., Melgarejo-Flores, B.G., González-Aguilar, G.A. and Miranda, M.R.A. 2013, Pectin–cinnamon leaf oil coatings add antioxidant and antibacterial properties to fresh-cut peach. Flavour Fragr. J. 28, 39–45.

Aider, M. 2010. Chitosan application for active bio-based films production and potential in the food industry: Review. LWT-Food Sci. Technol. 43, 837-842.

Alvarez, M.V., Ponce, A.G. and Moreira, M.D.R. 2013. Antimicrobial efficiency of chitosan coating enriched with bioactive compounds to improve the safety of fresh cut broccoli. LWT-Food Sci. Technol. 50, 78-87.

Beaulieu J.C. and Gorny, J.R. 2004. Fresh-cut Fruits. p. 17. In: Gross, KC, C.Y. Wang, and M.E. Saltveit (eds.), USDA Handbook Nº 66. The commercial storage of fruits, vegetables, and florist and nursery stocks. 3rd edition, Washington D.C.: Agricultural Research Service.

Berger, J., Reist, M., Mayer, J. M., Felt, O., Peppas, N. A. and Gurny, R. 2004. Structure and interactions in covalently and ionically crosslinked chitosan hydrogels for biomedical applications. Europ. J. Pharm. Biopharm. 57, 19-34.

Bigucci, F., Luppi, B., Cerchiara, T., Sorrenti, M., Bettinetti, G., Rodriguez, L. and Zecchi, V. 2008. Chitosan/pectin polyelectrolyte complexes: Selection of suitable preparative conditions for colon-specific delivery of vancomycin. Europ. J. Pharm. Sci. 35, 435-441.

Brand-Williams, W, Cuvelier, M.E., Berset, C. 1995. Use of a free radical method to evaluate antioxidant activity. Food Sci. Technol. 28, 25–30.

Cao, J., Li, X., Wu, K., Jiang, W. and Qu, G. 2015. Preparation of a novel $PdCl_2$–$CuSO_4$–based ethylene scavenger supported by acidified activated carbon powder and its effects on quality and ethylene metabolism of broccoli during shelf-life. Postharv. Biol. Technol. 99, 50-57.

Chen, X., Wu, W., Guo, Z., Xin, J., Li, J., 2011. Controlled insulin release from glucose-sensitive self-assembled multilayer films based on 21-arm star polymer. Biomater. 32, 1759-1766.

Cuero, R., Duffus, E., Osuji, G. and Pettit, R. 1991. Aflatoxin control in preharvest maize: Effects of chitosan and two microbial agents. J. Agric. Sci. 117, 65–169.

De Dicastillo, C.L., Bustos, F., Guarda, A., Galotto, M.J. 2016. Cross-linked methyl cellulose films with murta fruit extract for antioxidant and antimicrobial active food packaging. Food Hydrocoll. 60, 335-344.

De Ritter, E. and Purcell, A.E. 1981. Carotenoids Analytical methods. In: Carotenoids as colorants and vitamin A precursors. ed: Bauernfeind JC. Academic Inc London LTD. Pp. 815-820.

Di Maio, L., Scarfato, P., Galdi, M.R., Incarnato, L., 2014. Development and Oxygen Scavenging Performance of Three-LayerActive PET Films for Food Packaging. J. Appl. Polym. Sci. 132, 1-10.

Decher, G. 1997. Fuzzy nanoassemblies: Toward Layered Polym. Multicomp. Sci. 277, 1232–1237.

Del Hoyo-Gallego, S., Pérez-Álvarez, L., Gómez-Galván, F., Lizundia, E., Kuritka, I., Sedlarik, V., Laza, J.M. and Vila-Vilela, J.L. 2016. Construction of antibacterial poly(ethylene terephthalate) films via layer by layer assembly of chitosan and hyaluronic acid. Carbohydr. Polym. 143, 35–43.

Dizaj, S.M., Lotfipour, F., Barzegar-Jalali, M., Zarrintan, M.H. and Adibkia, K. 2014. Antimicrobial activity of the metals and metal oxide nanoparticles. Mater. Sci. Engineer. C. 44, 278-284.

Donath, E. Sukhorukov, G.B., Caruso, F., Davis, S.A. and Möhwald, H. 1998. Novel hollow polymer shells by colloid-templated assembly of polyelectrolytes. Angew. Chem. Int. Ed. Engl. 37, 2202–2205.

El Ghaouth, A., Arul, J., Asselin, A. and Benhamou, N. 1992. Antifungal activity of chitosan on post- harvest pathogens: Induction of morphological and cytological alternations in *Rhizopus stolonifer*. Mycol. Res. 96, 769–779.

European Commission. 2004. European Commission Regulation (EC) No 1935/2004 of 27 October 2004 on materials and articles intended to come into contact with food and repealing Directives 80/590/EEC and 89/109/EEC. Official Journal of the European Union, OJ L 338 (2004), pp. 4–17.

Facinó, R. M., Carini, M., Aldini, G., Berti, F., Rossoni, G., Bombardelli, E. and Morazzoni, P. 1996. Procyanidines from Vitis vinifera seeds protect rabbit heart from ischemia/reperfusion

injury: antioxidant intervention and/or iron and copper sequestering ability. Planta Med. 62, 495-502.

Flessner, R.M., Jewell, C.M., Anderson, D.G. and Lynn, D.M. 2011. Degradable polyelectrolyte multilayers that promote the release of siRNA. Langmuir. 27, 7868-7876.

Fuentes-Perez, M., Nogales-Delgado, S., Ayuso, M. C. and Bohoyo-Gil, D., 2014. Different peach cultivars and their suitability for minimal processing. Czech J. Food Sci. 32, 413,421.

González-Buesa, J., Arias, E., Salvador, M.L., Oria, R. and Ferrer-Mairal, A. 2011. Suitability for minimal processing of non-melting clingstone peaches. Int. J. Food Sci. Technol. 46, 819–826.

Janeiro, P., Brett, A.M.O., 2004. Catechin electrochemical oxidation mechanisms. Anal. Chim. Acta 518, 109-115.

Kołodziejczyk, K. Milala, J., Sójka, M., Kosmala, M. and Markowski, J. 2010. Polyphenol oxidase activity in selected apple cultivars. J. Fruit Ornamental Plant. Res. 18, 51–61.

Li, F., Biagioni, P., Finazzi, M., Tavazzi, S. and Piergiovanni, L. 2013. Tunable green oxygen barrier through layer-by-layer self-assembly of chitosan and cellulose nanocrystals. Carbohyd. Polym. 92, 2128-2134.

Li, Y., Liu, F., Xia, B., Du, Q., Zhang, P., Wang, D. and Xia, Y. 2010. Removal of copper from aqueous solution by carbon nanotube/calcium alginate composites. J. Hazard. Mat. 177, 876-880.

Li, Y., Xia, B., Zhao, Q., Liu, F., Zhang, P., Du, Q. and Xia, Y. 2011. Removal of copper ions from aqueous solution by calcium alginate immobilized kaolin. J. Environ. Sci. 23, 404-411.

Luna-Guzmán, I. and Barrett, D.M. 2000. Comparison of calcium chloride and calcium lactate effectiveness in maintaining shelf stability and quality of fresh-cut cantaloupes. Postharv. Biol. Technol. 19, 61-72.

Lurie, S. and Crisosto, C.H. 2005. Chilling injury in peach and nectarine. Postharv. Biol. Technol. 37, 195-208.

Martín-Diana, A.B., Rico, D., Barry-Ryan, C., 2008. Green tea extract as a natural antioxidant to extend the shelf life of fresh-cut lettuce. Innov. Food Sci. Emerg. Technol. 9, 593–603.

Mascheroni, E., Guillard, V., Nalin, F., Mora, L. and Piergiovanni, L. 2010. Diffusivity of propolis compounds in Polylactic acid polymer for the development of anti-microbial packaging films. J. Food Engineer. 98, 294-301.

McHugh, T.H. and Senesi, E. 2000. Apple wraps: A novel method to improve the quality and extend the shelf life of fresh-cut apples. J. Food Sci. 65, 480-485.

Michalak, A. 2006. Phenolic compounds and their antioxidant activity in plants growing under heavy metal stress. Polish J. Environ. Stud. 15, 523–530.

Newman, A.W. and Kwok, D.Y. 1999. Contact angle measurement and contact angle interpretation. Adv. Colloid Interface Sci. 81, 167–249.

Robles-Sánchez, R.M., Rojas-Graü, M.A., Odriozola-Serrano, I., González-Aguilar, G. and Martin-Belloso, O. 2013. Influence of alginate-based edible coating as carrier of antibrowning agents on bioactive compounds and antioxidant activity in fresh-cut Kent mangoes. LWT-Food Sci. Technol. 50, 240-246.

Rocha, A.M.C.N. and Morais, A.M.M.B. 2003. Shelf life of minimally processed apple (cv. Jonagored) determined by colour changes. Food Control. 14, 13-20.

Rojas-Grau, M.A., Oms-Oliu, G., Soliva-Fortuny, R. and Martin-Belloso, O., 2009. The use of packaging techniques to maintain freshness in fresh-cut fruits and vegetables: a review. Int. J. Food Sci. Technol. 44, 875-889.

Rojas-Graü, M.A., Raybaudi-Massilia, R.M., Soliva-Fortuny, R.C., Avena-Bustillos, R.J., McHugh, T.H. and Martín-Belloso, O. 2007. Apple puree-alginate edible coating as carrier of antimicrobial agents to prolong shelf-life of fresh-cut apples. Postharv. Biol. Technol. 45, 254-264.

Senanayake, N. 2013. Green tea extract: chemistry, antioxidant properties and food applications – A review. J. Functional Foods. 5, 1529 –1541.

Siroli, L., Patrignani, F., Serrazanetti, D.I., Tabanelli, G., Montanari, C., Tappi, S., Rocculi, P., Gardini, F. and Lanciotti, R. 2014. Efficacy of natural antimicrobials to prolong the shelf life of minimally processed apples packaged in modified atmosphere. Food Cont. 46, 403-411.

Soliva-Fortuny, R.C., Grigelmo-Miguel, N., Odrizola-Serrano, I., Gorinstein, S. and Martin-Belloso, O. 2001. Browning evaluation of ready-to-eat apples as affected by modified atmosphere packaging. J. Agric. Food Chem. 49, 3685–3690.

Srinivasa, P., Baskaran, R., Ramesh, M., Prashanth, K.H. and Tharanathan, R. 2002. Storage studies of mango packed using biodegradable chitosan film. Europ. Food Res. Technol. 215, 504-508.

Sutherland, B.A. Rahaman, R.M.A. and Appleton, I. 2006. Mechanism of action of green tea catechins. With a focus on ischemia-induced. J. Nutr. Biochem. 17, 291-306.

Tang, Z., Wang, Y., Podsiadlo, P., Kotov, N. A., 2006. Biomedical applications of layer-by-layer assembly: from biomimetics to tissue engineering. Advan. Mater. 18, 3203-3224.

Wang, H.J., An, D.S., Rhim, J.W. and Lee, D.S. 2015. A Multi-functional Biofilm Use d as an Active Insert in Modified Atmosphere Packaging for Fresh Produce. Packag. Technol. Sci. 28, 999-1010.

Wohl, B.M. and Engbersen, J.F. 2012. Responsive layer-by-layer materials for drug delivery. J. Controlled Release. 158, 2-14.

Yoneda, S. and Nakatsubo, F. 1998. Effects of the hydroxylation patterns and degrees of polymerization of condensed tannins on their metal-chelating capacity. J. Wood Chem. Technol. 18, 193-205.

6. CHAPTER IV:

Comparison of cellulose nanocrystals obtained by sulfuric acid hydrolysis and ammonium persulfate, to be used as coating on flexible food-packaging materials.

(Co-author of the article Published on Cellulose, 2016, 23: 779-793)

6.1. ABSTRACT

Cellulose nanocrystals (CNCs), extracted from trees, plants, or similar cellulose-containing materials, can be used in combination with other materials to improve their performance or introduce new applications. The main purpose of this study was to compare and understand the potentialities of two types of CNCs, one produced by sulfuric acid hydrolysis (H_2SO_4) and the other one produced by a less common treatment with ammonium persulfate (APS), as coatings for Poly(ethylene terephthalate) (PET) films. The results showed that CNCs produced through the APS treatment showed higher charge densities, due to the carboxylic groups formed during the process, higher crystallinity, higher clarity of the solution and, as a consequence, higher transparency of the coating, while producing a similar crystallinity pattern. These characteristics provide a higher oxygen barrier with respect to the CNCs produced by the H_2SO_4 treatment, together with the availability of active sites for potential surface modification or chemical grafting. Both CNC coatings showed oxygen permeability coefficients that were lower than synthetic resins commonly used in flexible packaging. Furthermore, they did not significantly affect the optical properties of the substrate, while revealing good friction coefficients. . Due though to the moisture sensitivity of the coating and its non-sealable nature, similar to EVOH or PVOH oxygen barrier synthetic resins, CNCs developed using APS will need to be laminated with another plastic layer such as a polyolefin. They could then be used to enhance the final properties of packaging solutions as an alternative to conventional food-packaging materials for perishable food products, while reducing their environmental impact with a thin layer of a bio-based polymer.

KEYWORDS: cellulose nanocrystals, ammonium persulfate, oxygen permeability, film coating.

6.2. INTRODUCTION

Cellulose, the most abundant natural polymer on earth, can potentially become a widely-used renewable nanomaterial for various applications in both its forms: cellulose nanocrystals (CNCs) and cellulose nanofibrils (CNFs) (Li et al. 2015; Dufresne 2012). Two main approaches are commonly used for obtaining cellulose nanoparticles: mechanical treatments and acid hydrolysis, the latter being the classical method for CNC production.

The production of nanocellulose by acid hydrolysis is the most classical procedure for cellulose fragmentation (Nickerson and Habrle 1947; Favier et al. 1995; Håkansson and Ahlgren 2005; Bondeson et al. 2006; Elazzouzi-Hafraoui et al. 2008). The structure of cellulose is highly-debated in the scientific field (Belbekhouche et al. 2011; Nishiyama et al. 2009), but the measure of chemical reactivity showed the rupture of hydrogen bonding between O3H and the ring oxygen O5 only in the region of defects that are periodically present along the microfibril and due to the biological synthesis of the cellulose (Nishiyama et al. 2009). The dimensions and the morphologies of these particles mainly depend on the cellulose source and the process being used. Different acids have been tested and used in nanocellulose production (sulfuric, hydrochloric, phosphoric, hydrobromic and maleic acid (Filpponen 2009; Filson and Dawson-Andoh 2009; Okano et al. 1999) leading to distinct properties and morphologies of the CNCs. Concentrated sulfuric acid is the most common medium for the hydrolysis process, because it determines the formation of surface-charged sulfate ester groups on the cellulose chains which promote water dispersion of the nanoparticles, avoiding the aggregation phenomena observed using hydrochloric acid (Araki et al. 2000). This process is easy to apply and low energy-consuming, but it can be time-consuming, not eco-friendly and pre-treatments are necessary, starting from lignocellulosic matrices (Espino et al. 2014). This method is not able to eliminate lignin, hemicelluloses and other impurities within plant raw materials.

An alternative to these processes is ammonium persulfate (APS) (Leung et al. 2011). APS is a chemical that is widely-used as a strong oxidizer in polymer chemistry (Jayakrishnan and Shah 1984), as a cleaning and bleaching agent and as an etchant in various industries (Turrentine 1906). It has low long-term toxicity, high water solubility and low cost. Ammonium persulfate is generally preferred to potassium and sodium persulfates because of its higher solubility, lower pH, lower density and viscosity.

Persulfates decompose thermally in aqueous solutions by two independent reactions, which occur simultaneously (Kolthoff and Miller 1951):

(A) an un-catalyzed reaction leading to the symmetrical rupture of the O-O bond and the formation of two sulfate-free radicals which disappear reacting with water and producing anion bisulfate and atomic oxygen;

$$A:\ S_2O_8^{=} \overset{T}{\rightarrow} 2SO_4^{-\circ}$$

$$2SO_4^{-\circ} + 2H_2O \overset{T}{\rightarrow} 2HSO_4^{-} + 2HO^{\circ}$$

$$2HO^{\circ} \overset{T}{\rightarrow} H_2O + {}^{1}/_{2}\, O_2$$

(B) an acid-catalyzed reaction leading to the unsymmetrical rupture of the O-O bond to form sulfur tetroxide and bisulfate.

$$B: S_2O_8^{=} + H^{+} \overset{T}{\rightarrow} HS_2O_8^{-}$$

$$HS_2O_8^{-} \overset{T}{\rightarrow} SO_4 + HSO_4^{-}$$

$$SO_4 \overset{T}{\rightarrow} SO_3 + {}^{1}/_{2}\, O_2$$

In diluted acidic solutions, sulfur tetroxide decomposes to form atomic oxygen and sulfuric acid, but if the acidic concentration increases (> 0.5M), the sulfur tetroxide reacts with water (Gall et al. 1943; Beer and Muller 1962) leading to mono peroxysulfuric acid (Caro's acid, H_2SO_5), which is patented as an effective delignification agent (Springer,Minor 1991).

$$SO_4 + H_2O \overset{T}{\rightarrow} H_2SO_5$$

$$H_2SO_5 + H_2O \overset{T}{\rightarrow} H_2O_2 + H_2SO_4$$

Therefore, the uniqueness of this treatment is that a simultaneous hydrolysis and oxidation process of cellulose fibers occurs on the surface and within the inner amorphous regions, due to the fast penetration of free radical ions (SO_4^{-}) and H_2O_2 through the lumen of the fibers. In addition, the effectiveness of the phenomena is related to the progressive increase in acid concentration and the generation of peroxysulfuric acid.

Recent literature reports that APS is able to produce CNCs from different types of lignocellulosic materials containing up to 20% of lignin. The process has been patented as an effective method to produce CNCs from renewable biomass (Leung et al. 2012; Leung et al. 2011). The reaction conditions, such as reaction time, temperature and APS concentration, can be tuned to provide satisfactory yields and crystals with different aspect ratios. Moreover, this treatment gives the opportunity to obtain carboxylated CNCs and to increase the degree of crystallinity (Cheng et al. 2014). It is well known that carboxyl groups on the surface of materials can provide active sites for template synthesis of nanoparticles, surface modification and chemical grafting (Ifuku et al.

2009; Qi et al. 2011; Arola et al. 2012). The oxidized cellulose obtained by APS treatment shows a higher charge density that can improve interface interactions. Furthermore, the polymer crystallinity generally leads to better mechanical properties and higher gas barrier properties (Lasoski and Cobbs 1959; Salame 1989; Miller and Krochta 1997).

These specific characteristics of the CNCs obtained through the APS treatment, taken together with the huge availability of lignin containing cellulose sources in agricultural biomasses as well as in industrial byproducts, addressed our research towards the potential uses of these carboxylated cellulose nanocrystals as coatings for high-performing and more sustainable flexible packaging materials (Li et al. 2013b; Li et al. 2013a). A process able to attain large amounts of CNCs from cheap and largely-available sources would be of interest to the sector producing packaging materials, in that it would supply novel materials that perform better and are more sustainable, and come from renewable sources. So far, however, to our best knowledge, an accurate comparison does not exist between CNCs obtained by the two processes and addressed to their potential use as coating for flexible packaging materials., In this paper, therefore, we propose a comparison between the cellulose nanocrystals obtained by sulfuric acid hydrolysis and APS oxidation-hydrolysis starting from the same cotton linters, and a characterization of PET films coated with the two differently-obtained CNCs, intended for food packaging applications.

6.3. MATERIALS AND METHODS

6.3.1. Materials

Cotton linters used as raw material to produce CNCs were kindly supplied by Innovhub (Milan, Italy). Sulfuric acid 96%, ammonium persulfate ≥98%, hydrochloric acid 37%, sodium hydroxide ≥97%, ion exchange resin Dowex Marathon MR-3 were purchased from Sigma-Aldrich (Milan, Italy).

Poly(ethylene terephthalate) (PET) film, having a thickness of 12±0.5 μm, was provided by Sapici s.p.a (Cernusco sul Naviglio, Italy)

6.3.2. CNC extraction by Sulfuric Acid hydrolysis

Cellulose nanocrystals (CNCs) were obtained from cotton linters by a common procedure used by many Authors (Dong et al. 1996; Li et al. 2013b). Milled cotton linters were hydrolyzed by 64% w/w sulfuric acid under vigorous stirring at 45 °C for 45 minutes (fibers/acid ratio 1:17.5 g/mL). To quench the reaction, the mixture was diluted ten times with deionized water (18 MΩ cm, Millipore Milli-Q Purification System). The solution was centrifuged 5 times at 10000 rpm for 15 minutes with the addition of deionized water each time in order to remove the excess acid until the supernatant became turbid. For further purification, the centrifuged solution was posed inside dialysis tubes (Molecular Weight Cut off 12000 Da) immersed in deionized water for 72 hours to remove any acid still present and the low molecular weight contaminants. The suspension was then sonicated (UP 400S 400 W, Hielscher ultrasonics GMBH, Teltow, Germany) repeatedly (cycles 0.7, time 5 minutes at 70% output) to bring cellulose crystals to colloidal dimensions. During the ultrasonic treatment, the suspension was cooled with an ice water bath to avoid overheating. Ion exchange resin was added to the sonicated suspension (resin/solution ratio 10:1 g L^{-1}) scavenging any residual ions. After that, the suspension was filtered under vacuum, using Munktell filter discs GF/C 1.2 μm in order to remove the largest fiber agglomerates and any microfibers possibly present. The cellulose content of the resulting aqueous suspension was determined by drying several samples (1 mL) at 105 °C overnight. The pH of purified suspensions was adjusted to 8 by 1M NaOH in order to gain fully-charged CNCs.

Secondly, the dispersion was frozen at -18 °C overnight and then moved to a freeze dryer (LIO-10P, Cinquepascal, Trezzano sul Naviglio, Italy). Finally, the freeze-dried powder obtained was stored in tightly-closed bottles under dry conditions.

6.3.3. CNC extraction by Ammonium Persulfate treatment

The CNCs were produced from cotton linters by the hydrolyzing-oxidative method proposed by Leung and coworkers in 2011 (Leung et al. 2011). Milled cotton linters and 1M ammonium persulfate (APS) (ratio between fibers and APS 10:1 g L^{-1}) were introduced into a large beaker, onto a magnetic stirrer hotplate, equipped with a Vertex Digital thermoregulator (VELP Scientifica, Usmate, Italy). The mixture was heated and continuously stirred at 75 °C for 16 hours, limiting the evaporation by means of an aluminum foil cover. The suspension of the CNCs obtained was centrifuged at 10000 rpm for 15 minutes with the addition of deionized water in order to rinse the suspension. The centrifugation and washing procedure was repeated 4 times until the pH of the suspension was around 4. In order to have the sodium form of CNCs, NaOH 1M was added until the suspension reached pH 8 and then it was sonicated for 15 minutes (0.7 cycles, 70% output). The purified suspension was frozen at -18 °C overnight and freeze-dried. Finally, the freeze-dried powder obtained was stored in tightly closed bottles under dry conditions.

6.3.4. Morphological characterization of the CNCs

Drops of aqueous dispersions of CNCs 0.5% w/w were deposited on carbon-coated electron microscope grids, negatively stained with uranyl acetate and allowed to dry. The samples were analyzed with a Hitachi Jeol-10084 transmission electron microscope (TEM) operated at an accelerating voltage of 80kV. Representative micrographs were selected for measuring the diameter and length of the nanocrystals by digital image analysis (Image-Pro Plus software). The aspect ratio was also calculated. Average lengths and diameters of the crystals were determined by analyzing 70 crystals.

In addition, the hydrodynamic size distributions of diluted aqueous dispersions of the CNCs were determined by dynamic light scattering (DLS) (Malvern Instruments Nano Series Zetasizer optical units). Measurements were performed at 23.0 ± 0.1 °C with a class 14 mW continuous wave He–Ne laser light (λ = 632.8 nm). The scatterers in solution were undergoing Brownian motions, constantly changing their instantaneous positions and thus causing temporal fluctuations in the scattered light intensity. By applying correlation analysis and the Stokes-Einstein relation, the hydrodynamic dimension and the size distribution of the scatterers was calculated (Berne,Pecora 2000). Prior to DLS measurement, the samples were diluted to 1:500 (w/w) with distilled water that was previously adjusted to pH 8 and maintained at 25 °C through stirring until measurement.

1 ml of the diluted solution was injected in the measurement cell after 30 s homogenization with an ultrasonic bath.

6.3.5. Determination of the degree of oxidation (DO) of the CNCs, charge density and clarity of the CNC solutions.

Conductometric titrations were performed to determine the carboxylic acid content of the CNCs. 50 mg of dry powders of CNCs were suspended into 15 mL 0.01M HCl for complete protonation of the COOH groups, and sonicated for 10 mins to disperse the nanocrystals. The CNC suspensions were then titrated against 0.01M NaOH and the carboxylic acid contents were determined from the resulting conductivity curves. The DO of the CNCs was calculated using the following equation:

$$DO = \frac{162(V_2 - V_1)C}{w - 36(V_2 - V_1)C}$$

where (V_2-V_1) is the volume of NaOH (L) required to deprotonate the carboxylic acids groups, C is the concentration (M) of NaOH, w is the weight of the CNCs samples, the values 162 and 36 correspond to the molecular weight of an anhydroglucose unit (AGU) and the molecular weight difference between an AGU and sodium gluconate, respectively.

The degree of oxidation (DO) was also quantified used FTIR spectra. The FTIR spectroscopy was performed with a Perkin Elmer instrument (Spectrum 100), equipped with ATR, at room temperature, on the CNCs in their acidic form (pH=2). The data was collected over 64 scans with resolutions of 4 cm^{-1} and the DO was calculated by the ratio of the intensity of the carbonyl peak (absorbance bands at 1735 cm^{-1} (ν (C=O) in the acid form)) to that of the band near 1060 cm^{-1}, relating to the backbone structure of cellulose. The equation used in this case is the following:

$$D0 = 0.01 + 0.7(I1735 - I1060)$$

Surface charge density was estimated using the dimensions of the CNC determined by TEM, assuming a cylindrical shape and a density of 1.6 g/cm^3 for cellulose nanocrystals (Beck-Candanedo et al. 2005). The clarity of the CNCs' water solution at 7% w/w was also tested after ultrasound treatment for 15 minutes (0.7 cycles, 70% output). The turbidity of the solution was measured using a spectrophotometer at λ=600nm.

6.3.6. Cristallinity evaluation by Solid-state nuclear magnetic resonance (NMR) spectroscopy and by X-ray diffraction (XRD).

All NMR spectra (three replications for each type of CNC) were acquired at room temperature on a Bruker AVANCE-600 spectrometer (Bruker Spectrospin GmbH, Rheinstetten, Germany), equipped with a 4 mm broad-band CP-MAS probe for solid state measurements. About 100 mg of a CNC sample were directly pressed into a 4 mm ZrO_2 rotor without further treatment. 13C spectra were acquired at 150.9 MHz using Cross Polarization (CP) and Magic Angle Spinning (MAS) at 6-10 kHz (Pines et al. 1973). Proton decoupling was achieved with a GARP-based composite pulse. Standard acquisition parameters were as follows: Spectral width: 75.7 kHz; acquisition time: 3.4 ms; relaxation delay: 2 s (fast acquisition conditions); contact time for Cross Polarization: 1 ms; number of scans: 7000-24000. The contact time was optimized by systematic variation of the corresponding pulse within the 0.3-3.0 ms range. Adamantane was used as the external chemical shift reference.

Measurement of X-ray diffraction was conducted using an X-ray diffractometer (D8-Advance Bruker AXS GmbH) at room temperature with a monochromatic Cu-Ka radiation source (Wavelength 1.5418 Å) in the step-scan mode with a 2θ angle ranging from 5° to 59.98° with a step size of 0.02 and 2750 number of points. The freeze-dried CNC powders were placed on the sample holder and leveled to obtain uniform X-ray exposure.

Diffraction peaks were profile-fitted using the WinPLOTR program (Roisnel et al. 2001). Peaks were fitted by a Pseudo-Voigt function with a fixed Lorentzian component η=0.75 and refinable background, peak width at half maximum (pwhm), position, and intensity.

NMR analysis was used to provide the relative masses of crystalline and amorphous material. A Gaussian function was used to perform the deconvolution of the C4 peaks. CI was calculated by dividing the area of the crystalline peak (integrating the peak from 87 to 93 ppm) by the total area assigned to the C4 peaks (integrating the region from 80 to 93 ppm).

XRD diffraction were carried out to determine the crystal type (polymorph). Diffraction patterns from cellulose Iα and Iβ were calculated based on the published atomic coordinates and unit cell dimensions contained in modified “crystal information files” (.cif). Diffraction intensities, output by Mercury program (3.0) from the Cambridge Crystallographic Data Centre, was compared with the experimental data (French, 2014, Nishiyama et al., 2012).

6.3.7. Thermogravimetric analysis (TGA)

TGA was carried out to determine the thermal stability of the different kinds of CNCs by employing a thermogravimetric analyzer Perkin Elmer, TGA 4000. Samples were heated from 30 °C to 800 °C under air or nitrogen atmosphere at a heating rate of 10 °C min^{-1}; three replications were done for each CNC type.

6.3.8. Coating process

A 7% wt CNC water dispersion (pH = 8) was coated onto PET 12 μm film, according to ASTM D823-07, practice C. After activation of the external side of the substrate by using a corona treater, (Arcotech GmbH, Monsheim, Germany), the CNC solution was coated by an automatic film applicator (model 1137, Sheen Instruments, Kingston, UK) at a constant speed of 2.5 mm s^{-1}. Water was evaporated using a constant mild air flow (25 ± 0.3 °C for 5 minutes).

6.3.9. Transparency, Haze and Water Resistance of the coatings

The transmittance of the sample was measured at 550 nm, according to the ASTM D 1746-70, by means of a Perkin-Elmer L650 UV-VIS spectro-photometer. Haze (%) was measured in accordance with ASTM D 1003-61 with the same instrument equipped with a 150 mm integrating sphere. Each sample was replicated three times, by analyzing four spots for each replica. The moisture sensitivity of the hydrophilic coatings was determined by using an empirical test, measuring the weight losses after 4 days of immersion in a water bath at 37 $\pm$ 0.5 °C, of ten samples (diameter 12 mm) cut from the two CNC coated PET films. Samples of the two kinds of CNCs were submerged in distilled water, avoiding any floating then wiped, dried and weighed to measure the weight loss (%).

6.3.10. Thickness

The thickness of the two different CNC coatings was measured analyzing the cross section by Scanning Electron Microscopy (SEM). Scanning electron microscopy images were obtained from a Sigma Field Emission microscope (Carl Zeiss Microscopy, LLC) at 5 kV accelerating voltage and 6 mm working distance, with a 30 m width slit. The samples were first gold-sputtered (Sputtering Polaron E 5100) for 30 s (rate 1 nm s−1) with argon and 18 mA current intensity.

6.3.11. Oxygen Permeability measurements

The oxygen permeability (PO_2) of CNC-coated plastic films was assessed (mL m^{-2} d^{-1} bar^{-1}) by an isostatic method (Multiperm, Extra_Solution S.r.l. Capannori, Italy) at 23 °C and two different relative humidity values (0% and 50% RH), complying with ASTM D-3985. The oxygen permeability coefficients of the CNC coating alone (i.e., KPO_2 of the coating) were calculated using the following equation (Crank 1979) and assuming that the substrate surface (PET film) did not interact with the CNC coating above and that the interface between them negligibly affected the final permeation measure.

$$\frac{L}{KPO_2(coating)} = \frac{1}{PO_2(coated\ film)} - \frac{1}{PO_2(bare\ film)}$$

6.3.12. Contact angles and surface energies

Self-standing films of the two different CNCs were obtained by casting, leaving their suspension evaporate at pH 7 for one night at 30 °C in Petri dishes Ø 9 cm. Their surface-free energies (SFE) were determined by measuring static contact angles of polar Milli-Q water (18.3 MΩ cm) and apolar diiodomethane (99%, Sigma Aldrich), using an OCA 15 Plus angle goniometer (Data Physics Instruments GmbH, Filderstadt, Germany), then elaborated by the Owens-Wendt-Rabel and Kaelblem (OWRK) method (Owens and Wendt 1969; Kaelble 1970). The measurements of static contact angles were performed at room temperature, on five different positions for each sample. The sessile drop method was used, by gently dropping a droplet of 4.0 ± 0.5 μL of each liquid onto the substrate. The instrument was equipped with a high-resolution CCD camera and a high performance digitizing adapter. SCA20 and SCA21 software (Data Physics Instruments GmbH, Filderstadt, Germany) were used, respectively, for contact angle measurements and surface energy calculation. According to the OWRK theory, the SFE is divided into two distinct parts, i.e. the polar γ_s^P and dispersive γ_s^D. These components are the square values, respectively, of slope and intercept of the following first order equation:

$$\frac{\gamma_l(1+\cos\theta)}{2\sqrt{\gamma_l^D}} = \sqrt{\gamma_s^P}\left(\frac{\sqrt{\gamma_l^P}}{\sqrt{\gamma_l^D}}\right) + \sqrt{\gamma_s^D}$$

Knowing, therefore, the polar and dispersive components (γ_l^P, γ_l^D) of at least two liquids (the ones used in this work are reported in Table 6.1), and the corresponding apparent contact angles of these

liquids onto the solid surface of interest, a linear regression permits to estimate the SFE components γ_s^P and γ_s^D.

Table 6.1 Surface tension parameters of the liquids used in contact angle determination (in mJ/m^2) at 20 °C (van Oss 2003)

Liquid	γ_l	γ_l^D	γ_l^P
Water	72.8	21.8	51
Diiodomethane	50.8	50.8	0

6.3.13. Coefficient of Friction

The static (μ_S) and dynamic (μ_D) friction coefficients (COF) were measured by a dynamometer (model Z005, Zwick Roell, Ulm, Germany), according to the standard method ASTM D 1894-87. Firstly, the uncoated side of CNC-coated film was attached on a specific sled (6.2×6.2 cm^2, 197.99 g), while the un-coated film was covered on the sliding plane (exposing the un-treated side). Then the sled was connected to the force sensor of a dynamometer and horizontally pulled by the instrument on the covered sliding plane. The raw data (pulling force) was recorded and analyzed by TestXpert software V10.11 (Zwick Roell, Ulm, Germany).

6.4. RESULTS AND DISCUSSION

6.4.1. CNC characterization

The two different processes used on the same batch of cotton linters each produced cellulose nanocrystals that then were characterized to determine the differences in the CNCs obtained.

The CNCs were characterized in terms of morphology with TEM (Fig. 6.1a; Fig. 6.1b) and hydrodynamic size distribution (DLS), (Fig. 6.2). Electron micrographs show quite similar rod-like shapes with comparable rod diameters (Tab. 6.2) for both sets of CNCs.. The higher values were measured for the
CNCs achieved through the APS process.

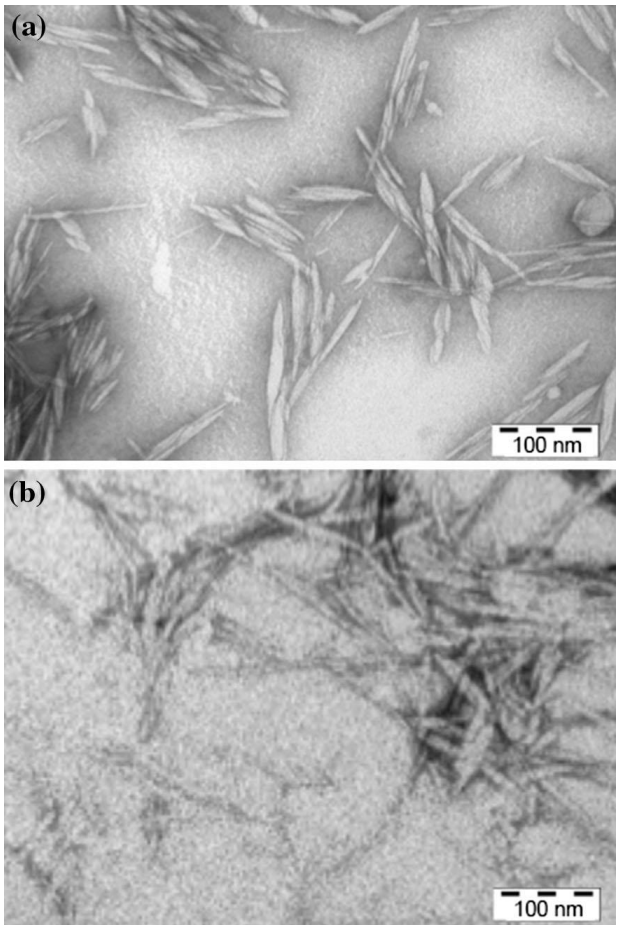

Figure 6.1a Transmission Electron Migrograph (TEM) of cotton linters nanocrystals obtained by APS

Figure 6.1b Transmission Electron Migrograph (TEM) of cotton linters nanocrystals obtained by H_2SO_4

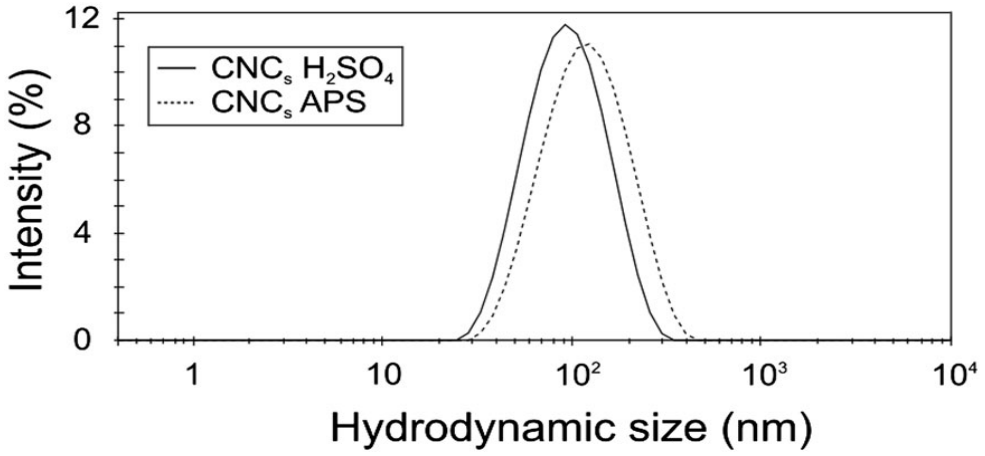

Figure 6.2 CNC hydrodynamic size distributions obtained with DLS

The fact that the CNCs are not spherical poses some issues on the sizes calculated by DLS, which analyzes the data in spherical approximation, mathematically treating the CNCs as spheres moving with Brownian motion independently from their real physical morphology. Particularly, when a rod-like particle is subjected to Brownian motion, it will be dragged along and rotate, in a similar way to a spherical particle. Differently from spheres, the hydrodynamic stresses will depend on the relative orientation of the rods, causing an anisotropic motion of the scatterer (Mewis and Wegner 2012). Prolated rod-like structures of length L are detected by DLS as equivalent Brownian spheres with a smaller average size (Kroeger et al. 2007). The average TEM Length dimension matches the DLS measured size distribution (Tab. 6.2 and Fig. 6.2), indicating the good overlap between size distribution in CNC solution and electron micrographies (EM) of drop-casted CNCs. Such an average size persistence in presence of strong capillary forces associated to drying and absorption before EM measurements underlines the stability of the morphology of both the CNCs obtained (Kralchevsky and Nagayama 1994).

Table 6.2 TEM/Image and hydrodynamic size distribution of dispersed CNCs.

CNC	TEM-Image ProPlus			DLS	
	Length (nm)	**Diameter (nm)**	**L/d**	**Nanocrystal size in uniform spherical approximation (nm)**	*PDI**
$CNCs_{H_2SO_4}$	110 ± 47	6.7 ± 2.3	16.4 ± 8.9	80.8	0.19
$CNCs_{APS}$	121 ± 46	6.2 ± 0.9	19.7 ± 8.0	101.2	0.23

* polydispersity index, defined as $PDI = (\sigma/D)^2$, is a measure of the width of particle size distribution

The length of the nanocrystals, in particular, can be relevant in networking consolidation during the coating process. The similar values and the uncertainty of the measures of the aspect ratio of crystals from the two preparations leads to assume similar dimensions of the crystals. Other important analyses for the goal of this research are the chemical indexes assessed by XRD, NMR, FTIR and conductometric titrations. NMR analysis with deconvolution based on a Gaussian Equation is often used to interpret the diffraction profile to provide the relative masses of crystalline and amorphous material in a given sample (Nishiyama et al. 2013). In this specific case, the values are 62.6±1.1 % for $CNCs_{H_2SO_4}$ and 63.8±1.2% for $CNCs_{APS}$ therefore no significant difference in crystallinity content is present.

More interesting is the analysis of X-ray diffraction patterns of our samples, and their comparison to XRPD patterns of the cellulose Iα and Iβ phases (Nishiyama Y, 2003; Nishiyama Y, 2002) simulated using the Mercury program.

Experimental and simulated patterns are shown stacked in Fig. 6.3. The position and relative intensities of the most intense peaks of both $CNCs_{H_2SO_4}$ and $CNCs_{APS}$ are more consistent with the Iβ phase. Thus, the peaks discussed in the following crystallite-size analysis were indexed according to the higher-symmetry Iβ phase. A spurious peak is visible at 2θ=32° in the $CNCs_{H_2SO_4}$ pattern, due to contamination occurring during CNC production through the H_2SO_4 process in form of K_2SO_4.

Crystallite size was evaluated on the three main peaks by means of the Scherrer equation (Patterson 1939), which relates the peak width β and the peak position θ to the minimum coherent diffraction length τ.

$$\tau = \frac{K\lambda}{\beta \cos\theta}$$

The value of the sample "shape factor" K can range from 0.6 to 2.08. In the present analysis K was set to 1.0, as previously used by Nishiyama (Nishiyama et al 2012). Peak width at half maximum (pwhm) was determined using WinPLOTR as described in Paragraph 2.6. The crystallite size values thus calculated are reported in Table 6.3 together with the respective pwhms. Width of the (200) peak in $CNCs_{APS}$ is smaller than in $CNCs_{H_2SO_4}$, resulting in crystallite sizes τ=6.3 nm and τ=5.5 nm, respectively. These two τ values account for 16 and 14 coherently stacked planes in the direction perpendicular to the (200) planes. Both values fall short of the 19 theorical interplanar spacings expected for the 100-chain crystal (τ=7.4 nm), as reported in previous works on CNC (Nishiyama et al, 2012). The values in Table 6.3 indicate that a preferential stacking of chains along (200) occurs, and good agreement is found with the size obtained from TEM (shown in Table 6.2). However, a larger size of $CNCs_{H_2SO_4}$ was inferred from TEM analysis, since TEM is not able to discriminate the amorphous and the crystalline parts of the sample.

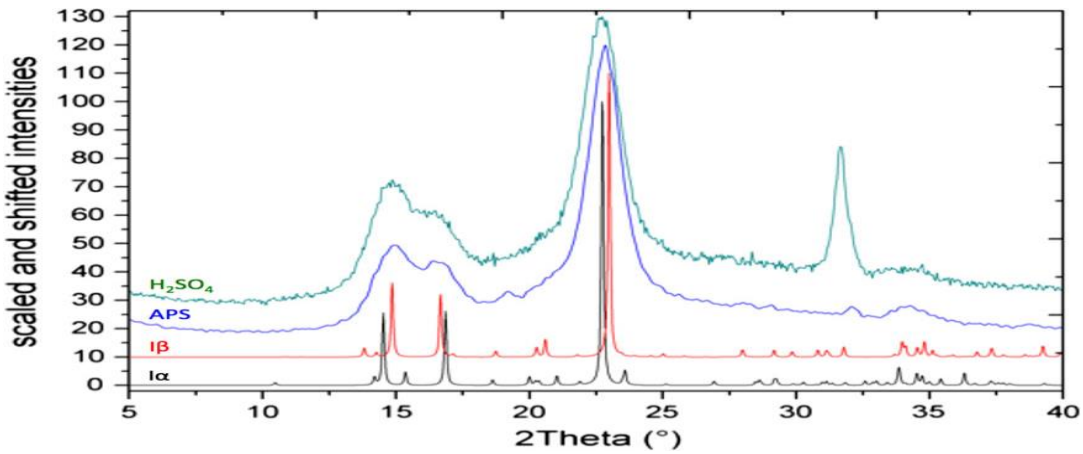

Figure 6.3. Powder diffraction patterns calculated with Mercury software based on cellulose Iα (Black line) and Iβ (red line) crystal structure (pwhm = 0,1°) and experimental powder diffraction patterns obtained by CNCs from APS (blu line) and from H_2SO_4 (green line)

Table 6.3. Crystallite size values with the respective pwhm

CNCs	Crystalline Plane (Miller index of Iβ)	pwhm [deg]	Peak position (2θ) [deg]	τ (nm)
APS	1 -1 0	1.45	14.79	6.1
	1 1 0	2.23	16.58	4.0
	2 0 0	1.41	22.83	6.4
H_2SO_4	1 -1 0	1.47	14.69	6.1
	1 1 0	2.65	16.35	3.4
	2 0 0	1.64	22.69	5.5

Because of the strong oxidative potential of the APS treatment, an essential characterization of the two different CNCs produced is related to the degree of oxidation and an assessment of the charge density. Both FTIR spectra and conductometric titrations were carried out for this purpose and the overall results obtained are reported in Table 6.4. FTIR spectra of $CNCs_{APS}$ (Fig. 6.4) clearly show the typical absorption bands of carboxylic groups. The two peaks recognizable in the inset of Fig. 6.4 are referable, according to Lam (Lam et al. 2013), to C=O stretching peaks of the carboxylic group (1733 cm^{-1}) and to $COO^-NH_4^+$ (1630 cm^{-1}), respectively.

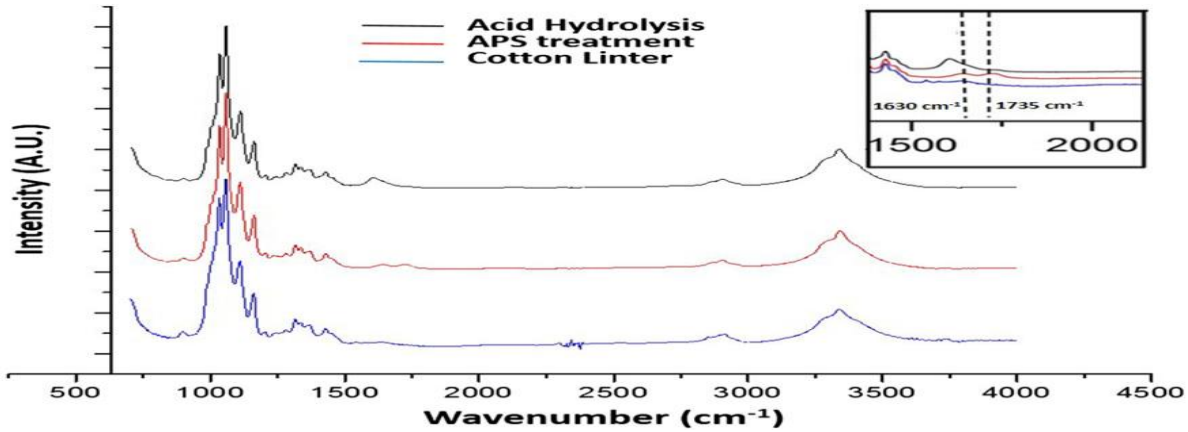

Figure 6.4. FTIR spectra and enlargement recorded for raw cotton linters (blue line), from the CNCs obtained by sulfuric acid hydrolysis (black line) and CNC-COOH produced by APS treatment (red line)

Concentration of COOH groups resulted to be 0.98 mmol g^{-1} of cellulose nanocrystals, leading to an oxidation degree around 0.15. According to Elazzouzi-Hafraoui (Elazzouzi-Hafraoui et al. 2009) and assuming that all the glucose units on the surface of each nanocrystalline cellulose

particle are completely carboxylated, the charge content measured provides an estimate of the diameter of the nanocrystals in the range of 6 and
10 nm (Yang et al., 2013) and this value is in agreement with the data obtained with TEM and XRD analyses. The charge density that was accounted for with $CNCs_{APS}$ is 4.5 times the value obtained for sulfuric acid hydrolysis and this achievement seems consistent with the goal of producing a suspension that can be casted, as a thin and functional coating, on the activated surface of flexible packaging materials.

Table 6.4 Extraction yield (%), degree of oxidation (DO) and charge density of the CNCs

CNCs	**Yield (%)**	**DO**		**COOH content (mmol g^{-1})**	**Sulfur Content (mmol g^{-1})**	**Charge density (e/nm^2)**
		Conductimetric	**FTIR**			
$CNCs_{H_2SO_4}$	52.7	-	-	-	0.21 ± 0.9	0.32
$CNCs_{APS}$	34.4	0.15	0.16	0.98 ± 0.10	-	1.46

The results concerning the degree of oxidation and the charge densities of the two different CNCs appear well-correlated to the values of contact angles and surface energies, measured on specimens obtained by casting the cellulose nanocrystals from their 7% suspension in water (pH = 7), and reported in Table 6.5. Both the samples presented water contact angles consistent with high hydrophilicity: this was largely expected due to their cellulosic origins. The value, however, of sample from the APS process is lower, showing a much higher wettability. Surface free energies (SFE) were also measured using the static contact angles of apolar diiodomethane, by means of the Owens-Wendt-Rabel and Kaelblem (OWRK) method, and they too showed a significant difference between the two samples. CNCs from the APS process had a surface-free energy which was 13.6% higher than that of the CNCs coming from sulfuric acid hydrolysis. This was mainly due to the polar part of this energy (32.54 versus 21.71 mN/m), in accordance with the large presence of carboxyl groups in the cellulose nanocrystals obtained using ammonium persulfate. It

is reasonable to assume that such a high surface energy can be useful in anchoring the CNC layer onto a common activated substrate.

Table 6.5: Static contact angles (θ) and Surface Energy (SFE) of the CNCs in form of thin casted films.

CNC	θ Water	θ DIM	Polar part (mN/m)	Dispersive part (mN/m)	SFE (mN/m)
$CNCs_{H_2SO_4}$	45.72 ± 1.69	44.39 ± 1.87	21.72	37.34	59.09
$CNCs_{APS}$	29.29 ± 1.73	49.67 ± 3.23	32.54	34.46	67.01

The yields recorded for the two processes are rather different, with the APS treatment yielding just 34,4% in comparison with almost 53% of the sulfuric acid hydrolysis. It is worth noting that these values are only indicative and related to a specific lab-scale production process. In particular, they strongly depend on the preparation condition and post-treatment filtration. The extraction yield should correspond to the proportion of crystalline domains of the cellulosic raw materials, but usually lower yields are obtained. Possibly, continued action of reactive agents like acids for a long time could cause dissolution of cellulose in crystallites (Dufresne 2012), or other reaction by-products.

Thermal stability of the CNCs was also tested, given its importance for thermoplastic applications where the processing temperature is often above 200 °C. In the literature, different degradation temperatures for nanocrystals are reported because the degradation temperature depends on different experimental variables (Roman and Winter, 2004).

In this case (Fig. 6.5), TGA curves report a small loss (about 6%) from 30 °C until 250 °C, where cellulose undergoes its most important degradation. Even if the TGA analysis was performed in the temperature range between 30 °C and 800 °C, only the range from 100 °C to 500 °C is reported in Fig. 6.5, because this is the zone where the differences between the samples are more visible and the behavior is more influenced by the CNCs' production process and by the initial humidity of the samples. During the hydrolysis reaction, for example, the sulfate or hydroxyl groups are introduced on the surface of the nanoparticles, giving at the same time improved stability of the aqueous suspension and lower thermal stability.

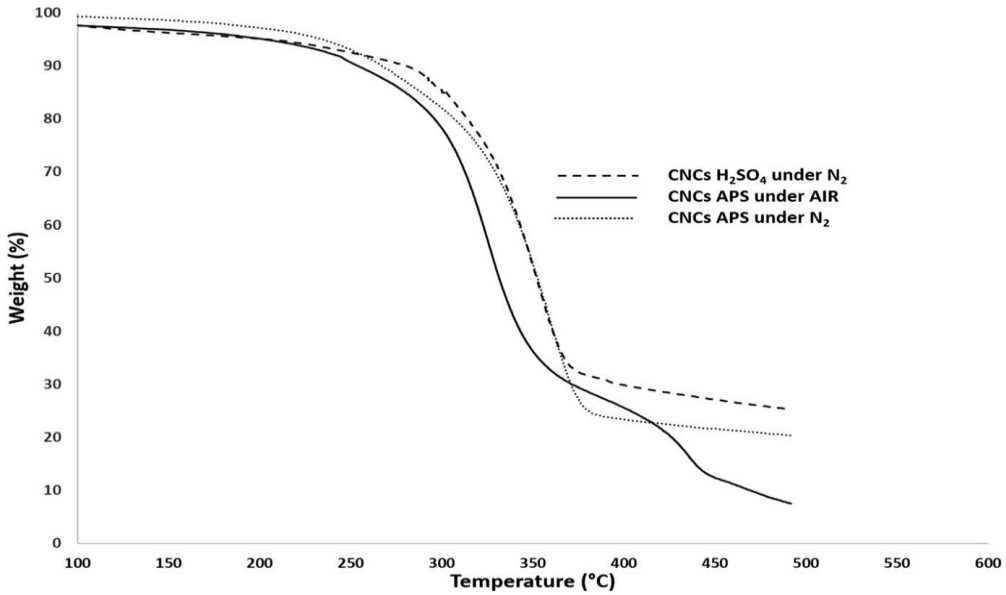

Figure 6.5. TGA plots, from 100 °C to 500 °C, of CNCs from H_2SO_4 hydrolysis, CNC-COO-Na^+ in Nitrogen atmosphere and CNC-COO-Na^+ in air

Increasing quantities of sulfate and hydroxyl groups led to lower degradation temperatures (Fig. 6.5), and a broader degradation temperature range was observed in comparison to unhydrolyzed samples, as shown in the literature (Roman and Winter 2004). Similarly, the COOH form of CNCs is reported as being more stable than the $COONa^+$ form (Lam et al. 2012). This was true in our case also, with the $COONa^+$ form being more stable in a water solution than the COOH form, but less thermostable. Complete decomposition of the CNCs to volatile products including CO_2 was observed at T > 400 °C. This phenomenon could be attributed to depolymerization and decomposition of the cellulose chain. The presence of sulfate groups on nanocrystals leads to charred residue at 350 °C. Heating in air causes oxidation of the hydroxyl groups, resulting, as the temperature increases, in increases of carbonyl, carboxyl and hydroperoxide groups, with free radicals also appearing. The thermal degradation temperature in this case is higher, as shown in Fig. 6.5.

6.4.2. Coated PET film characterization

The turbidity of the APS solution used for coating preparation is lower than the H_2SO_4 one, and this could be related to the surface charge density reported in Table 6.4. Indeed, in the case of the APS solution, the higher surface charge density induces a more efficient electrostatic interaction with water (i.e. a tighter hydrogen bonds network), leading to more stable CNC dispersion.

The nanocrystals were used in the form of 7% water dispersion at pH 8 as lacquers for coating the properly corona-treated side of thin PET films. The thickness of the coatings obtained were well below 1 µm but enough to affect the optical properties, reducing the transparency and increasing the haze (Tab. 6.6) in comparison with the uncoated PET film (T% 84.2, Haze 2.8) After solution deposition on the substrate, the strong capillary and surface forces due to drying and adsorption triggered a rearrangement of the crystal structure.

Cellulose is known to have a very high transparency in solid, non-porous forms. In this case, we are in the presence of a decrease of transparency of the PET film, and this decrease is higher in the case of the CNCs from the H_2SO_4 treatment (Tab. 6.6). Moreover, SEM micrographs of the coatings surface, recorded at 1KK and 100KX magnification, showed homogenous surface of the coatings with the presence of some holes (Fig. 6.6), with a more pronounced roughness in CNC coatings from H_2SO_4 than from APS. This can be correlated with the higher decrease in transparency of the coating produced with CNCs from H_2SO_4.

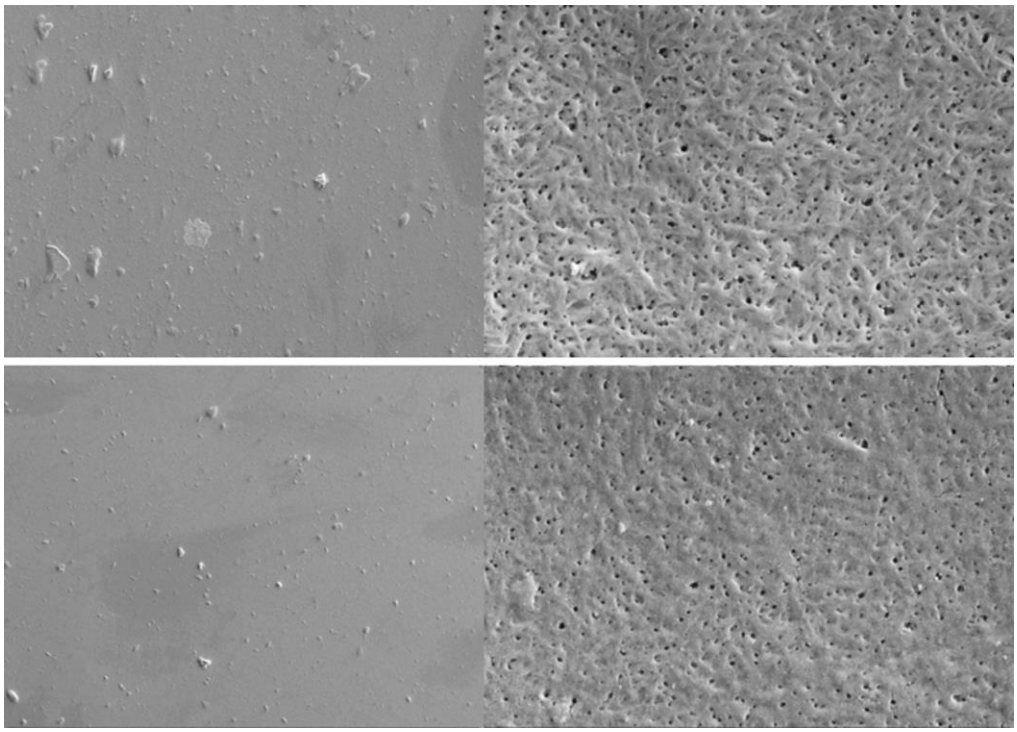

Figure 6.6: SEM micrographs at 1KX and 100KX magnification of the coatings' surface produced by CNCs from H_2SO_4 (up) and APS (down).

SEM observation of the same sample but in cross-section permitted to verify that the surface of the coating is homogeneous in thickness, with values for both the coatings around 450±50 nm (Fig. 6.7).

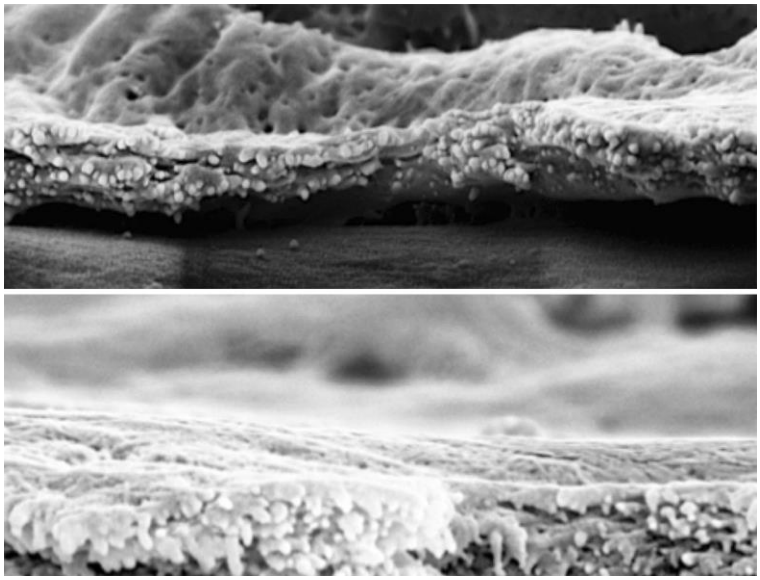

Figure 6.7. SEM micrographs at 180KX magnification of the cross-section of the films containing the coatings of the CNCs from H_2SO_4 (up) and APS (down).

At the same time, a test of the water resistance showed that the APS coating was removed by about 49.2%, while the sulfuric acid CNC layer was almost completely removed (87.4%). Despite its empiricism, the test perceptibly reveals a higher stability of the APS coating compared to that from H_2SO_4. In Table 6.6, the coefficients of friction (COF, both dynamic and static), measured for the two coated films, are reported. The values pertinent to the sulfuric acid CNC coating are quite similar to the ones obtained in a previous work (Li et al. 2013a), for various films (OPET, OPP, Cellophane and OPA) coated with the same CNCs. The achievement of similar COF values for different coated films were assumed as evidence of a complete and uniform covering of the substrates. The values obtained for APS CNC-coated PET are significantly lower, both as dynamic and static coefficients. This achievement can be interpreted as a possible better performance on the automatic machineries for converting the coated material or for a potential packaging operation, but it also confirms a very good adhesion to the plastic film and a compact and uniform coating offered by the cellulose nanocrystals.

Table 6.6: Optical properties, clarity of the CNCs in water dispersion (7%), water resistance and coefficients of friction (COF).

Coating	Clarity (Abs 600 nm)	Haze (%)	Transparency (%)	Water Resistance (% losses)	COF (μ_D)	COF (μ_S)
CNCs $_{H_2SO_4}$	3.1 ± 0.1	5.99 ± 0.11	77.48 ± 0.02	87.4 ± 3.0	0.28 ± 0.01	0.31 ± 0.01
CNCs $_{APS}$	1.8 ± 0.05	6.19 ± 0.10	79.55 ± 0.01	49.2 ± 3.3	0.21 ± 0.01	0.24 ± 0.01

Owing to the highly hydrophilic nature of these coatings and the results obtained in previous researches (Li et al. 2013a), the most promising property of such CNC coatings is its gas barrier. Oxygen permeability was therefore measured at two different relative humidity values at room temperature for both the coated PET films and the uncoated substrate. The results obtained are presented in Table 6.7 and show a very sharp reduction of gas diffusion trough the PET film, once coated by the CNCs. To get the same permeability, just increasing the plastic thickness, a 1.5 mm thick PET film would be necessary to have the same performance offered by the sulfuric acid nanocellulose coating. In the case of the APS CNC-coated film, the thickness of the "standard"

PET sheet having the same permeability should be around 8.2 mm. The very high oxygen barrier demonstrated by the APS CNC coating, which is much higher than that of the majority of synthetic barrier resins commonly used in food packaging applications, realistically derives from the inherent morphological, chemical and physical characteristics of these nanocrystals, which lead to low diffusion. The apparent higher moisture sensitivity of the CNCs from the APS process, which show a higher increase of permeability when measured at 50% RH in comparison with film coated with H_2SO_4 CNCs, is consistent with the higher wettability shown by the optical contact angle evaluation (Tab. 6.4), and can be attributed to the higher charge density. In any case, the moisture sensitivity of the coating, as happens for EVOH or PVOH oxygen barrier synthetic resins, does not permit the use of such materials at high relative humidity (80% or higher). This could be overcome by providing a sealable layer, that is a poliolefinic and moisture barrier, to the possible final laminate in a real application.

Table 6.7. Oxygen permeability (PO_2) and permeability coefficients (KPO_2) of CNC coated films and coatings alone.

Sample	**PO_2 (mL $m^{-2}d^{-1}$ bar^{-1}) 0%RH, 23 °C**	**PO_2 (mL $m^{-2}d^{-1}$ bar^{-1}) 50% RH, 23 °C**
$PET_{uncoated\ film}$	74.95 ± 1.83	87.96 ± 1.13
$CNC_{H_2SO_4\ coated\ PET}$	1.06 ± 0.07	5.99 ± 2.21
$CNC_{APS\ coated\ PET}$	0.17 ± 0.01	3.53 ± 1.92
Sample	**KPO_2 (mL µm $m^{-2}d^{-1}$ bar^{-1}) 0%RH, 23 °C**	**KPO_2 (mL µm $m^{-2}d^{-1}$ bar^{-1}) 50%RH, 23 °C**
$PET_{uncoated\ film}$	899.4 ± 1.83	1,055 ± 1.13
$CNC_{H_2SO_4\ coating\ alone}$	0.48 ± 0.01	2.89 ± 0.01
$CNC_{APS\ coating\ alone}$	0.075 ± 0.01	1.65 ± 0.01

6.5. CONCLUSIONS

In this paper, the advantage of using CNCs derived from APS for improving the performance of common food-packaging materials, while increasing their possible sustainability, was proved. Transparency, friction coefficient, wettability of the coating and crystallinity were always better for the CNC coatings obtained by the APS process, and especially the oxygen barrier property revealed a very interesting and promising behavior. These advantages must be correlated to the higher charge density (due to the presence of carboxylic groups), which in turn give rise to a more performing coating and availability of functional groups that can be used for grafting the CNCs to other molecules that could be involved in a lamination process. The tests demonstrated, however, that due to its intrinsic nature the hydrophilic coating was very sensitive to moisture and was neither thermoplastic nor thermo-sealable, as shown in the Differential Scanning Calorimetry analysis (Online Resource 1). Such a high-performing coating, in the case of a practical application such as food-packaging material, must therefore be protected by means of a hydrophobic and sealable polymeric layer. This is nevertheless the same problem that must be faced when synthetic barrier polymers, such as polyvinyl alcohol (PVOH) or ethylene vinyl alcohol copolymer (EVOH) are used. Due to the fact that the CNC coating showed oxygen permeability coefficients which were lower than the synthetic resins, they could be a viable alternative, having increased gas barrier properties, while reducing the dependency on oil-based derivatives.

Acknowledgements

The authors wish to acknowledge Professor Francesco Demartin and Dr. Stefano Checchia, Department of Chemistry, University of Milan and Dr. Giorgio Capretti of INNOVHUB-SSI, Milan, for technical support in analysis and scientific support.

6.6. REFERENCES

Arola, S., Tammelin, T., Setala, H., Tullila, A, and Linder, M.B. 2012. Immobilization-Stabilization of Proteins on Nanofibrillated Cellulose Derivatives and Their Bioactive Film Formation. Biomacromol. 13, 594-603.

Beck-Candanedo, S., Roman, M. and Gray, D.G. 2015 Effect of Reaction Conditions on the Properties and Behavior of Wood Cellulose Nanocrystal Suspensions. Biomacromol. 6,1048-1054.

Beer, F. and Muller, J. 1962. Process for the production of caro's acid salts and solutions thereof. In Google Patents. https://www.google.com/patents/US3036885. Accessed 08 July 2015.

Belbekhouche, S., Bras, J., Siqueira, G., Chappey, C., Lebrun, L., Khelifi, B., Marais, S. and Dufresne, A. 2011. Water sorption behavior and gas barrier properties of cellulose whiskers and microfibrils films Carbohyd. Polym. 83, 1740–1748.

Berne, B.J. and Pecora, R. 2000. Dynamic light scattering: with applications to chemistry, biology, and physics. Courier Corporation, New York.

Bondeson, D., Mathew, A. and Oksman, K. 2006. Optimization of the isolation of nanocrystals from microcrystalline cellulose by acid hydrolysis. Cellulose. 13, 171-180.

Cheng, M., Qin, Z., Liu, Y., Qin, Y., Li, T., Chen, L. and Zhu, M. 2014. Efficient extraction of carboxylated spherical cellulose nanocrystals with narrow distribution through hydrolysis of lyocell fibers by using ammonium persulfate as an oxidant. J. Mater. Chem. A. 2, 251-258.

Crank, J. 1979. The mathematics of diffusion. Oxford university press.

Dong, X.M., Kimura, T., Revol, J.F. and Gray, D.G. 1996. Effects of Ionic Strength on the Isotropic−Chiral Nematic Phase Transition of Suspensions of Cellulose Crystallites. Langmuir. 12, 2076-2082.

Dufresne, A. 2012. Nanocellulose: from nature to high performance tailored materials. Walter de Gruyter, Berlin.

Elazzouzi-Hafraoui, S., Nishiyama, Y., Putaux, J.L., Heux, L., Dubreuil, F. and Rochas, C. 2008. The shape and size distribution of crystalline nanoparticles prepared by acid hydrolysis of native cellulose. Biomacromol. 9, 57-65.

Elazzouzi-Hafraoui, S., Putaux, J.L. and Heux, L. 2009. Self-assembling and chiral nematic properties of organophilic cellulose nanocrystals. J. Phys. Chem. B. 113, 11069-11075.

Espino, E., Cakir, M., Domenek, S., Román-Gutiérrez, A.D., Belgacem, N. and Bras, J. 2014. Isolation and characterization of cellulose nanocrystal sfrom industrial by-productsof Agave tequilana and barley. Ind. Crop. Prod. 62, 552-559.

Favier, V., Canova, G.R., Cavaillé, J.Y., Chanzy, H., Dufresne, A. and Gauthier, C. 1995. Nanocomposite materials from latex and cellulose whiskers. Polym Adv. Technol. 6, 351-355.

Filpponen, I. 2009. The Synthetic Strategies for Unique Properties in Cellulose Nanocrystal Materials. Dissertation, North Carolina State University.

Filson, P.B. and Dawson-Andoh, B.E. 2009. Sono-chemical preparation of cellulose nanocrystals from lignocellulose derived materials. Biores. Technol. 100, 2259-2264.

French, A.D. 2014. Idealized powder diffraction patterns for cellulose polymorphs. Cellulose. 21, 885-896.

Frounchi, M. and Dourbash, A. 2009. Oxygen Barrier Properties of Poly(ethylene terephthalate) Nanocomposite Films. Macromol. Mater. Eng. 294, 68-74.

Gall, J.F., Church, G.L. and Brown, R.L. 1943. Solubility of Ammonium Persulfate in Water and in Solutions of Sulfuric Acid and Ammonium Sulfate. J. Physi. Chem.-Us. 47, 645-649.

Garvey, C.J., Parker, I.H. and Simon, G.P. 2005. On the Interpretation of X-Ray Diffraction Powder Patterns in Terms of the Nanostructure of Cellulose I Fibres. Macromol. Chem. Phys. 206, 1568-1575.

Håkansson, H. and Ahlgren, P. 2005. Acid hydrolysis of some industrial pulps: effect of hydrolysis conditions and raw material. Cellulose. 12, 177-183.

Hult, E.L., Iversen, T. and Sugiyama, J. 2003. Characterization of the supermolecular structure of cellulose in wood pulp fibres. Cellulose. 10, 103-110.

Ifuku, S., Tsuji, M., Morimoto, M., Saimoto, H. and Yano, H. 2009. Synthesis of silver nanoparticles templated by TEMPO-mediated oxidized bacterial cellulose nanofibers. Biomacromol. 10, 2714-2717.

Jayakrishnan, A. and Shah, D.O. 1984. Phase-transfer-catalyzed polymerization of acrylonitrile. J. Appl. Polym. Sci. 29, 2937-2940.

Kaelble, D.H. 1970. Dispersion-Polar Surface Tension Properties of Organic Solids. J. Adhesion. 2, 66-81.

Kolthoff, I. and Miller, I. 1951. The Chemistry of Persulfate. I. The Kinetics and Mechanism of the Decomposition of the Persulfate Ion in Aqueous Medium. J. Am. Chem. Soc. 73, 3055-3059.

Kralchevsky, P.A. and Nagayama, K. 1994. Capillary forces between colloidal particles. Langmuir. 10, 23-36.

Kroeger, A., Deimede, V., Belack, J., Lieberwirth, I., Fytas, G. and Wegner, G. 2007. Equilibrium length and shape of rodlike polyelectrolyte micelles in dilute aqueous solutions. Macromol. 40, 105-115.

Lam, E., Leung, A.C.W., Liu, Y., Majid, E., Hrapovic, S., Male, K.B. and Luong, J.H.T. 2013. Green Strategy Guided by Raman Spectroscopy for the Synthesis of Ammonium Carboxylated Nanocrystalline Cellulose and the Recovery of Byproducts. ACS Sustainable Chem. Eng. 1, 278-283.

Lasoski, S.W. and Cobbs, W.H. 1959. Moisture permeability of polymers. I. Role of crystallinity and orientation. Polym. Sci. 36, 21-33.

Leung, A., Hrapovic, S., Lam, E., Liu, Y.L., Male, K.B., Mahmoud, K.A. and Luong, J.H.T. 2011. Characteristics and Properties of Carboxylated Cellulose Nanocrystals Prepared from a Novel One-Step Procedure. Small. 7, 302-305.

Leung, C.W., Luong, J.H.T., Hrapovic, S., Lam, E., Liu, Y., Male, K.B., Mahmoud, K. and Rho, D. 2012. Cellulose nanocrystals from renewable biomass. In. Google Patents https://www.google.com/patents/US8900706. Accessed 08 July 2015.

Li, F., Biagioni, P., Bollani, M., Maccagnan, A. and Piergiovanni, L. 2013. Multi-functional coating of cellulose nanocrystals for flexible packaging applications. Cellulose. 20, 2491-2504.

Li, F., Biagioni, P., Finazzi, M., Tavazzi, S. and Piergiovanni, L. 2013. Tunable green oxygen barrier through layer-by-layer self-assembly of chitosan and cellulose nanocrystals. Carbohyd. Polym. 92, 2128-2134.

Li, F., Mascheroni, E. and Piergiovanni, L. 2015. The potential of nanocellulose in the packaging field: a review. Packaging Technol. Sci. 28, 475-508..

Mewis, J. and Wagner, N.J. 2012. Colloidal suspension rheology. Cambridge University Press.

Miller, K.S. and Krochta, J.M. 1997. Oxygen and aroma barrier properties of edible films: A review. Trends Food Sci. Technol. 8, 228-237.

Nickerson, R.F. and Habrle, J.A. 1947. Cellulose Intercrystalline Structure. Ind. Eng. Chem. 39, 1507-1512.

Nishiyama, Y. 2009. Structure and properties of the cellulose microfibril. J. Wood Sci. 55, 241-249.

Nishiyama, Y., Johnson, G.P. and French, A.D. 2012. Diffraction from nonperiodic models of cellulose crystals. Cellulose. 19, 319-336.

Nishiyama, Y., Kim, U.J., Kim, D.Y., Katsumata, K.S., May, .RP. and Lagan, P. 2003. Periodic disorder along ramie cellulose microfibrils. Biomacromol. 4, 1013-1017.

Nishiyama, Y., Sugiyama, J., Chanzy, H. and Langan, P. 2003. J. Am. Chem. Soc. 125, 14300–14306.

Nishiyama, Y., Langan, P. and Chanzy, H. 2002. J. Am. Chem. Soc. 124, 9074–9082.

Okano, T., Kuga, S., Wada, M., Araki, J. and Ikuina, J.P. 1999. Nisshin Oil Mills Ltd. Japan Patent JP 98/151052.

Owens, D.K. and Wendt, R.C. 1969. Estimation of the surface free energy of polymers. J. Appl. Polym. Sci. 13, 1741-1747.

Park, S., Baker, J.O., Himmel, M.E., Parilla, P.A. and Johnson, D.K. 2010. Cellulose crystallinity index: measurement techniques and their impact on interpreting cellulase performance. Biotechnol. Biofuels. 3, 1.

Patterson, A. 1939. the sherrer formula for X-ray particle size determination. Phys. Rev. 56, 978-982.

Pines, A., Gibby, M.G., Waugh, J.S.. 1973. Proton-enhanced NMR of dilute spins in solids. J. Chem. Phys. 59, 569-590.

Qi, A., Chan, P., Ho, J., Rajapaksa, A., Friend, J. and Yeo, L. 2011. Template-free synthesis and encapsulation technique for layer-by-layer polymer nanocarrier fabrication. ACS nano. 5, 9583-9591.

Roisnel, T. and Rodríguez-Carvajal, J. 2001. WinPLOTR: A Windows tool for powder diffraction pattern analysis." Materials Science Forum *378-3*, 118-123.

Roman, M. and Winter, W.T. 2004. Effect of Sulfate Groups from Sulfuric Acid Hydrolysis on the Thermal Degradation Behavior of Bacterial Cellulose. Biomacromol. 5, 1671-1677.

Salame, M. 1989. The use of barrier polymers in food and beverage packaging, vol. 1. Plastic film technology. Technologic Publishing Co. Inc., Lancaster USA.

Segal, L., Creely, J.J., Martin, A.E. and Conrad, C.M. 1959. An Empirical Method for Estimating the Degree of Crystallinity of Native Cellulose Using the X-Ray Diffractometer. Tex. Res. 29, 786-794.

Sinha-Ray, S. and Okamoto, M. 2003. Polymer/layered silicate nanocomposites: a review from preparation to processing. Prog. Polym. Sci. 28, 1539-1641.

Springer, E.L. and Minor, J.L. 1991. Delignification of lignocellulosic materials with monoperoxysulfuric acid. United States Patent 5,004,523 issued Apr. 2, 1991.

Turrentine, J.W. 1906. Action of Ammonium Persulphate on Metals. J. Phys. Chem. 11, 623-631.

Van Oss, C.J. 2003). Long-range and short-range mechanisms of hydrophobic attraction and hydrophilic repulsion in specific and aspecific interactions. J. Mol. Recognit. 16, 177-190.

Yang, H., Alam, M.N., van de Ven, T.G.M. 2013. Highly charged nanocrystalline cellulose and dicarboxylated cellulose from periodate and chlorite oxidized cellulose fibers. Cellulose. 20, 1865–1875.

7. CHAPTER V:

Cellulose nanocrystals from lignocellulosic raw materials, for oxygen barrier coatings of food packaging films.

(Co-author of the article Submitted to Packaging Technology and Science)

7.1. ABSTRACT

Cellulose nanocrystals (CNCs) provide unique, renewable top-down nano particles on which coatings with improved gas barrier properties and new functionalities can be prepared. In this paper, the potential of obtaining such high performing nanocrystals from low-cost lignocellulosic by-products or raw materials is proved by a comparison study on CNCs obtained both from Cotton linters and Kraft pulp, by means of APS (Ammonium Persulfate) process. Morphological and chemical characterization of the nanocrystals obtained, as well as the main functional properties of PET coated films, showed quite similar characteristics and performances of CNCs obtained from pure cellulose raw material (Cotton linters) and the nanoparticles produced from a potential waste of paper making processes (Kraft pulp). In particular, the gas barrier properties of the coating produced with CNCs coming from Kraft pulp resulted very interesting, providing oxygen and carbon dioxide permeability values hundreds of times lower than those of equal thickness of common barrier synthetic polymers, over a broad range of temperatures. The results obtained seem relevant not only for the outstanding performances achieved, but also because they evoke a possible positive example of industrial symbiosis in the packaging field, merging together the requirements and needs of paper and plastic industries and addressing the way for a better waste and materials management.

KEYWORDS: film coating, gas permeability, cellulose nano-crystals, lignocellulosic materials, APS process.

7.2. INTRODUCTION

Over the years, cellulose has been largely and commonly used for industrial purposes in general and in packaging applications in particular, due to its availability, biodegradability, and mechanical properties (Li et al., 2015; Keijsers et al., 2013; Clark et al., 2007). Cellulose is the main constituent of higher plants tissues, and is also found in marine animals (tunicates), in algae, fungi, bacteria and invertebrates in small quantities (Knoshaug eet al., 2012; Moon et al., 2011; Shoda and Sugano, 2005). As well as in natural resources, however, it is also hugely abundant in a number of wasted biomasses, industrial by-products, recycle streams and rubbishes (Shill et al., 2011; Nashar et al., 2004). From a chemical point of view, it is a linear polysaccharide formed by a chain of β-1,4 linked D-glucose where each subsequent glucose molecule is inverted 180°, therefore the fundamental unit is frequently taken to be *cellobiose*, a dimer of glucose. The degree of glucose polymerization in cellulose is found in the range of 3,000-15,000, corresponding to quite high molecular weights. Hydrogen bonds and van der Waals forces between hydroxyl groups and oxygen atoms within cellulose molecule chains cause the formation of elementary fibrils which are further aggregated into larger microfibrils and cellulose fibers. Microfibrils, generally within 5-50 nm in diameter and several micrometers in length, have crystalline and amorphous regions. Because of the susceptibility of these amorphous regions of cellulose microfibrils to different treatments, they are selectively hydrolysed under optimized conditions. With the removal of the cellulose amorphous parts, highly ordered structures, the cellulose nanocrystals (CNCs), can be extracted. CNCs have different geometrical dimensions depending on the source of cellulosic material and hydrolysis conditions, but they are within 2-20 nm in width and hundreds of nm in length, generally (Eichhorn et al., 2010; Habibi et al., 2010). At nanoscale dimensions, while maintaining low densities, biodegradability and low eco-toxicological characteristics, CNCs show excellent mechanical and barrier properties which expand their potential use in different applications, making them very attractive for packaging applications (Li et al., 2015; Khan et al., 2014); in particular, their good oxygen barrier properties have been already demonstrated as coatings and composites' constituent (Nair et al., 2014; Li et al, 2013a; Li et al, 2013b).

Therefore, the obtainment of CNCs from ligno-cellulosic sources is of great interest, taking into account the large availability and low cost of such cellulosic materials in underused by-products and wastes. A promising process useful for this goal is the Ammonium Persulfate process proposed by Leung et al. (2011) and recently checked for its capability in CNCs production from cotton linters, in a comparison trial with the traditional sulphuric acid method (Mascheroni et al., 2016).

APS, a strong oxidizing agent with high water solubility, is able to produce carboxylated CNCs having high crystallinity and active carboxyl groups (Zhang et al., 2016; Yang et al., 2013; Leung et al., 2011), without special pre-treatments and in relatively short time. When the solution of ammonium persulfate is heated, free radicals are produced and hydrogen peroxide is also formed in the media under the acidic conditions. These chemicals are able to break down amorphous cellulose and produce carboxylated CNCs but, at the same time, they can destroy lignin and other possibly contaminants in the raw materials used (Lam et al., 2012; Leung et al., 2012). Moreover, the conversion of the hydroxyl groups to the carboxylate form offers active sites for enhancing the adhesion onto coating substrates in order to produce new high performing, but more sustainable multilayer materials for critical packaging applications.

Lignocellulosic materials basically consists of three biopolymers, i.e. cellulose, hemicellulose and lignin and, depending on their source, they may be highly contaminated by other different substances. Therefore, the obtainment of high crystalline nanoparticles, suitable for the coating process and able to adequately performing as flexible packaging materials, must be thoroughly tested case by case. The main goal of this paper is to evaluate the chance of producing CNCs from lignocellulosic side-products and wastes coming from pulp and paper industries, with the aim of producing a bio-based, high gas barrier coating, useful to improve a fundamental property of flexible packaging materials for sensitive foods, while enhancing their general sustainability. As a prototype of such side-products, we selected some Kraft pulp rich in hemicellulose content and with a medium amount of lignin, comparing the final properties obtained with those of CNCs coming from a quite pure source, such as cotton linters, with a special focus on the gas permeability properties.

7.3. MATERIALS AND METHODS

7.3.1. Materials

Cotton linters (CL) used as raw material to produce CNCs were kindly supplied by Innovhub (Milan, Italy), while Softwood Kraft Pulp (KP) was kindly supplied by Burgo Goup (Altavilla Vicentina, Italy) (Fig. 7.1). Ammonium persulfate ≥98%, hydrochloric acid 37%, sodium hydroxide ≥97% and the other chemicals used were purchased from Sigma-Aldrich (Milan, Italy). Poly(ethylene terephthalate) (PET) film, having a thickness of 12 ± 0.5 μm, was provided by Sapici spa (Cernusco sul Naviglio, Italy)

Figure 7.1. The raw materials used to obtain CNCs: Cotton linters (Left), Kraft pulp from softwood (Right).

7.3.2. Kraft pulp characterization

The pulp was initially delignified to remove the soluble lignin (Sluiter et al., 2008; Rowell et al., 1997). To 10 g of KP sample, 320 mL of hot distilled water, 2 mL acetic acid, and 4 g of sodium chlorite were added. The sample was heated to 70 °C and, after 60 minutes, 0.5 mL of acetic acid and 1 g of sodium chlorite were slowly added to further continue the delignification process. Additional 0.5 mL of acetic acid and 1 g of sodium chlorite were added to the solution every hour until the fibers were completely separated from the lignin. The delignification process performed lasted 4 hours with 3 additions and 1 hour without further addition, before vacuum filtration. The holocellulose obtained was then washed with acetone, air dried and stored in dry conditions.

Determination of α-, β -, and γ-cellulose

The TAPPI T 203 method was used. 1.5 g of holocellulose obtained from delignification process was extracted consecutively with 17.5% and 9.45% NaOH solutions at 25 °C. The soluble fraction, consisting of β and γ cellulose was determined volumetrically by oxidation with potassium dichromate solution, while α cellulose is estimated as the insoluble fraction derived by difference.

Lignin content and Kappa number

Acid insoluble lignin content determination was performed following the technical report NREL/TP-510-42618[22]. The Kappa number estimate was according TAPPI T 236 method.

7.3.3. CNCs extraction by Ammonium Persulfate treatment

The CNCs were obtained from Cotton linters (CL-CNCs) and Kraft pulp (KP-CNCs) by the hydrolyzing-oxidative method proposed by Leung and coworkers (2011) in 2011. Milled Cotton linters or water swollen Kraft Pulp were introduced into a large beaker together with 1M ammonium persulfate (APS) for Cotton and 1.5M for Kraft pulp. The ratio between fibers and APS solution was always 10:1 g L^{-1}, and the beaker was put onto a magnetic stirrer hotplate, equipped with a Vertex Digital thermoregulator (VELP Scientifica, Usmate, Italy). The mixture was heated and stirred at 75 $\pm$ 2 °C for 16 hours, limiting the evaporation by means of an aluminum foil cover. The suspension of the CNCs obtained was centrifuged at 10000 rpm for 15 minutes. The centrifugation and a washing step with deionized water were repeated 4 times until the pH of the suspension was around 4. Then NaOH 1M was added until the suspension reached pH 8 in order to have the sodium form of CNCs, after that it was sonicated for 10 minutes (0.7 cycles, 70% output). The purified suspension was frozen at -18 °C overnight and freeze-dried and then stored in dry conditions. The yields of CNCs production (%) were evaluated from the weight of freeze dried products, with reference to the mass of cellulosic raw materials treated with APS.

7.3.4. CNCs morphological characterization

Drops of aqueous dispersions of CNCs 0.5% w/w were deposited on carbon-coated grids for transmission electron microscope (TEM) observations, negatively stained with uranyl acetate and then allowed to dry. The samples were analyzed with a microscope operating at an accelerating voltage of 80kV (mod. Jeol-10084 Hitachi, Brugherio, Italy). Representative micrographs were selected for measuring the dimensions of nanocrystals by means of digital image analysis (Image-Pro Plus software). Scanning electron microscopy (SEM) images were also obtained from a Sigma Field Emission microscope (Carl Zeiss Microscopy LLC, Thornwood, NY) at accelerating 5 kV

voltage and 6 mm working distance, with a 30 m width slit. The samples were first gold sputtered (Sputtering Polaron E 5100) for 30 s (rate 1 nm s^{-1}) with argon and 18 mA current intensity.

In addition, by dynamic light scattering (DLS) measures (mod. Litesizer 500, Anton Paar, Graz, Austria), the equivalent hydrodynamic diameter of the CNCs were determined, as well as polydispersity index and an intensity weighted size distribution. The measurements were performed at 25.0 ± 0.1 °C with a 35 mW laser diode light (λ = 658 nm) and collecting the scattered light at 90°. Prior to DLS measurement, the samples were diluted to 1:500 (w/w) with distilled water that was previously adjusted to pH 8 and maintained at 25 °C through stirring until measurement. 4 mL of the diluted solution was poured in the measurement cell after 30 s homogenization by an ultrasonic water bath.

7.3.5. Zeta-potential and conductivity of the CNCs

Zeta potential of CNCs in the diluted suspension at pH 8 were determined by electrophoretic light scattering (ELS), using the PALS technology (mod. Litesizer 500, Anton Paar, Graz, Austria). Measures were at 25.0 $\pm$ 0.1 °C, by means of a 35 mW diode laser (λ = 658 nm) and at 15° detection angle. The same measures give the values of conductivity (mS cm^{-1}).

7.3.6. Degree of oxidation (DO) by FTIR spectrum of the CNCs

The degree of oxidation (DO) was quantified by FTIR spectra, collected using an instrument (mod. Spectrum 100, Perkin Elmer, Milano, Italy) equipped with Attenuated Total Reflectance accessory (ATR), at room temperature. 64 scans, with a resolutions of 4 cm^{-1}, were collected and the DO was calculated by the ratio of the intensity of the carbonyl peak (absorbance bands at 1735 cm^{-1} (ν (C=O) in the acid form)) to that of the band near 1060 cm^{-1} (related to the backbone structure of cellulose). The equation used is the following (Cheng et al., 2014; Habibi et al., 2006):

$$D0 = 0.01 + 0.7\left(\frac{I_{1735}}{I_{1060}}\right)$$

7.3.7. Weight-average molar mass of the CNCs by static light scattering (SLS)

The molecular mass of the cellulose nanocrystals was estimated by measuring static light scattering (mod. Litesizer 500, Anton Paar, Graz, Austria). The intensity of the scattered light is directly related to molecular mass and the scattering intensity of three different concentrations (0.01, 0.1, 1 mg/mL in water at pH 8.0), was measured at 25 °C and at 90° detection angle. Toluene

was used as reference and the hydrodynamic radius detected by DLS measures was applied. The Debye plot (Debye and Anacker, 1951) was then generated, whose intercept provided the weight-average molecular mass estimate.

7.3.8. Viscosity of CNCs dispersion

In order to determine the rheological properties of CNCs suspensions, frequency sweeps experiments were conducted, using a rotational rheometer (mod. Physica MCR 300, Anton Paar, Graz, Austria) with cone-plate geometry (ϕ = 50 mm, cone angle = 2°, minimum distance between plates = 50 micron). Strain was set equal to 5% and curves of complex viscosity as function of frequency were recorded. 30 points were taken ranging from 100 Hz to 0.1 Hz with logarithmic progression at 20 °C.

7.3.9. Thermogravimetric analysis (TGA) of the CNCs

TGA was carried out to compare the thermal stability of the two different kinds of CNCs using a thermogravimetric analyzer (mod. TGA 4000, Perkin Elmer, Milano, Italy). Samples were heated from 30 °C to 600 °C under air and at a heating rate of 10 °C min^{-1}; three replications were done for each CNC type. Three characteristics temperatures were measured: the onset temperature (To), the inflection point (Ti), and the maximum temperature related to significant weight loss (Tmax).

7.3.10. Coating process

A 8% (w/v) of CL-CNCs in water (pH = 8) was coated onto PET 12 μm films, following the ASTM D823-07, practice C. Due to high viscosity, two subsequent coatings of 4% KP-CNCs were accomplished on the same substrate. The CNCs dispersions were previously sonicated for 20 minutes (1.0 cycles, 100% output). The side of the PET substrates receiving the coating, was activated immediately before coating by a corona treatment (Arcotech GmbH, Monsheim, Germany). The coatings were performed by an automatic film applicator (mod.1137, Sheen Instruments, Kingston, UK) at a constant speed of 2.5 mm s^{-1}. Water was evaporated using a constant mild air flow (25 ± 0.3 °C for 5 minutes).

7.3.11. Thickness of the coatings

The measurement of coating thickness was accomplished by a gravimetric method. Four 10 × 10 cm^2 samples (PET films coated by the two kinds of CNCs) was cut and weighed (m_1, g). The

coating was then removed by running hot water (~70 °C) and the resulting bare film was dried and weighed (m_2, g). The coating thickness (L, cm) was calculated according to the following equation:

$$L = \frac{(m_1 - m_2)}{\rho \, x \, 100}$$

where ρ ~1.58 g cm^{-3} is the density of CNCs (Mazeau and Heux, 2003).

7.3.12. Water Resistance of the coatings

The water resistance of the coatings was determined by using an empirical test, measuring the weight losses after 4 days of immersion in a water bath at 37 $\pm$ 0.5 °C, of samples (10 × 10 cm^2) cut from the two CNCs coated PET films. Four samples of the two kinds of CNCs (CL and KP) coated films were submerged in water, avoiding any floating, then wiped, dried for one day at room temperature, and weighed to measure the weight loss (%).

7.3.13. Optical properties

The transmittance of the coated films was measured at 550 nm, according to the ASTM D 1746-70, by means of a UV-VIS spectro-photometer (mod. L650, Perkin-Elmer Milano, Italy). The haze (%) of the same samples was measured according to ASTM D 1003-61 with the same instrument equipped with a 150 mm integrating sphere. Each sample was replicated three times, analyzing four spots on each replica.

7.3.14. Contact angles and surface energies

Static contact angles of the substrate (uncoated PET film after the corona treatment) and the coated films were determined by using an OCA 15 Plus angle goniometer (Data Physics Instruments GmbH, Filderstadt, Germany). Milli-Q water (18.3 MΩ cm), formamide, and apolar diiodomethane (99%) were used to assess and characterize surface free energies (SFE). On the basis of the surface tension parameters of the liquids used (Tab. 7.1), the polar γ_s^P and dispersive γ_s^D parts of SFE were calculated by the Owens-Wendt-Rabel and Kaelblem (OWRK) method (Kaelble, 1970; Owens and Wendt, 1969). The sessile drop method was used, by gently dropping a droplet of 4.0 ± 0.5 μL of each liquid onto the substrate. The measurements were performed at room temperature, on five different positions for each sample. The instrument was equipped with a high-resolution CCD camera and a high performance digitizing adapter. SCA20 and SCA21

software (Data Physics Instruments GmbH, Filderstadt, Germany) were used, respectively, for contact angle measurements and surface energy calculation.

Table 7.1. Surface tension parameters ofthe liquids used in contact angle determination (in mJ/m^2) at 20 °C (van Oss, 2003; Dann, 1970)*.

Liquid	γ_l	γ_l^D	γ_l^P
Milli-Q Water	72.8	21.8	51.0
Diiodomethane	50.8	50.8	0
Formamide*	58.0	39.0	19.0

7.3.15. Coefficient of Friction

The friction coefficients (COF) static (μ_S) and dynamic (μ_D) were measured by a dynamometer (mod. Z005, Zwick Roell, Ulm, Germany). The uncoated side of CNC-coated films was tightly wrapped onto a sled (6.2×6.2 cm^2, 197.99 g), while the un-treated side of uncoated PET film was covered on the sliding plane. Then the sled was connected to the force sensor of a dynamometer and horizontally pulled by the instrument on the covered sliding plane. The pulling force data were recorded and analyzed by TestXpert software V10.11 (Zwick Roell, Ulm, Germany), according to the standard method ASTM D 1894-87.

7.3.16. Gas and water vapor permeability

All the gases and water permeability measures were performed by an isostatic permeabilimeter (mod. Multiperm, PERMTECH S.r.l., Pieve Fosciana, Italy) according to ASTM standard methods (D-3985 and F-1249 respectively). The oxygen and carbon dioxide permeability (P_{O2}, P_{CO2}, mL m^{-2} d^{-1} bar^{-1}) of uncoated PET film and KP-CNCs coated film was measured at 30, 34, 38, 42, 46 and 50 °C at 0% RH. The permeability coefficients of the CNCs coating alone (KP_{O2}, KP_{CO2}, mL µm m^{-2} d^{-1} bar^{-1}) were calculated using the following equations (Crank, 1979), assuming that the PET surface did not interact with the coating layer above, whose thickness is *L* (µm), and that the interface between them negligibly affected the final permeation measure.

$$\frac{L}{\mathrm{KP_{O2}(CNCs\ coating)}} = \frac{1}{\mathrm{P_{O2}(coated\ PET\ film)}} - \frac{1}{\mathrm{P_{O2}(PET\ film)}}$$

$$\frac{L}{\mathrm{KP_{CO2}(CNCs\ coating)}} = \frac{1}{\mathrm{P_{CO2}(coated\ PET\ film)}} - \frac{1}{\mathrm{P_{CO2}(PET\ film)}}$$

From the isostatic permeation curves obtained (Fig. 2), the diffusion coefficient (D_G, cm^2 s^{-1}) of each gas was estimated, according to the following equation (Hernandez and Gavara, 1999):

$$D_G = \frac{L^2}{7.2\ x\ t_{1/2}}$$

where L is the thickness (cm) and $t_{1/2}$ (s) is the time required to reach half of the maximum permeability value. Knowing the permeability and diffusion coefficients (KP_G, D_G) of each gas, their solubility (S_G, bar^{-1}) in the coating were estimated on the basis of:

$$S_G = \frac{KP_G}{D_G}$$

The oxygen permeability of the KP-CNCs coated film was also measured at 23° under 70, 50, 30, 20 and 10% RH on the coated side of the film, while the water vapor transmission rate (WVTR) was assessed at 38 °C, under a 90% RH difference.

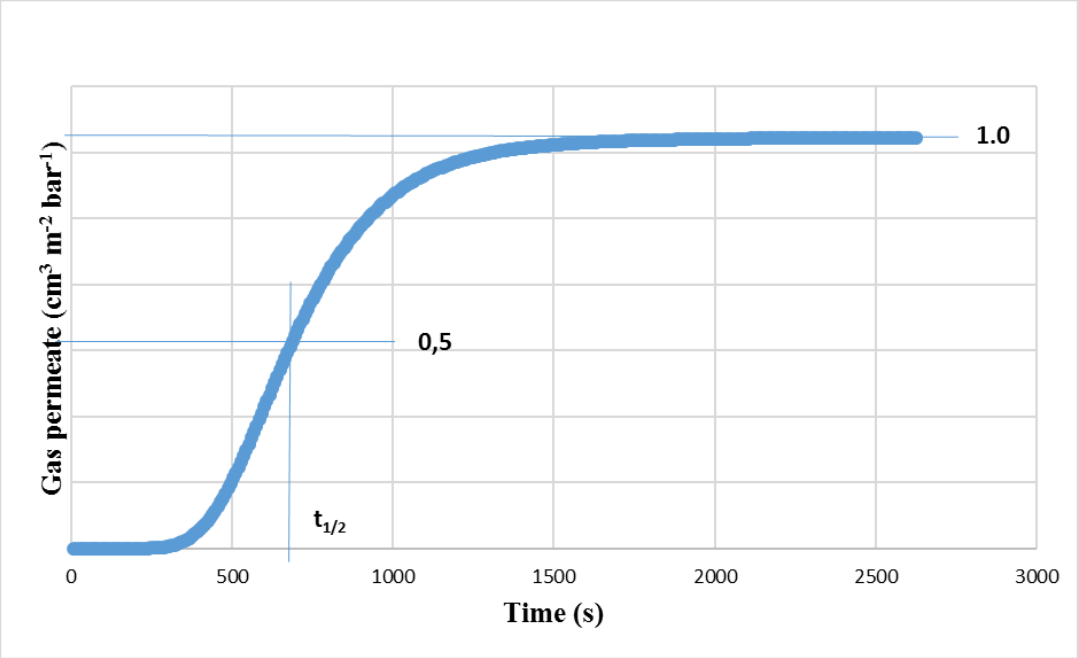

Figure 7.2. Gas permeation profile in isostatic method and $t_{1/2}$ identification.

7.4. RESULTS

Raw materials characterization

Cotton linters are by-products of the oil mills, mechanically and chemically purified (Sczostak, 2009), characterized by thin and short fibers (length 2-6 mm, diameter 6-12 μm). According to the provider's information they have only small amount of minerals and hemicellulose and, after purification, provide a cellulose content around 99%. The softwood Kraft pulp used to obtain the CNCs was analyzed according to the current TAPPI methods and the results are shown in Table 7.2. It was characterized on the basis of its amount of α, β, and γ cellulose, lignin content and kappa number. α-cellulose is commonly considered the not-degraded, higher molecular weight cellulose fraction, β-cellulose indicates degraded cellulose, γ-cellulose mainly consists of hemicellulose, while Kappa number, estimating the amount of chemicals required during bleaching of wood pulp, is approximately proportional to the residual lignin content of the pulp. The range for bleachable pulps are about 25-30, while higher values (45-90) are typical for less fine manufacturing such as sack paper or corrugated fiberboard. The Kappa number of the pulp used in this work is 35.5, a value consistent with the medium-high lignin content measured (about 8%). The degraded cellulose (β-cellulose) is limited but, much more important, the hemicellulose content (γ-cellulose) is high, denoting the complexity of the raw material selected.

Table 7.2. K number and main constituents of the softwood Kraft pulp used.

Kappa number	**α-cellulose (%)**	**β-cellulose (%)**	**γ-cellulose (%)**	**Lignin (%)**	**Minerals (%)**
35.5	79.9	0.37	12.52	7.9	0

7.4.1. Characterization and comparison of CNCs obtained from the two raw materials

The hydrolyzing-oxidative APS method used was effective in reducing the dimension, providing a significant oxidation of native cellulose and giving satisfactory yields of CNCs, which were assessed at 21.5% from Kraft pulp and 50% from Cotton linters. The lower yield obtained from the pulp is due to the complex composition of this raw material and, in particular, to the lignin content which depletes part of the reactants used to extract and oxidize the CNCs (Leung et al., 2015; Springer and Minor, 1991). The reported yields, moreover, were estimated by a gravimetric

method and it is not excluded the presence of some residual, non-cellulosic, components in the KP-CNCs. The de-lignification process of KP, anyway, has been quite fast, according to the observed colour change of the fiber dispersion during the process shown in Fig. 3. At the end of the process (16 hours) and after the steps of purification and freeze drying, it was possible to collect enough CNCs for further characterization analysis and coating process.

Figure 7.3. Lignin bleaching of Kraft Pulp during the APS process (Left: time zero; middle: after 2 h; right: after 12 h).

CNCs morphology

The CNCs dimensions were characterized in terms of their hydrodynamic diameter distribution by DLS measures, and in Fig. 4 the comparison of CNCs obtained from Kraft pulp and Cotton linters is presented for the relative frequency of the intensity of scattered light. The results indicate an average hydrodynamic diameter quite similar, around 120 nm, very close to previous results reported (Mascheroni et al., 2016; Li et al., 2013b; Elazzouzi-Hafraoui et al., 2008; Angles and Dufresne, 2001). It is well known that hydrodynamic diameter is estimated assuming spherical and non-permeable particles and is not expected to be equal to the length of CNCs rods, while it strongly correlates with particle lengths, generally resulting much shorter than actual values (Boluk et al., 2012). A summary of the parameters obtained by the DLS analysis is reported in Table 7.3 and the comparison reveals quite different polydispersity indexes, higher for KP-CNCs indicative of a more complex morphology.

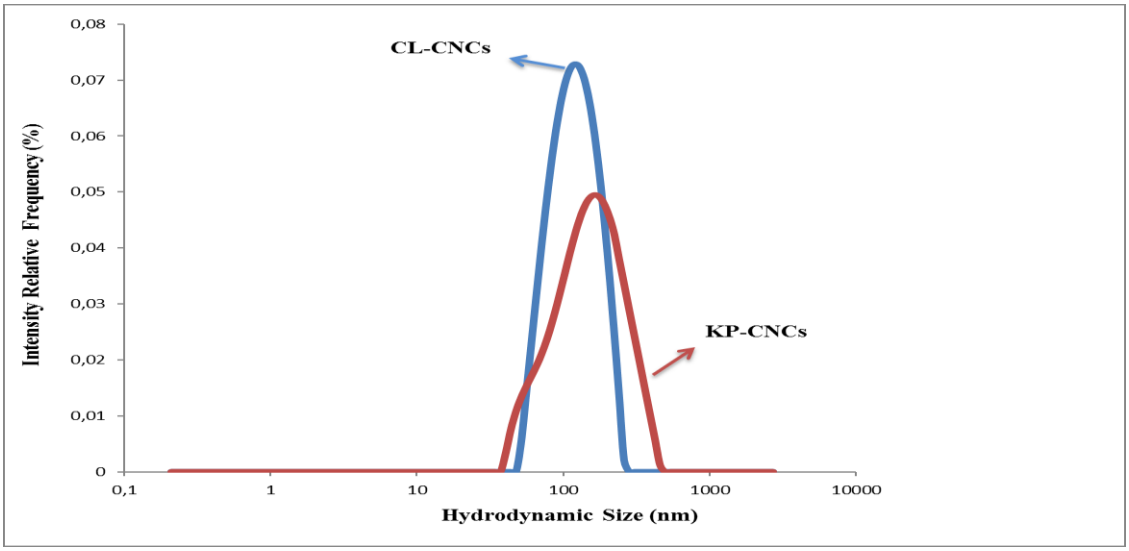

Figure 7.4. CNCs hydrodynamic intensity-weighted size distributions obtained by DLS.

Actually, a polydispersity index of 10% is suggested as a limit above which DLS can no longer be interpreted accurately (Baalousha et al., 2012) and both the two type of CNCs show higher values. Moreover, scattering intensities depend hugely (6^{th} power) on the particles' size, therefore with bi- or multi-modal distributions the peak of bigger nano-particles are visible, while the smaller are underestimated. In fact, the transmission electron microscope (TEM) observations reveal important differences in terms of morphology of the two kinds of CNCs. Electron micrographs (see Fig. 7.5) show only rod-like shape for CL-CNCs, while shape and dimension of KP-CNCs are composite, denoting both rod-like and many spherical nanoparticles. The presence of such spherical shape cannot be attributed to the APS process used but, very likely, to the cellulose source and, actually, several Authors have already described spherical cellulose nanocrystals and related this morphology to the use of hydrochloric acid and/or possible alkaline pre-treatment (Cheng et al., 2014; Lu and Hsieh, 2010; Lu and Hsieh, 2009; Wang et al., 2007; Zhang et al., 2007). In particular, it is worthy to underline that the Kraft process is based on alkaline treatment of the wood and may be the responsible of such a complex morphology. In order to check the unusual morphology, we acquired a SEM image of the KP-CNCs, reported on the right side of Fig. 7.5, which confirms the presence of both rod like and spherical nanoparticles, leading to a network that might be relevant for final performance of the coatings prepared.

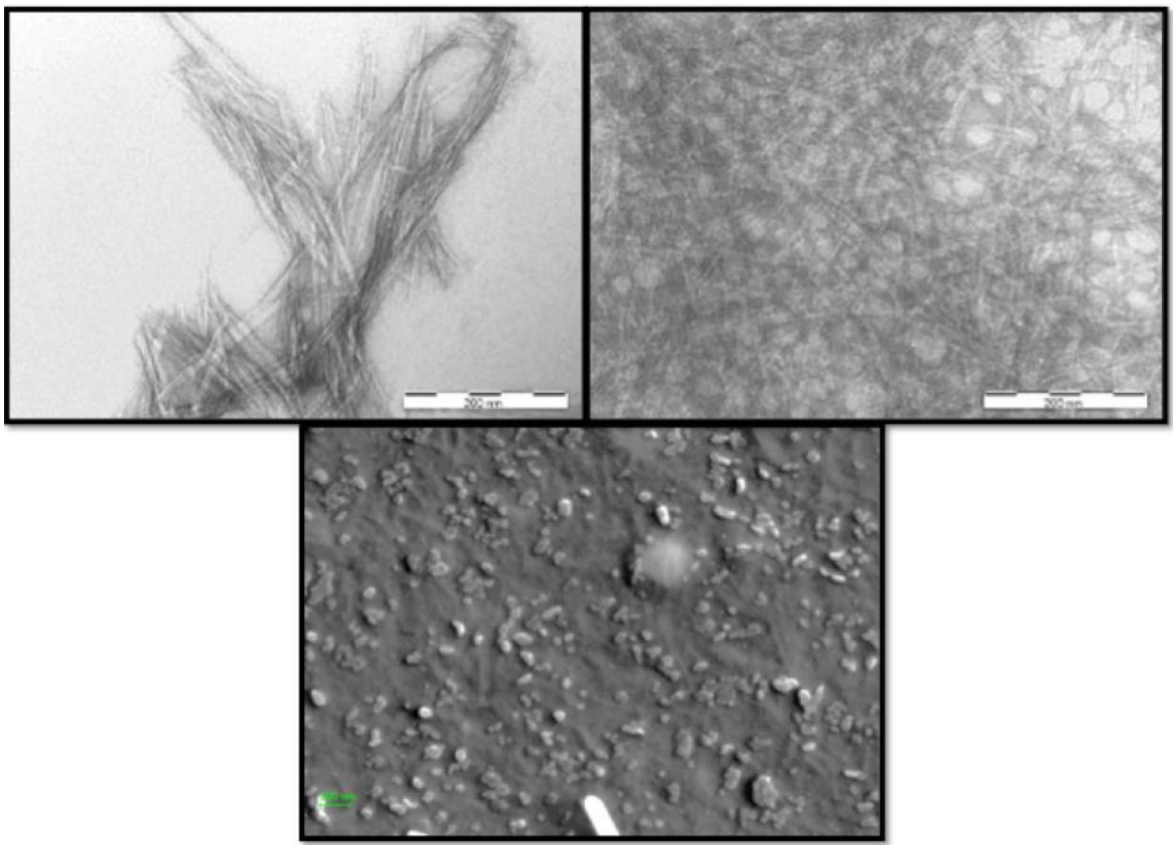

Figure 7.5. Electron micrographs of CNCs obtained from Cotton linters (left) and Kraft pulp (center) by TEM, and CNCs from Kraft pulp by SEM (right).

Table 7.3. Morphological information of CNCs from the two different raw materials.

Property	**CL-CNCs**	**KP-CNCs**
Rod Length/Diameter (nm) by TEM	≈ 120/6	≈ 200/6
Sphere Diameter (nm) by TEM	-	≈ 32
Hydrodynamic diameter by DLS (nm)	128.5	169.7
Polydispersity index,	17.9	25.8

** polydispersity defined as PDI = (σ/D)2, is a measure of the width of particle size distribution*

7.4.2. CNCs chemical characterization

Various chemical features were evaluated in order to compare the CNCs obtained from the lignocellulosic cellulose source, with those from cotton linters (Tab. 7.4). By means of light scattering techniques, besides the hydrodynamic diameter, an evaluation of the molecular mass of nano-particles were achieved using a static light scattering method, while the Zeta potential and the conductivity of CNCs dispersion were assessed using an ELS method (electrophoretic light

scattering). Collecting the FT-IR spectra of freeze dried CNCs in attenuated total reflectance mode, a check of the chemical structure and an evaluation of the degree of oxidation induced by the APS process were obtained. Zero shear viscosity (η_0) of the suspension used for the coating subsequent steps, was calculated using Cross equation (Cross, 1965):

$$\frac{\eta\text{-}\eta_\infty}{\eta_0 - \eta_\infty} = \frac{1}{1 + (K^2 \cdot \dot{\gamma}^2)^{(1-n)/2}} = \frac{1}{1 + (K \cdot \dot{\gamma})^{1-n}}$$

Data used for the equation as standard shear viscosity versus shear rate have been derived by experimental complex viscosity versus angular frequency data using Cox-Merz rule. In Cross equation, η_0 represents zero shear viscosity, η_∞ infinite shear viscosity, $\dot{\gamma}$ is shear rate, $(1 - n)$ is called Cross rate constant (with *n* known as non-Newtonian behavior index) and K is the Cross time constant. Finally, the thermal stability of CNCs from the two different sources was investigated using a thermo-gravimetric procedure (TGA).

Table 7.4. Chemical features of CNCs from the two different raw materials.

Property	**CNCs from CL**	**CNCs from KP**
Zeta Potential (mV)	-44.7 + 1.1	-40.1 + 0.8
Conductivity (mS cm^{-1})	0.113	0.126
Degree of Oxidation (DO)	0.16	0.20
Molecular Mass (kDa)	1.15 x10^6	3.86 x10^5
Viscosity (η0, Pa·s)	Non-detectable	2.62 x10^3
TGA (To, °C)	304.45	303.42
TGA (Ti, °C)	336.47	345.14
TGA (Tmax, °C)	388.02	369.39

T_0, T_i and T_{max} are three parameters usually indicated in the description of a thermal degradation process. Since cellulose KP-CNC exhibit a one-step degradation pathway, these three parameters are defined as, respectively, temperature in correspondence to the inflection point for the step, Ti, and temperatures at which the tangent in this point encounters the extensions of plateau regions when degradation starts, T_0, and finishes, T_{max}.

Zeta potential value is an assessment of the electro-kinetic potential in colloid dispersions, being related to the degree of repulsion between ions of like charges and particle-particle interaction. It provides information about the particles surface-solvent interface, and its measure is key to understanding dispersion stability and aggregation phenomena, i.e. is essential for potential use of CNCs as coating for flexible packaging materials. Both the CNCs produced, exceed the value of

40, assumed as essential to guarantee good stability of colloid dispersions (Hanaor, 2012). The lower value in KP-CNCs can be related to the higher viscosity, which affects the electrophoretic mobility in the electric field used for zeta potential assessment. KP-CNCs and CL-CNCs suspensions have very different rheological behaviors. KP-CNCs suspension shows shear thinning behavior, with a constant slope of viscosity in the frequency range considered and no Newtonian plateau at low shear rates: the slope of complex viscosity and of elastic and storage modulus is similar to the one observed when thickening agents are dispersed in fluids (Manrique et al., 2016; Makmoon et al., 2013). Data registered at frequencies higher than 12 Hz have not been reported since viscosity was under the detection limit of the instrument. CL-CNCs suspension shows very low viscosity, that becomes non detectable using the cone-plate geometry used for measurements. In particular, they appear to have viscosities lower from one to four orders of magnitude in the same conditions used for KP-CNC suspension and a different behavior in relation to the frequency applied. The higher viscosity of KP-CNCs, and its behavior in relation to frequency, is inconsistent with the difference observed in the molecular mass (lower than CL-CNCs), but could be related to the composite morphology noted for the nano-particles and to a residual of hemicellulose from the raw material. As the TEM microphotographs show, the spherical nanoparticles are entrapped into the network of rod-like CNCs, giving very likely a sort of rigidity to the system. The hemicellulose, on the other hand, are well known as gluing substances and can affect much the viscosity (Fitt et al., 1994; Goring, 1966). The conductivity values assessed on the two CNCs are similar and consistent with the degree of oxidation; i.e. they show a higher conductivity in the more oxidized nanoparticles. From the comparison of FT-IR spectra (data not shown) a confirmation of identical chemical structure of the two CNCs was obtained.

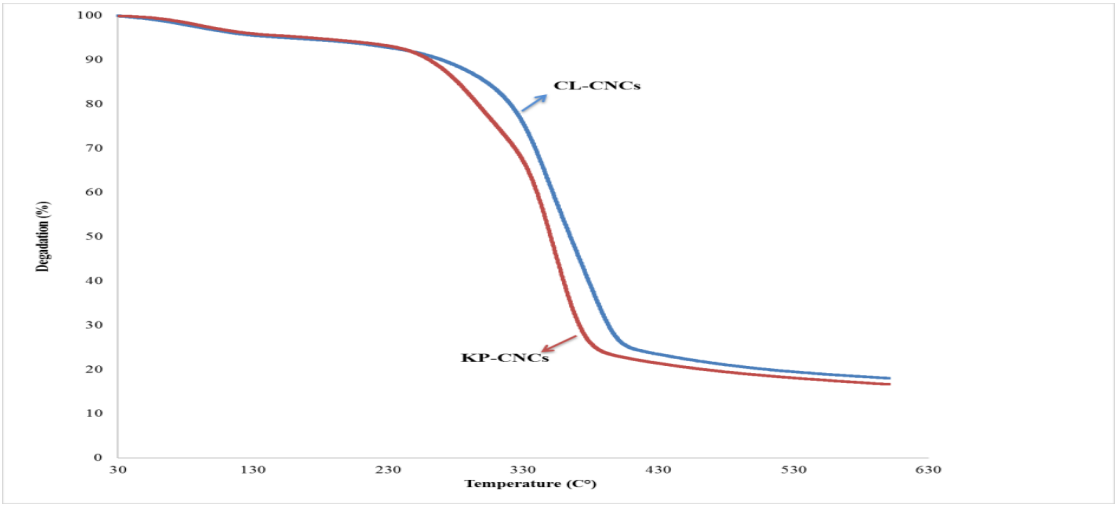

Figure 7.6. TGA plots, from 30 °C to 600 °C, of CNCs from Cotton linters and Kraft pulp in air.

The evaluation of the TGA values (Tab. 7.4 and Fig. 7.6) confirms the possible presence of some contaminants in the KP-CNCs. In fact, even if the onset temperatures (To) are very close (304.4 °C and 303.4 °C for the CL-CNCs and KP-CNCs respectively) the temperatures corresponding to the inflection point (Ti) and maximum value (Tmax) are quite different. In particular, the lower maximum temperature of nano-particles produced from Kraft pulp, for which the CNCs undergo a most important degradation, can be explained by the presence of substances less thermostable than pure cellulose, suggesting that a better optimization of the fragmentation process and of purification steps are required.

7.4.3. Characterization and comparison of PET films coated with CNCs obtained from the two raw materials

Chemical and physical features of the coated films

The coatings were realized on the same substrate (PET, 12 µm thick) after the same activation step by corona treatment, with the two different CNCs suspensions, providing the same amount of cellulose nano-crystals per surface unit. Due to the different viscosity, however, the CL-CNCs suspension was applied in one step, using a 8% (w/v) concentration, while the KP-CNCs suspension was applied in two subsequent steps, using a 4% (w/v) concentration. Nevertheless, the final thicknesses obtained were quite similar (Tab. 7.5) and also the adhesion strength (water resistance), evaluated by an empirical method on the two coatings, showed no significant differences and provides indications about a good stability and consistency of both the coatings. The coefficients of friction (COF), estimated both as dynamic and static values (Tab. 7.5), were a little higher than those obtained in previous papers[14,16] when a lower amount of CNCs was used

(7%), but always much lower than the substrate alone. The corona treated side of PET, in fact, shows much higher values in the 0.5-0.7 range (data not presented). Such difference in COF values is indicative of a well distributed coating onto the substrate surface and consistent with a good machinability of the coated films. KP-CNCs coated film had higher COF values than CL-CNCs, denoting once again some differences in the chemical nature of the coating, but the low standard deviations of the measures can be again assumed as proof of uniform covering of the substrate thus, good coating aptitudes of CNCs suspensions.

The optical properties evaluated on the coated films (haze and transparency) showed significant differences between the KP-CNCs and CL-CNCs coated PET, with lower transparency and higher haze values for the coating obtained from lignocellulosic raw material, but still acceptable for practical purpose, as Fig. 7.7 clearly demonstrates. It is also worthy to mention the clearly visible iridescence on the surface of KP-CNCs coated film, typical behaviour of one dimension crystallinity (Salas et al., 2014).

Figure 7.7. Transparency of the coated (KP-CNCs) and bare films.

An extensive evaluation of surface properties was conducted with the aim of characterizing the two coatings, and with the perspective of a laminating step, needed to protect and make sealable the coated film developed. The static contact angles of the two coatings (Tab. 7.5) were quite similar for water and the apolar solvent (diiodomethane) but different for the polar, organic solvent (formamide). More importantly, these results confirm previous data[14,16], highlighting the higher wettability of these coatings towards polar solvents (even organic) with respect to bare film (PET

showed 57.4 and 39.5 for water and formamide, respectively) and to CNCs obtained by the traditional H_2SO_4 hydrolyzing process[16]. The higher affinity of these coatings for water and polar solvents is also well demonstrated by the surface energy (SFE) values and their components. 68 mJ m^{-2} is a quite high SFE value, higher than the surface energy measured when H_2SO_4 was used to obtain CNCs from the same raw material, and much higher than typical values of PET bare film (Li et al., 2013b; Introzzi et al., 2012). The substrate used, in fact, has SFE around 45 mJ m^{-2} and a very small polar component (less than 5 mJ m^{-2}). These are classical achievements when hydrophilic polymer are considered (Li et al., 2013b; Introzzi et al., 2012; Nuraje et al., 2010) but, in this case, the powerful action of APS reagent in oxidation of cellulose is also to be underlined.

Table 7.5. Some features of PET film coated with CNCs obtained from the two different raw materials (average values ± s.d.).

	PET coated CL-CNCs	**PET coated KP-CNCs**
Coating thickness (nm)	756.3 ± 22.3	746.8 ± 89.5
Water resistance (%)	49.2 ± 3.3	47.8 ± 0.7
COF[a] static	0.35 ± 0.02	0.43 ± 0.02
COF[a] dynamic	0.26 ± 0.02	0.30 ± 0.01
Transparency (T%)	85.67 ± 0.3	81.7 ± 1.1
Haze (%)	1.89 ± 0.1	3.18 ± 0.9
OCA[b] water	23.6 ± 4.9	22.6 ± 3.6
OCA[b] diiodomethane	27.7 ± 3.5	33.9 ± 2.8
OCA[b] formamide	5.54 ± 0.7	12.9 ± 3.8
SFE[c] (mJ m^{-2})	68.85	68.18
SFE[c] polar part (mJ m^{-2})	29.37	31.20
SFE[c] dispersive part (mJ m^{-2})	38.49	36.98

[a]: coefficients of friction; [b]: optical contact angles; [c]: surface energies

Diffusional properties

The overall results obtained in the comparison of the CNCs coatings obtained using a pure cellulosic source (CL) and a lignocellulosic raw material (KP) demonstrate a substantial similarity between them and encouraged the potential use of KP-CNCs coating as an effective gas barrier coating, in real applications. Therefore, the investigation proceeded with a deep analysis of gas permeability properties of the PET film coated with the CNCs from the softwood Kraft pulp. Previous works clearly demonstrated the effectiveness of cellulose nano-crystals coatings, as gas

barrier layer in possible laminated flexible structures (Mascheroni et al., 2016; Fukuya et al., 2014; Li et al., 2013a; Li et al., 2013b; Aulin et al., 2010; Minelli et al., 2010; Frounchi and Dourbash, 2009), showing oxygen gas permeability values much lower than the ones currently provided by synthetic polymers, but only few data are available so far about CO_2 permeability, thermal and relative humidity sensitivity of such nano-coatings. At first, the CO_2 and O_2 permeability of un-coated and KP-CNCs coated PET films were measured in a range of temperatures from 30 to 50 °C, and the diffusional properties of the coating alone were calculated. In Fig. 7.8 the CO_2 and O_2 permeability of PET film (12 μm) and CNCs coating (0.74 μm) are presented in a log diagram (LnP vs 1/T), together with the apparent activation energies of permeabilities (Ea), estimated according to Arrhenius equation. The superior barrier properties of CNCs coating is well evident and it is worthy to note that P_{CO2}CNCs is about 4 log (Ln) lower than P_{CO2}PET, while P_{O2}CNCs is more than 5 log lower than P_{O2}PET. Moreover, the comparison of activation energies is also noticeable, showing that Ea of O_2 permeation is higher in PET than in CNCs, while for carbon dioxide is the opposite. It means that gas diffusion through the biopolymer coating is different with respect to the diffusion through PET film and the difference affects particularly the oxygen diffusion leading to a significant lesser thermal sensitivity of permeability in the nanocrystals. The concepts of "free volume" and cooperative movement of gas molecules and polymer chains are generally considered useful to explain gas permeability and its thermal sensitivity (Mokwena et al., 2012), and is worthy to note that the free volume inside KP-CNCs coating, as well as the chain mobility, must be affected by the particular morphology observed in these nano-particles, where the voids inside a network of rod like crystals are filled by spherical particles.

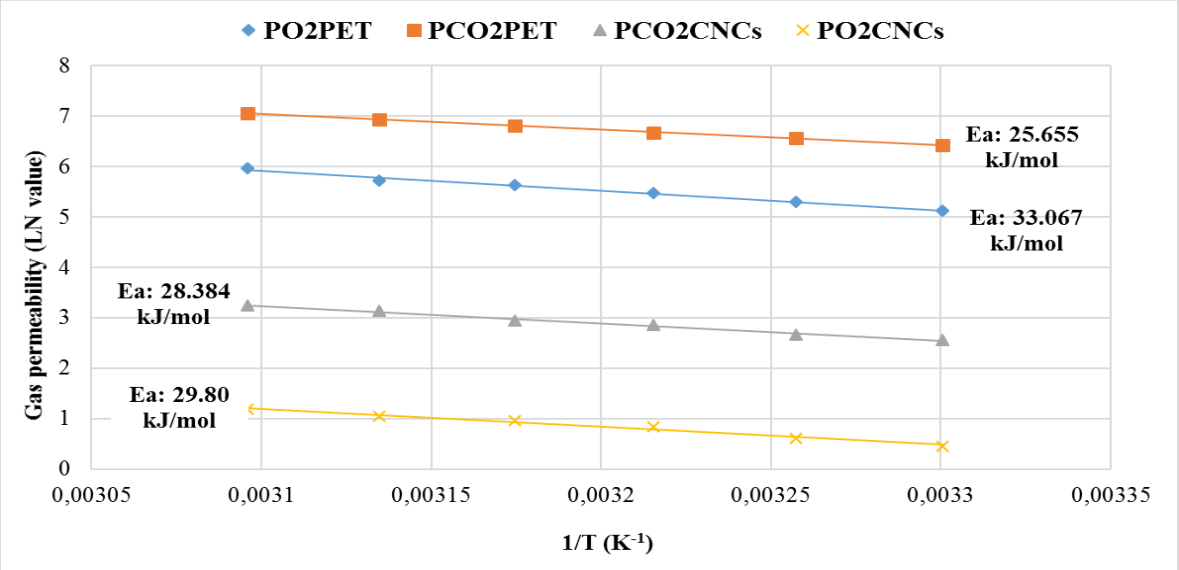

Figure 7.8. Arrhenius plot of oxygen and carbon dioxide permeabilities in PET and KP-CNCs coating.

Table 7.6. Permeability, diffusion and solubility coefficients of oxygen and carbon dioxide, in PET and KP-CNCs coating.

	KP_G at 30 °C (cm^3 µm m^{-2} bar^{-1} d^{-1})	**KP_G at 50 °C** (cm^3 µm m^{-2} bar^{-1} d^{-1})	**D_G at 30°C** (cm^2 s^{-1})	**D_G at 50°C** (cm^2 s^{-1})	**S_G at 30°C** (bar^{-1})	**S_G at 50°C** (bar^{-1})
O_2 in PET	2 004	4 694	3.78E-10	4.23E-10	0.612	1.282
O_2 in CNCs	1.2	2.5	4.07E-13[a]	5.32E-13	0.341[a]	0.544
CO_2 in PET	7 450	14 004	2.91E-10	4.46E-10	2.966	3.630
CO_2 in CNCs	9.7	19.1	7.81E-13	1.22E-12	1.44	1.82

[a] Values collected at 34 °C

In Table 7.6, the permeability coefficients (KP_{O2} and KP_{CO2}), calculated for the bare PET film and the CNCs coating, are presented at the minimum and maximum temperatures tested, together with diffusion and solubility coefficients. The barrier property provided by the coating is well evident and impressive. The KP_{O2} and KP_{CO2} of Kraft pulp CNCs coating are thousand times lower than the substrate, showing values which are 8-10 times lower than synthetic barrier polymers such as EVOH or PVOH and 50-60 times lower than O-MXD6 or PVDC. Such low values are mainly due to the strongly reduced diffusion coefficients which, at both the temperatures, are about one-thousandth of what has been measured in PET for oxygen and less than three-thousandth for carbon

dioxide. Solubility, on the contrary, is not dramatically reduced, sustaining the hypothesis of a relevant effect of the complex structure revealed for CNCs coming from the lignocellulosic raw material.

The high gas barrier assessed is, at the same time, proof of barrier properties of the nanoparticles, as well as of the uniformity of the thin coating realized onto the PET film, suggesting a realistic opportunity for coating processes based on these kind of CNCs. In any case, it is clear that this potential bio-barrier has to be protected from moisture absorption by a hydrophobic layer, which could also provide sealability to the final structure. In fact, the moisture sensitivity of the CNCs coating is quite high, as Fig. 7.9 shows, leading to an exponential increase of oxygen permeability when the relative humidity increases on the coated side. However, the loss of gas barrier properties is reversible, and if a drying step is provided to the coated film (data not shown) the permeability turns back to the original, low values. This point is of relevant importance and is currently under deeper investigation.

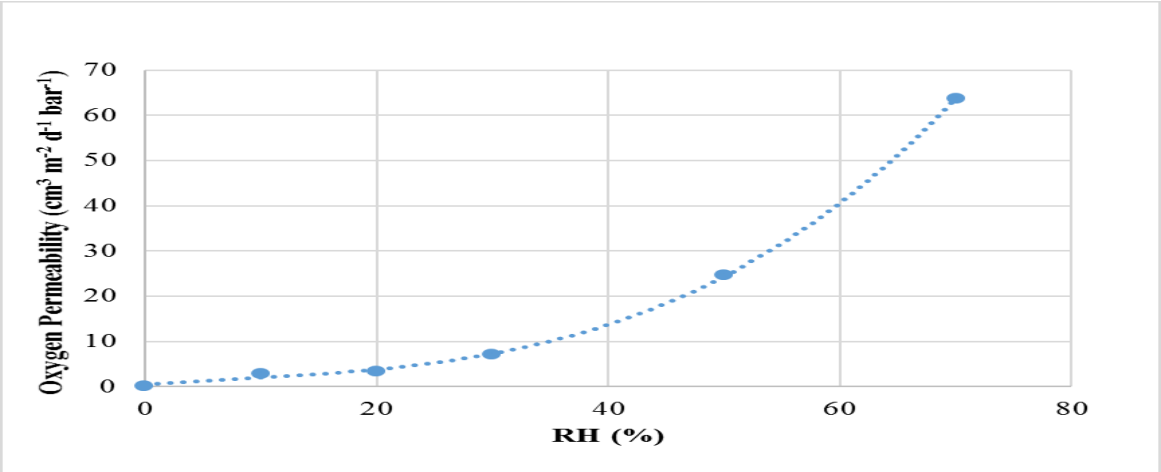

Figure 7.9. Oxygen permeability of KP-CNCs coated PET film, as function of relative humidity on the coated side.

7.5. CONCLUSIONS

The results obtained highlight that is possible to produce high performing coatings for common packaging materials, starting from un-expensive, largely available, and renewable raw materials and by-products. The cellulose nanocrystals, easily obtained from the softwood Kraft pulp, were able to deliver, in form of thin coating onto a PET film, a surprising high oxygen and carbon dioxide barrier, which was just slightly affected by the temperature raise. Even if in this work the gas barrier properties were mainly focused, it is well known that the cellulose nanocrystals can provide or enhance other interesting properties (mechanical, optical), and that CNCs can be used as template to provide an active behavior, such as antioxidant or antimicrobial, to the packaging materials. Therefore, it seems really appropriate to proceed in this kind of research, addressed to increase the sustainability of packaging materials, making possible to put in practice concepts of circular economy or industrial symbiosis. In the particular case considered in this work, i.e. the production of plastic films coatings based on CNCs from lignocellulosics coming from the paper industries, the APS process seems really promising. However, a "case by case" approach is advisable, to take into account individual differences in the cellulosic sources and in order to possibly adjust the process variables.

Acknowledgements

The authors wish to acknowledge Dr. Giorgio Capretti of INNOVHUB-SSI, Milan, for his scientific support. Mr. Alessio Busi, post-graduate Master student in the University of Milan, and Mr. Gerald Perry E. Marin, post-graduate Master student in the Lund University, are strongly acknowledged for their unrivaled technical support. Finally, TUBITAK, the Scientific and Technological Research Council of Turkey, is warmly thanked for its support.

7.6. REFERENCES

Anglès, M.N. and Dufresne, A. 2001. Plasticized Starch/Tunicin Whiskers Nanocomposite Materials. Mechanical Behavior. Macromol. 34, 2921-2931.

Aulin, C., Gallstedt, M. and Lindstrom, T. 2010. Oxygen and oil barrier properties of microfibrillated cellulose films and coatings. Cellul. 17, 559-574.

Baalousha, M. and, Lead, J. 2012. Rationalizing nanomaterial sizes measured by atomic force microscopy, flow field-flow fractionation, and dynamic light scattering: sample preparation, polydispersity, and particle structure. Environ. Sci. Technol. 46, 6134-6142.

Boluk, Y., Zhao, L. and Incani, V. 2012. Dispersions of nanocrystalline cellulose in aqueous polymer solutions: structure formation of colloidal rods. Langmuir. 28, 6114-6123.

Cheng, M., Qin, Z., Liu, Y., Qin, Y., Li, T., Chen, L. and Zhu, M. 2014. Efficient extraction of carboxylated spherical cellulose nanocrystals with narrow distribution through hydrolysis of lyocell fibers by using ammonium persulfate as an oxidant. J. Mater. Chem. A. 2, 251-258.

Clark, J.H. 2007. Green chemistry for the second generation biorefinery—sustainable chemical manufacturing based on biomass. J. Chem. Technol. Biotechnol. 82, 603-609.

Crank, J. 1979. The mathematics of diffusion. Oxford university press.

Cross, M.M. 1965. Rheology of non-Newtonian fluids: A new flow equation for pseudoplastic systems. J. Colloid Sci. 20, 417-437.

Dann, J.R. 1970. Forces involved in the adhesive process. J. Colloid Interface Sci. 32, 302-320.

Debye, P. and Anacker E.W. 1951. Micelle Shape from Dissymmetry Measurements. J. Phys. Chem. 55, 644-655.

Eichhorn, S.J., Dufresne, A., Aranguren, M., Marcovich, N.E., Capadona, J.R., Rowan, S.J., Weder, C., Thielemans, W., Roman, M., Renneckar, S., Gindl, W., Veigel, S., Keckes, J., Yano, H., Abe, K., Nogi, M., Nakagaito, A.N., Mangalam, A., Simonsen, J., Benight, A.S., Bismarck, A., Berglund, L.A. and Peijs, T. 2010. Review: current international research into cellulose nanofibres and nanocomposites. J. Mater. Sci. 45, 1-33.

Elazzouzi-Hafraoui, S., Nishiyama, Y., Putaux, J.L., Heux, L., Dubreuil, F. and Rochas, C. 2008. The shape and size distribution of crystalline nanoparticles prepared by acid hydrolysis of native cellulose. Biomacromol. 9, 57-65.

Fitt, L.E., Pienkowski, J.J. and Wallace, J.R. 1994. U.S. Patent No. 5,358,559. Washington, DC: U.S. Patent and Trademark Office.

Frounchi, M. and Dourbash, A. 2009. Oxygen Barrier Properties of Poly(ethylene terephthalate) Nanocomposite Films. Macromolecul. Mater. Engineer. 294, 68-74.

Fukuya, M.N., Senoo, K., Kotera, M., Yoshimoto, M. and Sakata, O. 2014. Enhanced oxygen barrier property of poly(ethylene oxide) films crystallite-oriented by adding cellulose single nanofibers. Polymer. 55, 5843-5846.

Goring, D. 1966. Thermal softening, adhesive properties and glass transitions in lignin, hemicellulose and cellulose. in Consolidation of the Paper Web. 555-575.

Habibi, Y., Lucia, L.A. and Rojas, O.J. 2010. Cellulose Nanocrystals: Chemistry, Self-Assembly, and Applications. Chem. Rev. 110, 3479-3500.

Habibi, Y., Chanzy, H. and Vignon, M. 2006. TEMPO-mediated surface oxidation of cellulose whiskers. Cellul. 13, 679-687.

Hanaor, D., Michelazzi, M., Leonelli, C. and Sorrell, C.C. 2012. The effects of carboxylic acids on the aqueous dispersion and electrophoretic deposition of ZrO_2. J. Europ. Ceramic Soc. 32, 235-244.

Hernandez, R.J. and, Gavara, R. 1999. Plastics Packaging: Methods for Studying Mass Transfer Interactions: a Literature Review. Pira International.

Introzzi, L., Fuentes-Alventosa, J.M, Cozzolino, C.A., Trabattoni, S., Tavazzi, S., Bianchi, C.L., Schiraldi, A., Piergiovanni, L. and Farris, S. 2012. “Wetting Enhancer” Pullulan Coating for Antifog Packaging Applications. Acs Appl. Mater. Interfaces. 4, 3692-3700.

Kaelble, D. 1970. Dispersion-polar surface tension properties of organic solids. J. Adhesion. 2, 66-81.

Keijsers, E.R.P., Yılmaz, G., van Dam, J.E.G. 2013. The cellulose resource matrix. Carbohydr. Polym. 93, 9-21.

Khan, A., Huq, T., Khan, R.A., Riedl, B. and Lacroix, M. 2014. Nanocellulose-Based Composites and Bioactive Agents for Food Packaging. Crit. Rev. Food Sci. Nutr. 54, 163-174.

Knoshaug, E., Shi, B., Shannon, T., Mleziva, M. and Pienkos, P. 2012. The potential of photosynthetic aquatic species as sources of useful cellulose fibers—a review. J. Appl. Phycol. 25, 1123-1134.

Lam, E., Male, K.B., Chong, J.H., Leung, A.C.W. and Luong, J.H.T. 2012. Applications of functionalized and nanoparticle-modified nanocrystalline cellulose. Trends Biotechnol. 30, 283-290.

Leung, C.W., Luong, J.H.T., Hrapovic, S., Lam, E., Liu, Y., Male, K.B., Mahmoud, K. and Rho, D.2012. Cellulose nanocrystals from renewable biomass. Google Patents.

Leung, A., Hrapovic, S., Lam, E., Liu, Y.L., Male, K.B., Mahmoud, K.A., Luong, J.H.T. 2011. Characteristics and Properties of Carboxylated Cellulose Nanocrystals Prepared from a Novel One-Step Procedure. Small. 7, 302-305.

Li, F., Mascheroni, E. and Piergiovanni, L. 2015. The Potential of NanoCellulose in the Packaging Field: A Review. Packaging Technol. Sci. 28, 475-508.

Li, F., Biagioni, P., Finazzi, M., Tavazzi, S. and Piergiovanni, L. 2013a. Tunable green oxygen barrier through layer-by-layer self-assembly of chitosan and cellulose nanocrystals. Carbohydr. Polym. 92, 2128-2134.

Li, F., Biagioni, P., Bollani, M., Maccagnan, A. and Piergiovanni, L. 2013b. Multi-functional coating of cellulose nanocrystals for flexible packaging applications. Cellul. 20, 2491-2504.

Lu P, Hsieh YL. 2010. Preparation and properties of cellulose nanocrystals: Rods, spheres, and network. Carbohydr. Polym. 82(2), 329-336.

Lu, P. and Hsieh, Y.L. 2009. Preparation of rod-like, network-structured, and spherical cellulose nanocrystals with excellent thermal and mechanical properties. Abstracts of Papers of the Am. Chem. Soc. 237pp.

Makmoon, T., Foungfuchat, A. and Jiratumnukul, N. 2013. Modified tapioca starch as a rheology modifier in acrylic dispersion system. Progress Organic Coat. 76, 959-962.

Manrique, Y.J., Sparkes, A.M., Cichero, J.A.Y., Stokes, J.R., Nissen, L.M. and Steadman, K.J. 2016. Oral medication delivery in impaired swallowing: thickening liquid medications for safe swallowing alters dissolution characteristics. Drug Develop. Ind. Pharm. 42, 1537-1544.

Mascheroni, E., Rampazzo, R., Ortenzi, M.A., Piva, G., Bonetti, S. and Piergiovanni, L. 2016. Comparison of cellulose nanocrystals obtained by sulfuric acid hydrolysis and ammonium persulfate, to be used as coating on flexible food-packaging materials. Cellul. 23, 779-793.

Mazeau, K. and Heux, L. 2013. Molecular Dynamics Simulations of Bulk Native Crystalline and Amorphous Structures of Cellulose. J. Physical Chem. B. 107, 2394-2403.

Minelli, M., Baschetti, M.G., Doghieri, F., Ankerfors, M., Lindstrom, T., Siro, I. and Plackett, D. 2010. Investigation of mass transport properties of microfibrillated cellulose (MFC) films. J. Membrane Sci. 358, 67-75.

Mokwena, K.K. and Tang, J. 2012. Ethylene Vinyl Alcohol: A Review of Barrier Properties for Packaging Shelf Stable Foods. Crit. Rev. Food Sci. Nutr. 52, 640-650.

Moon, R.J., Martini, A., Nairn, J., Simonsen, J. and Youngblood, J. 2011. Cellulose nanomaterials review: structure, properties and nanocomposites. Chem. Soc. Rev. 40, 3941-3994.

Nair, S.S., Zhu, J., Deng, Y. and Ragauskas, A.J. 2014. High performance green barriers based on nanocellulose. Sustainable Chem. Proc. 2, 1-7.

Nashar, D.E.E., Abd-El-Messieh, S.L., Basta, A.H. 2004. Newsprint paper waste as a fiber reinforcement in rubber composites. J. Appl. Polym. Sci. 91, 3410-3420.

Nuraje, N., Asmatulu, R., Cohen, R.E. and Rubner, M.F. 2010. Durable Antifog Films from Layer-by-Layer Molecularly Blended Hydrophilic Polysaccharides. Langmuir. 27, 782-791.

Owens, D.K. and Wendt, R.C. 1969. Estimation of the surface free energy of polymers. J. Appl. Polym. Sci. 13, 1741-1747.

Rowell, R., Young, R. and Rowell, J. 1997. Paper and composites from agro-based resources. Ch 7 pp. 257.

Salas, C., Nypelö, T., Rodriguez-Abreu, C., Carrillo, C. and Rojas, O.J. 2014. Nanocellulose properties and applications in colloids and interfaces. Curr. Opinion Colloid Interface Sci. 19, 383-396.

Sczostak, A. 2009. Cotton linters: an alternative cellulosic raw material. in Macromolecular Symposia. Wiley Online Library.

Sluiter, A., Hames, B., Ruiz, R., Scarlata, C., Sluiter, J., Templeton, D. and Crocker, D. 2008. Determination of structural carbohydrates and lignin in biomass. Lab. Anal. Proced. 1617pp.

Shill, K., Padmanabhan, S., Xin, Q., Prausnitz, J.M., Clark, D.S. and Blanch, H.W. 2011. Ionic liquid pretreatment of cellulosic biomass: Enzymatic hydrolysis and ionic liquid recycle. Biotechnol. Bioengineer. 108, 511-520.

Shoda, M., Sugano, Y. 2005. Recent advances in bacterial cellulose production. Biotechnol. Biopr. Engineer. 10, 1-8.

Springer, E.L., Minor, J.L. 1991. Delignification of lignocellulosic materials with monoperoxysulfuric acid. Google Patents.

van Oss, C.J. 2003. Long-range and short-range mechanisms of hydrophobic attraction and hydrophilic repulsion in specific and aspecific interactions. J. Molecul. Rec. 16, 177-190.

Wang, N., Ding, E.Y. and Cheng, R.S. 2007. Thermal degradation behaviors of spherical cellulose nanocrystals with sulfate groups. Polym. 48, 3486-3493.

Yang, H., Alam, M.N. and van de Ven, T.M. 2013. Highly charged nanocrystalline cellulose and dicarboxylated cellulose from periodate and chlorite oxidized cellulose fibers. Cellul. 20, 1865-1875.

Zhang, J., Elder, T.J., Pu, Y. and Ragauskas, A.J. 2007. Facile synthesis of spherical cellulose nanoparticles. Carbohydr. Polym. 69, 607-611.

Zhang, K., Sun, P., Liu, H., Shang, S., Song, J., Wang, D. 2016. Extraction and comparison of carboxylated cellulose nanocrystals from bleached sugarcane bagasse pulp using two different oxidation methods. Carbohydr. Polym. 138, 237-243.

8. FINAL REMARKS

The control of fresh-cut fruit decay is not an easy task at all. The involved variables are many and often in opposition to each other. If, inside the package, the oxygen content for PPO activity or other metabolic processes of senescence is reduced, this may have negative effects related to anoxia, such as off-odors or bad tastes. Now, since it is not possible to control all the involved variables, a strategy to hold some of theme, the ones that are deemed necessary according to the product is required. Regarding fresh-cut fruit, characterized by a very short shelf life, from 5 to 7 days, it is desirable to aim at controlling those variables that affect the visual appearance of the product, which influences the consumer in the purchase process. Therefore, if the consumer is guided by the visual sense it is necessary to present the product in excellent esthetical condition, with no browning but suitable color, without neglecting the safety of the product. All these considerations, however, must also take into account another variable, essential at industrial and market level, namely the control of the processing costs.

In this direction, the active packaging seems to play a very interesting match between the industrial point of view and that of the product preservation.

In this thesis, the studied and developed active packaging devices can be easily prepared on industrial scale, since the active substances were added into the devices in contact with the fruit. Some researchers suggest the use of edible coating or the dipping process to deliver the active substances, which do not replace the containing function of the packaging and expose the product by oxygen and/or water for long times during the treatment, with negative impacts on the final product. From this point of view the active packaging solutions allow to reduce the handling steps of product preparation and packaging, lowering the exposure to the main factors responsible of senescence acceleration, as well as microbial contamination by the operators.

In the present study, an interesting result was the use of active substances from natural sources. Some of them, such as the extract of *Posidonia oceanica*, cannot be used industrially for different reasons: the lack of legal authorization and high artificial growing as well as extraction costs. Other natural substances, such as green tea extract, chitosan or grape seed extract (wine industry waste) were very interesting for their antioxidant and antimicrobial properties and their low costs. However, from application point of view, some of these substances showed better efficacy when incorporated into the packaging rather than applied by dipping.

The proposed and developed active packaging devices showed several advantages. The active paper added by chitosan and Tetrahydrocurcumin (THC) protects against light, micro-organisms and enzymatic oxidation, and also acts as an absorbent pad toward released juice of fruit during

the storage period, mitigating the unpleasant vision of leachate juice in the package, which often leads to not purchase by the consumer. Furthermore, cellulose, chitosan and THC pad components do not involve an increase in pollution, considering their renewability. However, the limit of the paper pad is the action time, in fact, the advantages of this active packaging have occurred after four days required by the imbibition of the paper for the solubilization of the coating.

The developed active packaging through layer-by-layer (LbL) technique behaved differently. In this case, the release took place from the first day, although further studies are needed to understand how many layers are solubilized over the time. The study revealed that this active packaging was effective both from the microbiological and chemical point of view, slowing the quality decay of the fruit. The used polymers for device assembly were low costs components and the assembly method (positive polymer deposition, water dipping, negative polymer deposition, water dipping) allows automated application. The LbL active packaging has many advantages, the device is highly tailorable, the antimicrobial and/or antioxidant component can be changed depending on the planned application, assembling the layers by more suitable substances. Moreover, it is possible to change the number of the layers increasing them to achieve greater efficacy in relation to the expected food storage period. In addition, differently from what proposed in this study, it would be possible to incorporate the active layers directly in the packaging that contains the product (i.e. skin films). Ss future perspective, all the used methods could be applied on the same kind of fruit and the sensorial analysis could be carried out.

Finally, respect to the topic about cellulose nanocrystals (CNC) flexible packaging, this solution has the objective of EVOH use reduction, which can be replaced by CNC with the same gas barrier efficacy. The use of this solution as an alternative to the existing would allow a reduction in the economic and environmental impact of EVOH. Cellulose nanocrystals flexible film would find a valid use for the preservation of fresh fruit stored in high oxygen MAP or dried and dehydrated fruit.

APPENDIX

Postharvest Biology and Technology 124 (2017) 54–61

Contents lists available at ScienceDirect

Postharvest Biology and Technology

journal homepage: www.elsevier.com/locate/postharvbio

Evaluation of the antioxidant/antimicrobial performance of *Posidonia oceanica* in comparison with three commercial natural extracts and as a treatment on fresh-cut peaches (*Prunus persica* Batsch)

Giulio Piva[a], Daniela Fracassetti[b], Antonio Tirelli[b], Erika Mascheroni[b], Alida Musatti[b], Paolo Inglese[a], Luciano Piergiovanni[b], Manuela Rollini[b,*]

[a] SAF, Department of Agricultural and Forest Sciences, Università degli Studi di Palermo, Viale delle Scienze 4, 90128, Palermo, Italy
[b] DeFENS, Department of Food, Environmental and Nutritional Sciences, Università degli Studi di Milano, Via Celoria 2, 20133, Milano, Italy

ARTICLE INFO

Article history:
Received 17 May 2016
Received in revised form 12 September 2016
Accepted 6 October 2016
Available online xxx

Keywords:
Ready-to-eat fruit
Green tea
Posidonia oceanica
Dipping
Antimicrobials
Antioxidants

ABSTRACT

This research aimed at extending the choice of natural antimicrobials/antioxidants for food applications. Four plant extracts, *Posidonia oceanica* (PO), Green Tea (GT), Grape seeds (GS) and Grape skin (GK), were analyzed to determine their total phenolic content, antioxidant activity and *in vitro* antimicrobial performance. PO extract showed the highest total phenolic content (711 mg gallic acid/g extract) and antifungal activity against *Aspergillus niger* and *Penicillium chrysogenum*. The highest antioxidant (3.81 mg/L EC_{50}) and antibacterial activities (bactericidal against Gram positives and bacteriostatic against Gram negatives) were found for GT extract.

The best performing extracts (PO and GT) were applied by dipping on peach slices in storage trials. Microbiological and pomological parameters were evaluated during 7 d storage. Total aerobic count, *Pseudomonas* as well as yeasts and moulds populations, were reduced by about 0.5 log cfu/g, mainly up to 5 d in all treated samples compared to the control. Total soluble solids, titratable acidity and colour (L*a*b*) changes were also delayed in treated fruit.

1. Introduction

One of the most important research areas as rated by a large majority of food companies is the development of healthy foods, and the introduction of fresh cut produce onto the market, in order facilitate fruit consumption, is rapidly growing (Lung and Zhao, 2016).

Nevertheless, the high perishability of minimally processed fruit may lead to an increase in food waste and economic losses (Amani and Gadde, 2015). Throughout production process, cell breakage takes place causing juice leakage and leading to microbial contamination and growth. Moreover, the contact between enzymes and cell juice under oxygen exposure increases cell respiration and activation of fruit senescence. Specifically, minimally processed fruit, and peaches in particular, are very susceptible to flesh browning (Denoya et al., 2016). Therefore one of the current challenges for the agro-food companies is to lengthen cut fruit shelf life, consequently improving attractiveness to customers as well as food safety.

The food industry has been increasingly employing polyphenols to limit enzymatic oxidation which affects the shelf life of ready-to-eat fruit (Gyawali and Ibrahim, 2014). The beneficial properties of polyphenols on human health also have to be taken into account (Pandey and Rizvi, 2009).

As sources of polyphenols, several trials have been carried out using plant extracts from common or endemic species (Perumalla and Hettiarachchy, 2011) or alternatively from by-products of the agro-food industry (Balasundram et al., 2006). Nowadays, exploitation of by-products and/or residues represents one of the environmental and economic priorities. Several substances discarded from agro-food production can find alternative applications in different contexts. As examples, grape skin (GK) and seeds (GS) are the main wastes from the wine industry, nevertheless they are appreciated for their high phenolic content which includes flavonoids, phenolic acids and non-flavonoid compounds (Poudel et al., 2008). The hydroxyl groups of gallic acid, present in grape by-products, showed antimicrobial activity against *Bacillus cereus*, *B.*

* Corresponding author.
E-mail addresses: giuliopiva88@gmail.com (G. Piva), daniela.fracassetti@unimi.it (D. Fracassetti), antonio.tirelli@unimi.it (A. Tirelli), erika.mascheroni@gmail.com (E. Mascheroni), alida.musatti@unimi.it (A. Musatti), paolo.inglese@unipa.it (P. Inglese), luciano.piergiovanni@unimi.it (L. Piergiovanni), manuela.rollini@unimi.it (M. Rollini).

http://dx.doi.org/10.1016/j.postharvbio.2016.10.001
0925-5214/

Cellulose (2016) 23:779–793
DOI 10.1007/s10570-015-0853-2

ORIGINAL PAPER

Comparison of cellulose nanocrystals obtained by sulfuric acid hydrolysis and ammonium persulfate, to be used as coating on flexible food-packaging materials

Erika Mascheroni · Riccardo Rampazzo · Marco Aldo Ortenzi · Giulio Piva · Simone Bonetti · Luciano Piergiovanni

Received: 16 July 2015 / Accepted: 25 December 2015 / Published online: 13 January 2016

Abstract Cellulose nanocrystals (CNCs), extracted from trees, plants, or similar cellulose-containing materials, can be used in combination with other materials to improve their performance or introduce new applications. The main purpose of this study was to compare and understand the potentialities, as coatings for Poly(ethylene terephthalate) films, of CNCs obtained starting from the same cotton linters by two different processes: sulfuric acid hydrolysis and a less common treatment with ammonium persulfate (APS), able to provide also a cellulose oxidation. The results showed that CNCs produced through the APS treatment showed higher charge densities, due to the carboxylic groups formed during the process, higher crystallinity, higher clarity of the solution and, as a consequence, higher transparency of the coating. These characteristics provide a higher oxygen barrier with respect to the CNCs produced by the H_2SO_4 treatment, together with the availability of active sites for potential surface modification or chemical grafting. Both CNC coatings showed oxygen permeability coefficients that were lower than synthetic resins commonly used in flexible packaging. Furthermore, they did not significantly affect the optical properties of the substrate, while revealing good friction coefficients. Due though to the moisture sensitivity of the coating and its non-sealable nature, similar to EVOH or PVOH oxygen barrier synthetic resins, CNCs developed using APS will need to be laminated with another plastic layer such as a polyolefin. They could then be used to enhance the final properties of packaging solutions as an alternative to

Electronic supplementary material The online version of this article (doi:10.1007/s10570-015-0853-2) contains supplementary material, which is available to authorized users.

E. Mascheroni · R. Rampazzo · L. Piergiovanni
DeFENS, Department of Food, Environmental and Nutritional Sciences - PackLab, Università degli Studi di Milano, Via Celoria 2, 20133 Milan, Italy

M. A. Ortenzi
Department of Chemistry, University of Milan, Via Golgi 19, 20133 Milan, Italy

E. Mascheroni · M. A. Ortenzi · L. Piergiovanni (✉)
CRC Materiali Polimerici (LaMPo), Dipartimento di Chimica, Università degli Studi di Milano, Via Golgi 19, 20133 Milan, Italy
e-mail: luciano.piergiovanni@unimi.it

G. Piva
SAF, Department of Agricultural and Forest Sciences, Università degli Studi di Palermo, Via delle scienze 4, 90128 Palermo, Italy

S. Bonetti
Materials Science Department, University of Milano Bicocca, Via Cozzi 55, 20125 Milan, Italy

BARBARA DEL CURTO

ABSTRACT

A Edoardo

Progetto scientifico
Coordinamento editoriale
Barbara Del Curto
Eliana Farotto

Con testi di
Ilaria Alfieri
Mario Bisson
Giacomo Canali
Gabriele Candiani
Alberto Cigada
Luigi De Nardo
Graziano Elegir, Joana Mendes, Sara Diana
Paola Garbagnoli
Rosalba Lanciotti, Francesca Patrignani, Lorenzo Siroli
Claudio Dall'Agata, Lorenzo Faedi
Andrea Lorenzi
Roberto Montanari
Angelo Montenero
MariaPia Pedeferri
Luciano Piergiovanni, Riccardo Rampazzo, Giulio Piva
Agnese Piselli

Progetto grafico
Rossana Gaddi
Anna Paola Braga

Traduzione
Laura Monti

ISBN 978-88-902818-9-1
Edizioni Dativo Srl
Via Benigno Crespi 30/2 – 20159 Milano (Italy)
Tel. +39 0269007733 – fax +39 0269007664
info@dativo.it - www.dativoweb.net

PACKAGING NATURALMENTE TECNOLOGICO

INNOVAZIONI SOSTENIBILI
PER IL FOOD PACKAGING A BASE DI CARTA E CARTONE

NATURALLY
TECHNOLOGICAL
PACKAGING

SUSTAINABLE INNOVATION
IN PAPER AND BOARD FOOD PACKAGING

POLITECNICO MILANO 1863

comieco

3. 1
Protecting from Oxygen (and from other gases)

Luciano Piergiovanni, Riccardo Rampazzo[a]
Giulio Piva[a,b]

[a] **PackLAB - DeFENS** | Department of Food, Environmental and Nutritional Sciences
Milan State University

[b] **SAF** | Department of Agricultural and Forest Sciences
Palermo State University

Biographies

Luciano Piergiovanni *is full professor of Food Sciences and Technology at the Faculty of Agricultural and Food Sciences of the Milan State University, where he lectures on Conditioning Technologies and Essentials of Distribution Logistics, Quality, and Safety of Biotechnological Food and Food Production and Distribution System sustainability. He coordinated the Research Unit focused on Food Packaging issues, both for national and international projects. He has been the President of GSICA, the Italian Scientific Food Packaging Group, since 1999 and is the author of three text books and 6 chapters in Food Packaging books, as well as of 7 patents and more than 250 published papers.*

Riccardo Rampazzo *is a research fellow at the PackLAB of the Milan State University and at LAMPO, the Centre for Coordinated Research on Polymeric Materials established at the same institution. He published 5 scientific papers and his research is mainly focused on new flexible packaging solutions based on nanocellulose, as well as on the implementation of oxygen absorbers in packaging structures to extend the shelf-life of perishable foodstuffs.*

Giulio Piva *is a Ph.D. candidate in Agricultural, Forest, and Environmental Sciences at the SAF Department of the Palermo University and at the PackLAB of the Milan State University. He was a research intern at the Institut Polytechnique de Grenoble (INP) in France and at the Córdoba University in Spain. He published 5 scientific papers and his research is mainly focused on the implementation of new flexible packaging solutions based on nanocellulose and biopolymers to extend the shelf-life of prepared fresh fruits.*